Dissertation

The role of the STAT signaling pathway in the regulation of growth and apoptosis in malignant pleural mesothelioma

submitted by

Lisa ARZT, MSc.

for the Academic Degree of

Doctor of Medical Science

(Dr.scient.med.)

at the

Medical University of Graz

Institute of Pathology

under the Supervision of

Prof. Dr. Helmut H. Popper

2014

Declaration

I hereby declare that this dissertation is my own original work and that I have fully acknowledged by name all of those individuals and organizations that have contributed to the research for this thesis. Due acknowledgement has been made in the text to all other material used. Throughout this dissertation and in all related publications I followed the guidelines of "Good Scientific Practice".

Graz, July 2014 Lisa Arzt, MSc.

ACKNOWLEDGEMENTS

First of all I would like to thank my supervisor Dr. Helmut H. Popper for providing this research project and for being a great mentor. He offered me opportunities to present my work at several conferences, he helped me to publish my results in peer-reviewed journals, he supported me to become an independent researcher and he always found time to discuss my ideas and results while having one busy day after another.
I also express my gratitude to my thesis committee members Dr. Gerald Höfler and Dr. Hellmut Samonigg for their guidance and feedback.

I warmly thank BMA Iris Halbwedl for technical guidance and emotional support. I enjoyed pleasant and friendly working atmosphere and many helpful discussions. Thank you for being a friend and a teacher for the last 5 years!

I would like to thank several people working at the Institute of Pathology for excellent technical support: BMA Mohammed Al-Effah, BMA Hildegard Gleixner, BMA Margit Gogg-Kamerer and BMA Elisabeth Grygar.
Many thanks to BMA Theresa Maierhofer and BMA Karin Wagner, from the Center for Medical Research of the Medical University of Graz, for their technical assistance and friendly help.

Furthermore I am grateful to Dr. Franz Quehenberger from the Institute for Medical Informatics, Statistics and Documentation of the Medical University of Graz for fruitful discussions and his help with statistical analyses.

Finally I owe special gratitude to my family, my partner Gregor and my friends for unconditional support and encouragement throughout my career. Thank you so much for believing in me!

TABLE OF CONTENTS

ABBREVIATIONS

APS	ammoniumpersulfate
BAP1	BRCA associated protein 1
bp	basepairs
cDNA	complementary DNA
Cq	quantification cycle
DNA	deoxyribonucelic acid
dsRNA	double-stranded RNA
dTTP	deoxy-thymidine triphosphate
EDTA	ethylenediamintetraacedic acid
FBS	fetal bovine serum
FFPE	formalin-fixed and paraffin-embedded
H&E	hematoxylin-eosin
IHC	immunohistochemistry
IL-6	interleukin 6
INF-γ	interferon gamma
JAK	janus kinase
kDa	kilodalton
miRNA, miR	microRNA
MPM	malignant pleural mesothelioma
mRNA	messenger RNA
PBS	phosphate buffered saline
PCR	polymerase chain reaction
PIAS	protein inhibitors of activated STATs
qPCR	quantitative real-time polymerase chain reaction
RNA	ribonucleic acid
RNAi	RNA interference
rpm	randoms per minute
RT	reverse transcription
RT-free	reverse transcriptase free
SD	standard deviation
SDS	sodium dodecyl sulfate

SDS-PAGE	SDS - polyacrylamide gelelectrophoresis
siRNA	small interfering RNA
SOCS	suppressors of cytokine signaling
STAT	signal transducer and activator of transcription
TBS	tris buffered saline
TBS-T	TBS with 0.1% Tween-20
TEMED	N,N,N',N'-Tetramethylethylendiamine
TMA	tissue micro array
Tris	Tris(hydroxymethyl)aminomethane

ABSTRACT

Malignant pleural mesothelioma (MPM) is an aggressive tumor caused by former asbestos exposure with a mean overall survival of 12 months from diagnosis. The knowledge about prognostic factors of outcome is poor and MPM is resistant to conventional therapy.

Genetic predisposition even contributes to the development of MPM: BRCA1-associated protein 1 (BAP1) is a tumor suppressor gene that is frequently lost in MPM and germline mutations predispose to several different tumors including MPM. We wanted to know if BAP1 expression could be used as prognostic factor of outcome and we detected a significant effect of BAP1 expression on overall survival time: the higher the BAP1 expression (non-mutated BAP1), the shorter the overall survival.

From our recent study and published data we know that the regular rapid progressive type of MPM uses several signaling pathways regulating cell growth and survival.The JAK/STAT signaling pathway is the principal signaling mechanism for lots of cytokines or growth factors in mammalians.

Our investigations demonstrate that the STAT (signal transducer and activator of transcription) signaling pathway is totally deregulated. STAT1 is upregulated, phosphorylation of STAT1 on tyrosine 701 is induced by Interferon-gamma treatment and it is very likely that STAT1 functions as an oncogene through the STAT1/survivin pathway. Survivin is highly expressed in MPM and is associated with resistance to chemotherapy.

STAT3 is downregulated in MPM and only a very small part is activated by phosphorylation, which indicates that it has no oncogenic function in MPM. The negative regulators SOCS1 (suppressor of cytokine signaling) and SOCS3 were not detected on protein level and therefore STAT1 activation is not terminated. However, it was possible to detect SOCS messengerRNA (mRNA) in MPM cell lines. This means that the translation process is inhibited or affected by something. It is known that protein expression is controlled by non-coding RNAs and microRNAs (miRNA) are one class. They regulate the expression of target mRNAs and are expected to act as oncogenes or tumor suppressors. Therefore we aimed to quantify selected miRNAs in MPM which are thought to be involved in the regulation of the STAT signaling pathway.

Four upregulated miRNAs (miR-19b, miR-30b, miR-30c and miR-222)have been identified, possibly targeting SOCS1/3 and we tried to re-express SOCS1/3 in MPM cell lines by knocking down the identified miRNAs using single inhibitors or combinations of

inhibitors. With these experiments we aimed to answer if the STAT1/3 signaling cascade can be restored to a physiological level when SOCS proteins are expressed again. Since the knock-down had no effect on SOCS protein expression, it seems that the miRNAs identified by now, are not the (only) reason for the missing expression of SOCS1/3.

To clarify if components of the deregulated STAT signaling pathway have potential as therapeutic targets, it was investigated if the knock-down of STAT1 in MPM cell lines leads to an increased expression of apoptosis or cell-cycle related genes. The effect of STAT1 knock-down on the expression of STAT proteins was different in MPM cell lines: while CRL-5915 seems to compensate STAT1 knock-down by an upregulation of STAT5a, MSTO-211H and Hmeso show slightly upregulated expression levels of STAT3. Most of the genes investigated were found to be differentially expressed in all cell lines, but STAT1 knock-down seems to have an effect on cell cycle progression and apoptosis by the upregulation of CDKN1A in all MPM cell lines. However, it is very unlikely that cell cycle and apoptosis are regulated by only one gene especially because no cell growth inhibition was detected microscopically after STAT1 knock-down.

Understanding the role of STATs in MPM could be the first step into the development of a targeted therapy for these tumors.

ZUSAMMENFASSUNG

Die Rolle des STAT Signalwegs auf die Regulierung von Wachstum und Apoptose im malignen Pleuramesotheliom

Das maligne Pleuramesotheliom (MPM) ist ein aggressiver Tumor, verursacht durch den Kontakt mit Asbest. Die durchschnittliche Überlebensdauer beträgt 12 Monate. Man weiß wenig über die Mechanismen, die zur Tumorentstehung führen und MPM ist resistent gegenüber konventioneller Therapie.

Genetische Prädisposition trägt auch zur Entstehung von MPM bei: BAP1 (BRCA1-associated protein 1) ist ein Tumorsuppressor-Gen das in MPM häufig fehlt und Keimbahnmutationen tragen zur Entstehung unterschiedlicher Tumore bei, einschließlich MPM. Wir wollten wissen, ob eine BAP1 Expression Hinweise auf die Überlebenszeit liefern kann und wir haben einen signifikanten Effekt der BAP1 Expression auf die Überlebenszeit detektiert: je höher die BAP1 Expression (nicht-mutiertes BAP1), desto kürzer ist die Überlebenszeit.

Durch aktuelle Studien und publizierte Daten weiß man, dass einige Signalwege, die Zellwachstum und Überleben regulieren, beim MPM eine Rolle spielen. Der JAK/STAT Signalweg ist der Haupt-Signalweg für viele Zytokine und Wachstumsfaktoren.

Unsere Untersuchungen zeigen, dass der STAT (signal transducer and activator of transcription) Signalweg im MPM vollkommen dereguliert ist. STAT1 ist hochreguliert, eine Phosphorylierung von STAT1 an Tyrosin 701 wird durch Interferon-gamma induziert und es ist sehr wahrscheinlich, dass STAT1 durch den STAT1/Survivin Signalweg wie ein Onkogen funktioniert. Survivin ist im MPM stark exprimiert und wird mit Resistenz gegenüber Chemotherapie assoziiert.

STAT3 ist herunterreguliert und nur ein kleiner Anteil ist durch Phosphorylierung aktiviert, was darauf hinweist, dass STAT3 im MPM nicht wie ein Onkogen funktioniert. Die negativen Regulatoren SOCS1(suppressor of cytokine signaling) und SOCS3 wurden auf Protein-Ebene nicht detektiert.Das bedeutet, dass eine STAT1 Aktivierung nicht durch SOCS1 beendet wird. Allerdings war es möglich SOCS-messengerRNA (mRNA) in MPM Zelllinien zu detektieren. Das bedeutet, dass der Translationsprozess beeinflusst wird. Es ist bekannt, dass Proteinexpression durch nicht-kodierende RNAs kontrolliert wird und eine Klasse davon sind microRNAs (miRNA). Daher war ein Ziel der Studie die

Quantifizierung ausgewählter miRNAs im MPM, die den STAT Signalweg regulieren sollen.

Es wurden vier hochregulierte miRNAs (miR-19b, miR-30b, miR-30c and miR-222) identifiziert, die SOCS1/3 als Target haben und es wurde versucht, dass SOCS1/3 durch einen knock-down der miRNAs wieder exprimiert werden. Durch diese Experimente sollte beantwortet werden ob die STAT1/3 Signalkaskade wieder „normal" funktioniert, wenn SOCS Proteine exprimiert werden. Da der miRNA knock-down keinen Effekt auf die Expression der SOCS Proteine hatte, scheint es, dass diese miRNAs nicht der (einzige) Grund für die fehlende Expression von SOCS1 und SOCS3 sind.

Um zu klären ob Komponenten des STAT Signalwegs Potential als therapeutische Targets haben, wurde untersucht ob ein STAT1 knock-down in MPM Zelllinien zu einer erhöhten Expression von Apoptose- oder Zellzyklusgenen führt. Die Effekte des STAT1 knock-downs waren unterschiedlich: während CRL-5915 einen STAT1 knock-down anscheinend durch eine erhöhte Expression von STAT5a kompensiert, wurde in MSTO-211H und Hmeso eine erhöhte STAT3-Expression festgestellt. Die meisten untersuchten Gene waren in den 3 MPM Zelllinien unterschiedlich exprimiert aber STAT1 knock-down scheintdurch die Hochregulierung von CDKN1A einen Einfluss auf Zellzyklus-Progression und Apoptose zu haben. Allerdings ist es sehr unwahrscheinlich dass Zellzyklus und Apoptose nur durch ein Gen reguliert werden vor allem weil mikroskopisch keine Inhibierung des Zellwachstums festgestellt werden konnte, nachdem STAT1 herunterreguliert wurde.

Versteht man die Rolle des STAT Signalwegs im MPM, kann das der erste Schritt in Richtung einer neuen, effektiven Therapie sein.

1. INTRODUCTION

1.1 Malignant pleural mesothelioma

Malignant mesothelioma is an aggressive cancer which arises from the mesothelial lining of the pleura, peritoneum, pericardial cavities as well as the tunica vaginalis and is mainly caused by asbestos. Mesothelial cells are mostly flat and thin and they make up a protective layer of tissue called the mesothelium. [1, 2] Malignant pleural mesothelioma (MPM) (see **Figure 1**) is the most common form (>90%), followed by the peritoneum (6-10%).

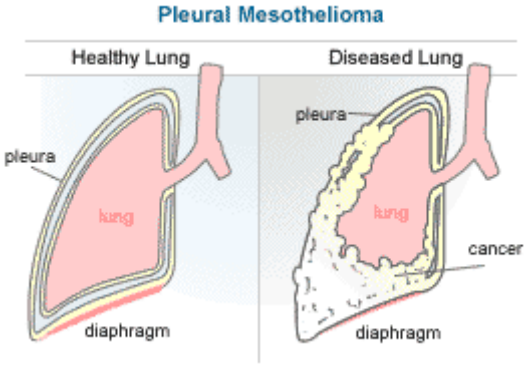

Figure 1: Schematic picture of a healthy lung (left side) and malignant pleural mesothelioma (right side) (from: www.malignantpleuralmesothelioma.org)

Three histological subtypes of malignant pleural mesothelioma are recognized:

- Epithelioid subtype: ~ 50%
- Sarcomatoid subtype: ~ 20%
- Biphasic subtype: ~ 30%

The most common epithelial pattern comprises mesothelial cells arranged in tubulo-papillary or trabecular formations and those mesotheliomas are predominantly composed of acinar structures and are sometimes morphologically identical to a variety of adenocarcinomas. Sarcomatoid mesotheliomas show a fibroblastic pattern with focal storiform arrangement of cells. The biphasic subtype is a mixture of the epithelioid and sarcomatoid subtype. [1]

The median survival of MPM patients ranges from 7 to 24 months depending on the histological subtype, stage of disease and treatment options. [3] MPM is a very rare tumor

which causes about 3000 deaths each year in the United States as well as 5000 deaths each year in Western Europe. The incidence is increasing worldwide with an expected peak in 2020 in Europe [4] or e.g. 2027 in Japan. Like the US even Japan has not banned the use of asbestos entirely and only restricted its use. Therefore future risks are not eliminated. [2, 5]
The long latency period in MPM pathogenesis (20 to 50 years) is responsible for the late diagnosis of this disease. Typical symptoms are progressive dyspnea, which is usually the result of pleural effusion and/or steady chest pain, which is caused by significant chest wall invasion. Patients may also suffer from dry cough, weight loss, fever, fatigue or night sweats. These symptoms are nonspecific – therefore the time from initial presentation until diagnosis is often 3 to 6 months. [4]
MPM has low chemo- and radio-sensitivity and most patients are not amenable to radical surgery. Systemic therapy is the only potential treatment for the bigger part of these patients and the standard of care is the combination of pemetrexed and cisplatin as front line chemotherapy. [6]

1.2 Incidence and causes

Malignant mesothelioma was first recognized in 1870, but the link between mesothelioma and asbestos was first reported in 1960. [7] 80% of MPM patients have a history of asbestos exposure but only 2-10% of individuals with asbestos exposure develop MPM. [4] This can be explained by a threshold value: this is a minimal lower limit below which asbestos fibres cannot cause the tumor. [8] Therefore genetic predisposition for MPM may play a role, as well as Simian Virus 40 (SV40) infection or the inhalation of erionite. [4]

1.2.1 Asbestos

Asbestos is the name for a group of six fibrous silicate minerals that are divided in two groups: (A) serpentine and (B) amphibole (see **Figure 2**) based on their chemical composition and crystalline structure. Chrysotile (so called white asbestos, softer and curled shape) is the only one commercially used among the serpentine minerals while the commercially used amphiboles are actinolite, anthophyllite, amosite, crocidolite and tremolite. [2, 5]
Asbestos has extraordinary fire-resistant properties and was used mostly in the ship-building and construction industries. Although the industrial use was largely eliminated in most countries [4] (not the case in e.g. India where the use of asbestos continues to

increase and only few precautions are taken [5]), asbestos is still present in old buildings where it was used as insulation and fire retardant. Natural disasters like tornados or manmade disasters like the terrorist attacks on the World Trade Center on September 11, 2011 could destroy those buildings and expose millions of people to asbestos.[2, 4] The WHO estimates that about 125 million people worldwide are currently exposed to asbestos. [9]

1.2.2 Erionite

It is often assumed that only asbestos, but no other mineral fibers, cause cancer. This is not true. One such naturally occurring fibrous mineral is erionite (see **Figure 2**). The exposure to erionite is less widespread but it is much more potent in causing mesothelioma than asbestos. [5]

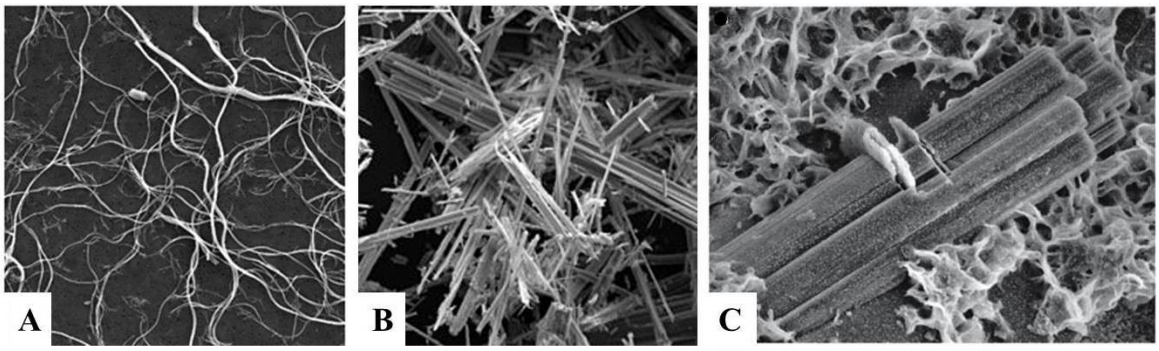

Figure 2: Different types of fibrous minerals.
(A) serpentine (from http://www.complicheck.com/asbestos-info.html,
(B) amphibole (from http://www.mesotheliomalungs.org) and
(C) erionite[10]

1.2.3 Simian Virus 40

Whether Simian Virus 40 (SV40), a small, circular double-stranded DNA polyomavirus of monkey origin, is involved in MPM pathogenesis or not is still unclear. Human population was most probably infected through contaminated poliovirus and adenovirus vaccines between 1955 and 1963.

SV40 induces various tumors including mesotheliomas when injected into hamsters. The primary oncogenic effect is thought to be through binding and inactivation of p53 and the products of the retinoblastoma-susceptibility gene. [6, 11] Two studies were set up to assess the presence of SV40 in mesotheliomas by DNA PCR to clarify if SV40 infection causes MPM. Many samples were positive and both laboratories had problems with

reproducibility. Years later, López-Ríos et al. could show that contamination by common laboratory plasmids containing SV40 sequences causes false-positive results and they stated that asbestos exposure should be considered to be the most likely risk for developing MPM. [11]

1.3 Chromosomal aberrations

Due to the fact that only a small percentage of individuals exposed to asbestos develop MPM, it is suggested that genetics influences mineral fiber carcinogenesis and that genetic predisposition plays a role. Germline mutations of the BRCA-associated protein 1 (BAP1) gene have been linked to high incidence of malignant mesothelioma in some U.S. families. [12] BAP1 is a nuclear- localized deubiquinating enzyme with an ubiquitin carboxy-terminal hydrolase function. [13] It is supposed to be a tumor suppressor gene with a role in cell proliferation and growth inhibition. [14, 15]*BAP1* is located on chromosome 3p21, a region which is deleted in mesotheliomas. [16] Several molecular alterations have been reported in MPM which may cause a number of pathological processes. Some of the changes can be caused by the direct effect of asbestos fibers on the mitotic spindle apparatus or on mesothelial cells and macrophages, inducing them to generate mutagenic reactive oxygen species (ROS). The asbestos or erionite fibers also induce hormone, growth factor and cytokine production due to an inflammatory response, resulting in mesothelial cell proliferation. [5]

No specific chromosome abnormalities characterize MPM, but a number of recurrent anomalies have been identified:

- monosomy for chromosome 4 and particularly for chromosome 22
- polysomy for chromosomes 5,7 and 20
- loss at 1p21-p22, 3p21, 6q15-q21, 9p21-p22 and 22q12
- deletion of chromosome bands 9p13-22: in 50% of MPM, three tumor suppressor (p14, p15 and p16) genes are located in this region; the absence of p16 and p14 maybe important in transformation and proliferation of MPM cells [6]
- missense or nonsense mutations in neurofibromatosis type 2 (NF2) gene [5]

1.4 Cellular pathways and inflammation

The capacity of asbestos to induce ROS is only one factor that contributes to asbestos carcinogenesis. ROS lead to increased growth factor signaling, proliferation and signal transduction pathway stimulation in response to tissue damage (see **Figure 3**). [2] The main targets are:

- Epidermal Growth Factor Receptor (EGFR/ERK)
- Phosphoinositol-3-kinase (PI3K/AKT)
- Hepatocyte Growth Factor Receptor (cMet, HGFR)
- Platelet-derived growth factor receptor (PDGFR)

Overexpression of EGFR has been observed in MPM, especially in the epithelioid subtype. An important molecule involved in downstream signaling from EGFR is PI3K. [6] PI3K, AKT and the downstream mTOR, have been shown to be activated in mesotheliomas and are involved in cell growth and survival. Inhibition of mTOR enhances apoptosis of mesothelioma cells *in vitro*. Similar to EGFR signaling, activation of HGF and c-Met leads to cell proliferation and motility. Even HGF and c-Met are found to be highly expressed in mesotheliomas.

The generation of oxidants by macrophages even activates the mitogen-activated protein kinase (MAPK) signaling and the resulting activator protein 1 (AP-1) transcriptional activity. They have been linked to mesothelial cell transformation. Asbestos may even directly initiate AP-1 activity through EGFR and downstream pathways. [5]

Vascular endothelial growth factor (VEGF) expression correlates with microvessel density in mesothelioma and high microvessel density is associated with poor survival. [6] The Wnt signaling pathway is abnormally activated in human mesotheliomas as indicated by the accumulation of β-catenin, which is a downstream component. [5]

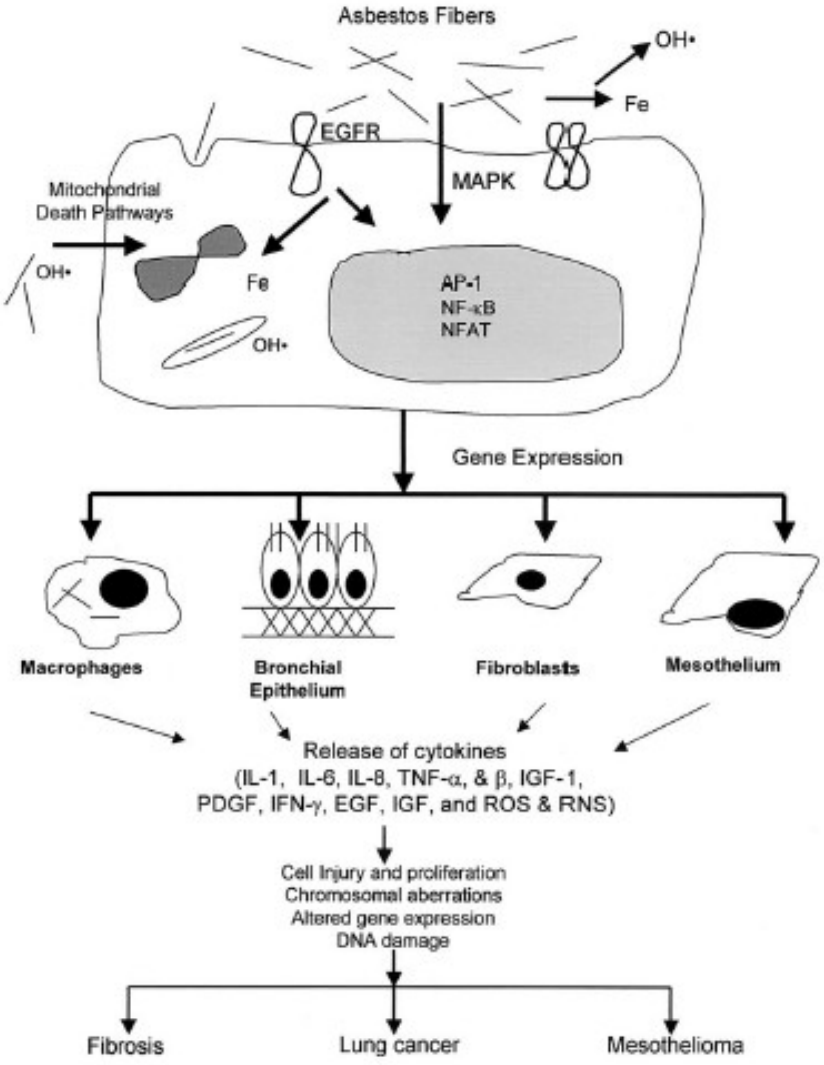

Figure 3: Hypothetical schema of the role of oxidants in asbestos-related cell signaling, injury and disease.[17]

As mentioned above, asbestos fibers induce hormone, growth factor and cytokine production and two such cytokines - tumor necrosis factor alpha (TNF-α) and interleukin - 1beta (IL-1β) - are linked to asbestos-related carcinogenesis. Asbestos induced cell necrosis causes the release of high-mobility group protein B1 (HMGB1), which is a critical regulator in the initiation of asbestos-mediated inflammation leading to the release of TNF-α and subsequent NF-κB signaling. It was shown that TNF-α induced NF-κB signaling is the critical link between carcinogenesis and inflammation in different cancer models including mesotheliomas. HMGB1, TNF-α and IL-1β are potential targets for inhibitors of asbestos-induced inflammation leading to mesothelioma. [5] Immunotherapy may even be a useful tool in treating MPM. [18] A high response rate has been achieved in

stage I MPM after Interferon-gamma (IFN-γ) treatment. [19] Other groups have shown that recombinant human IFN-γ inhibited the growth of human mesothelioma cell lines. This inhibition was enhanced by the addition of chemotherapeutic agents or cytokines like tumor necrosis factor. [20-23] Previous studies have shown that part of the IFN-γ effect on human mesothelioma cell lines is mediated directly through the activation of the JAK/STAT1 signaling pathway [24] and this pathway was found to be deregulated. [25, 26]

1.5 The JAK/STAT signaling pathway

Janus kinase (JAK) activation induces several biological responses like cell proliferation, differentiation, cell migration and apoptosis. STATs are a highly conserved family of latent transcription factors that are activated differentially by various extracellular ligands including growth factors, cytokines and hormones. [27]

Cytokines are recognized by cell surface receptors which oligomerize after ligand binding. This induces the recruitment of members of the JAK family (JAK1-3 and Tyk2). Members of the JAK family cross-phosphorylate each other and even phosphorylate the cytoplasmic domains of the receptors on tyrosine residues. This is necessary for the provision of STATs. They get phosphorylated as well and dimerize before they enter the nucleus and activate transcription by binding specific DNA sequences. Seven different STAT proteins (STAT1-4, STAT5a, STAT5b and STAT6) are known. They have a conserved tyrosine residue near the C-terminus. This residue is phosphorylated by JAKs. The dimerization of STATs through the interaction with SH2 domains is enabled by the phosphotyrosines. [27, 28]

Three protein families act as inhibitors and regulators of cytokine signaling:

- SHP: Src homology 2 domain containing phosphatases
- PIAS: protein inhibitors of activated STATs
- SOCS: suppressor of cytokine signaling

Activated JAKs or the receptors can be dephosphorylated by constitutively expressed SHP-1. SHP dephosphorylate many proteins and are therefore not a selective inhibitor of phosphorylated STATs. PIAS proteins sumoylate STATs, which leads to an inhibition of the transcriptional activation. Like SHPs, PIAS proteins are constitutively expressed and do not only target STATs. Therefore their physiological function differs from that of SOCS

proteins which are induced in response to cytokine signaling and STAT activation and therefore represent a classical negative feedback loop (see **Figure 4**). [29-32]

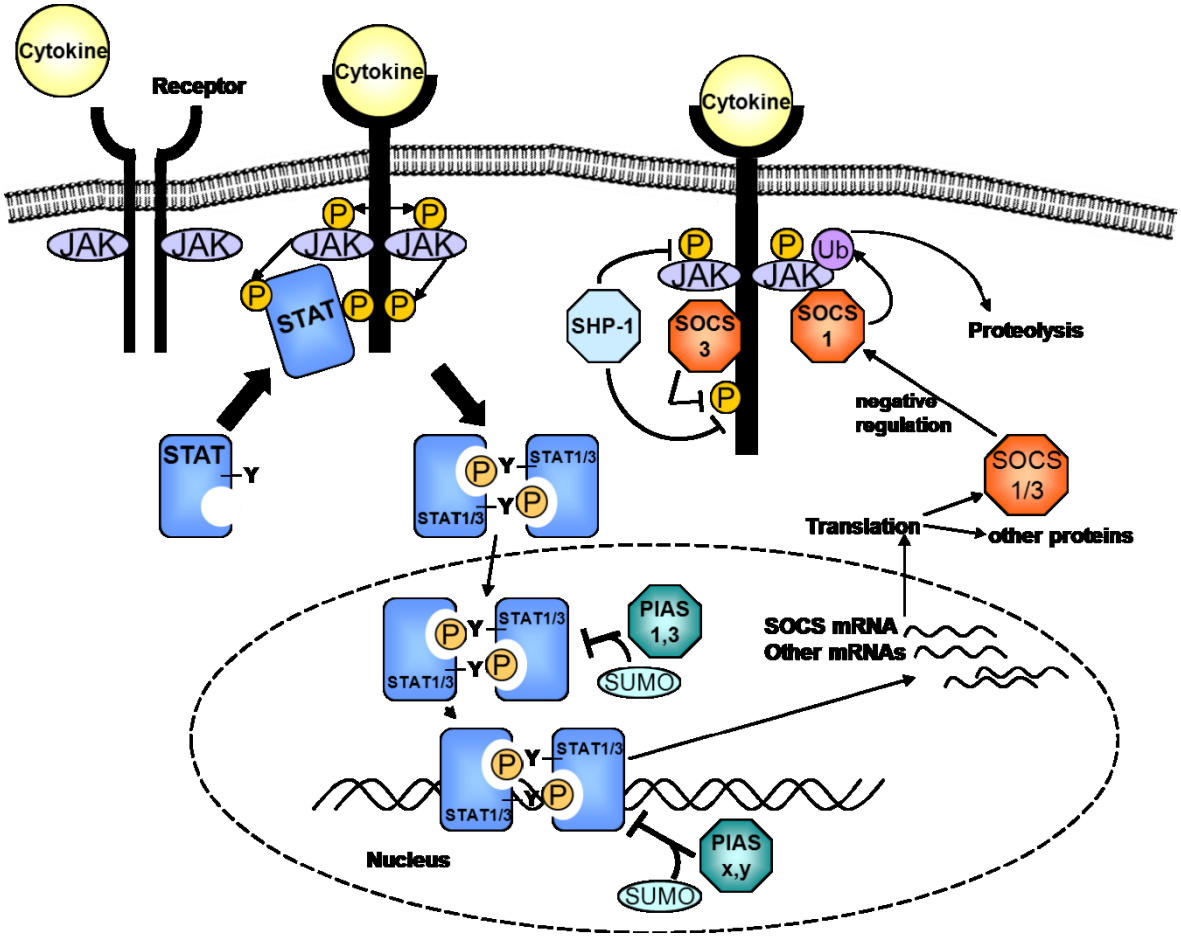

Figure 4: The JAK/STAT signaling pathway and its regulation. SOCS represent a classical negative feedback-loop, PIAS proteins sumoylate STATs which leads to an inhibition of the transcriptional activation. [33]

STATs bind to specific DNA loci and start transcription of their respective SOCS which then block STAT binding to JAKs by binding to phosphotyrosine residues in cytokine receptors or JAKs. [34-36] SOCS proteins suppress cytokine signaling in three different ways:

- by binding to JAKs
- by competing with STATs for binding sites on the receptors
- by targeting proteins for proteasomal degradation [30, 37]

It was reported previously that STAT1 is upregulated whereas STAT3 is downregulated in this particular cancer. Furthermore it seems that the negative feedback loop for STAT1 is

not functioning: PIAS1 was found to be downregulated and the expression of SOCS1 was totally missing. [25, 26] Furthermore a statistically significant inverse correlation between phosphorylated STAT1 and microRNA-30d* (= hsa-miR-30d-3p) was detected leading to the conclusion that this microRNA is a potential regulator of the upregulated STAT1. [26]

1.6 Mechanism of RNA interference

RNA interference (RNAi) – also known as post-transcriptional gene silencing – is a biological mechanism, which regulates the expression of protein-coding genes. The RNAi pathway was discovered in 1998 when Andrew Fire and Craig Mello initiated a potent sequence-specific degradation of cytoplasmic messengerRNAs (mRNA) containing the same sequence as the double-stranded RNA (dsRNA) trigger, by injecting dsRNA into the nematode *Caenorhabditis elegans*. [38, 39]

The first applications used long dsRNA, but this was not effective in most mammalian cells since it induced the antiviral interferon response and this usually leads to cell death. [40] Investigating the mechanism of RNAi in different organisms revealed the conservation of a cellular machinery that cleaves long dsRNA into duplexes of 21-28 nucleotide small interfering RNA (siRNA) molecules, which guide the sequence-specific degradation of mRNAs. [41] By elucidating siRNA structure, it was discovered that siRNAs can reduce gene expression in mammalian cells without triggering the interferon response. [42]

The RNAi pathway (see **Figure 5**) is based on two steps: first, the dsRNA is processed into a siRNA by the RNase III enzyme Dicer. In the second step, siRNAs are integrated into the effector complex, the RNA induced silencing complex (RISC). The siRNA is unwound during RISC assembly and the siRNA subsequently guide the RISCs to the complementary RNA molecules, where the single-stranded RNA hybridizes with mRNA targets. Gene silencing is a result of nucleolytic degradation of the targeted mRNA. [43-45]

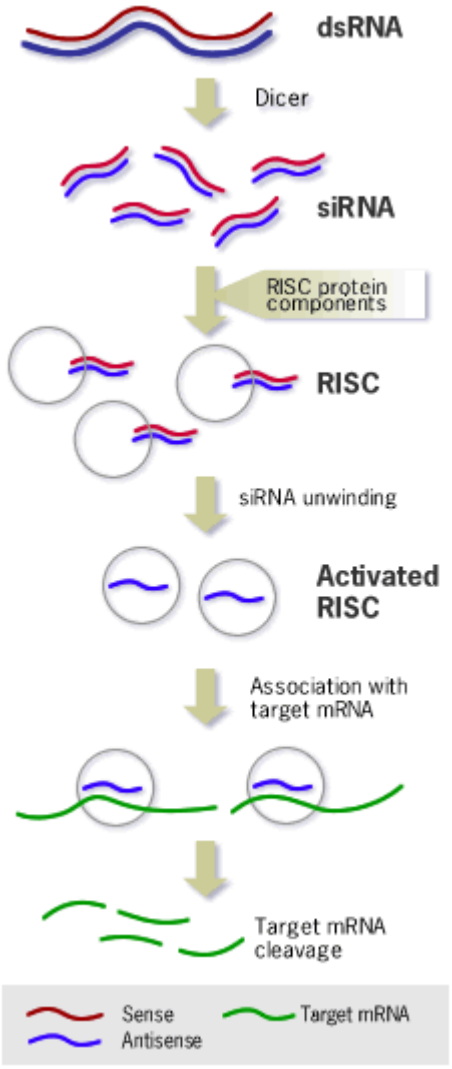

Figure 5: Mechanism of RNA interference. From: http://www.integratedhealthcare.eu/1/en/rna_interference/1498/

1.6.1 siRNA

SiRNAs can be synthetically produced to study gene function through the mechanism of RNA interference. Therefore, cells are transfected *in vitro* with siRNA and the target mRNA gets degraded. This gene knockdown results in reduced gene expression and gives hints of the physiologic function of the target gene. SiRNAs are naturally used by cells to regulate gene expression. Therefore they are non-toxic and effective and hold great therapeutic promise. [46]

1.6.2 microRNAs

SiRNAs resemble microRNAs (miRNA), one class of small, non-coding RNAs which regulate protein expression either by mRNA degradation or by preventing mRNA from being translated. They are supposed to act as oncogenes and tumor suppressors and regulate various developmental and physiological processes. Furthermore they represent a useful tool in the development of novel therapeutic approaches. [47]

1.6.2.1 Biosynthesis

MiRNAs are usually about 19-25 nucleotides in size and regulate the expression of target mRNAs, usually at their 3' untranslated region. [47-49] Mature miRNAs are processed via a two-step-pathway (see **Figure 6**).

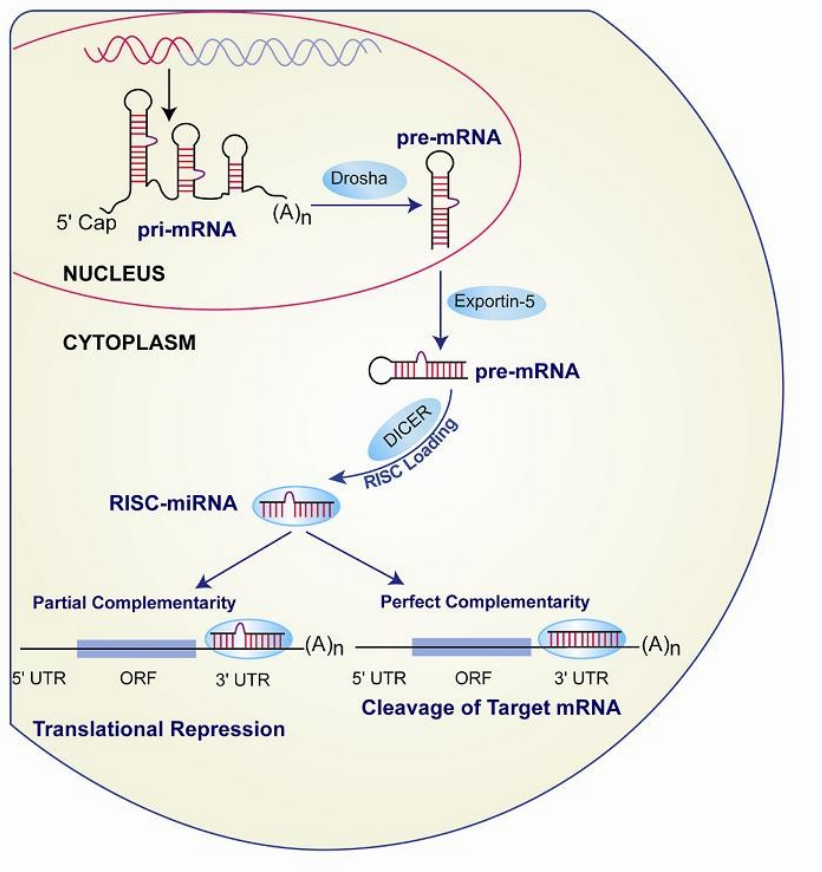

Figure 6: Schema of miRNA biogenesis. From http://www.genscript.com/siRNA_technology.html

They are first transcribed by RNA polymerase II into primary miRNAs (pri-miRNA). Pri-miRNAs have a length of about 60-70 nucleotides and contain hairpin-loop domains. This hairpin-loop region is cleaved in the nucleus by the RNase III enzyme Drosha in complex

with a double-strand RNA-binding protein called DiGeorge syndrome critical region 8 (DGCR8). [50-54] The resulting precursor-miRNA (pre-miRNA) is then exported from the nucleus to the cytoplasm by the Ran-GTP dependent transporter Exportin-5. Pre-miRNAs are cleaved again by the RNase III enzyme Dicer in partnership with another RNA-binding protein called transactivation-responsive RNA-binding protein. The mature-miRNA accumulates as a single-stranded species comprising one arm of each pre-miRNA and it is incorporated into the RISC that carries out the function of silencing gene expression. [51, 55, 56]

MiRNAs inhibit their target mRNAs by base-pairing to complementary sequences. An animal miRNA typically makes imperfect base pair contacts. [51] If there isn't complete complementation, the silencing is achieved by preventing translation. [57]

1.6.2.2 miRNAs and cancer

MiRNAs, which show an increased expression in tumors, are considered as oncogenes. They are called "oncomirs" and they promote tumor development by negatively inhibiting tumor suppressor genes and genes that control cell differentiation or apoptosis. If the expression of miRNAs is decreased in cancerous cells, they are considered to be tumor suppressor genes which act through an inhibition of oncogenes. [58]

MiRNAs with a well-known cancer association have been identified for a wide variety of human tumors. One example for an oncogene is the miR-17-92 cluster: members of this cluster are known to be upregulated in colorectal and lung cancer as well as lymphomas. The expression of this cluster was found to be significantly upregulated in tumor tissues compared to normal tissues, especially in the most aggressive forms of tumors. [58, 59] This cluster is even known as "Oncomir-1" since the miRNAs included are thought to promote cellular events including, for example, increased proliferation or decreased apoptosis. [60] An example for a tumor suppressor is let-7: it acts by regulating cell-proliferation pathways and by inhibiting the RAS oncogene. The expression of let-7 was found to be decreased in human lung cancer. [61-63]

The expression profiles of different miRNAs may even help to distinguish between tumors, e.g. malignant mesothelioma and lung adenocarcinoma. Different groups found that the expression of the miR-200 family is decreased in malignant mesothelioma samples compared to lung cancers in different types of samples (FFPE or fresh frozen biopsy samples). [64, 65] A 3-microRNA ratio (combining the expression levels of iR-200c, miR-

192 and miR-193a-3p) was developed which enables the accurate identification of malignant pleural mesothelioma.[64]

Pass et al. aimed to identify miRNAs associated with survival: they were able to identify miR-29c* (or miR-29c-5p) to be significantly downregulated in tumors of patients with short survival. [66] Furthermore they identified the loss of miR-31 expression that can be correlated with the deletion of 9p22, which is frequently found in malignant mesothelioma. [67] MiR-126 was found to be downregulated in pleural mesothelioma patients compared to other asbestos-exposed or control individuals. [68] Increased expression levels of miR-625-3p discriminated between malignant mesothelioma patients and asbestos-exposed controls without malignant mesothelioma with an accuracy of 82%. [69]

These are only a few examples showing the functions of miRNAs and their roles as oncogenes, tumor suppressors, diagnostic markers or prognostic factors of outcome. Furthermore, it has been shown recently that miRNA inhibitors can be used for disease treatment. MiR-122 was found to be associated with hepatitis C virus (HCV) infection: the stability of HCV is dependent on the interaction between HVC genome and miR-122, which is expressed in the liver. A locked nucleic acid–modified DNA phosphorothioate antisense oligonucleotide was generated, that sequesters mature miR-122 and therefore inhibits its function. A clinical study (phase 2a) was performed and patients with chronic HCV genotype 1 infection showed prolonged dose-dependent reductions of HCV RNA levels when using the miR-122 inhibitor. [70] An early-stage clinical trial is currently performed with a miR-34a replacement therapy for the treatment of liver cancer and cancers with liver involvement. [71]

1.6.2.3 Inhibition of miRNAs

The inhibition of miRNAs by e.g. locked nucleic acid can also be used to investigate the function of a miRNA in a certain tumor or to prove online target prediction.

Locked nucleic acid (LNA™) nucleosides are a class of nucleic acid analogues in which the ribose ring is locked by a methylene bridge (see **Figure 7**). They contain the common nucleobases that appear in DNA or RNA and are able to form base pairs according to standard Watson-Crick base-pairing rules.

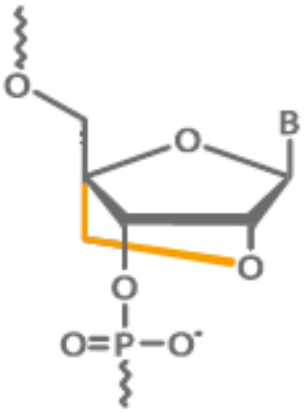

Figure 7: The structure of LNA™

LNA™ oligonucleotides are defined as DNA or RNA nucleotides containing one or more LNA™ nucleosides. The physical properties are very similar to those of RNA and DNA and this is why conventional experimental protocols can be easily adjusted to their use. LNA™ is a powerful tool in many molecular biological applications e.g. the inhibition of miRNA expression.

The high affinity of LNA™ oligonucleotides to complementary nucleic acids means that LNA™:RNA duplexes are much more stable than those formed between DNA and RNA. Therefore they are extremely potent antisense inhibitors and can be easily transfected by using standard techniques (for more information see http://www.exiqon.com/lna-technology). [72]

1.7 Aim of the study

Since deregulation of STAT1 signaling is associated with development of cancer and the fact that STAT1 is highly expressed in MPM, one aim of the study was to investigate whether STAT1 signaling contributes to MPM pathogenesis. The oncogenic potential of STAT1 was investigated as well as the expression of STAT1 inhibitors and the impact of IFN-γ, which has been shown to have an antiproliferative effect in MPM. Six mesothelioma cell lines have therefore been stimulated with IFN-γ and protein expression levels were assessed by Western Blot. Furthermore the impact of STAT1 expression on apoptosis – and cell cycle related genes was investigated. STAT1 expression was knocked-down by using siRNA and gene expression was detected by real-time PCR (Human JAK/STAT signaling pathway PCR Array).

As mentioned above, not only asbestos but even genetic predisposition contributes to the development of MPM. Germline *BAP1* mutations gene have been linked to high incidence of malignant mesothelioma in U.S. families and BAP1 seems to play a role in many different tumors. By performing an immunohistochemical staining on 123 tumor tissue samples, the questions if asbestos exposure has an influence on BAP1 expression and if BAP1 expression could be used as a prognostic factor of outcome were aimed to be answered.

Based on the promising results of previous studies the big aim of this study was to quantify further miRNAs in malignant pleural mesothelioma, which are thought to be involved in the JAK/STAT signaling pathway and which may be responsible for the deregulation of this pathway, especially the missing expression of the negative feedback loop.

Therefore a miRNA profiling has been performed to identify extremely up- or downregulated miRNAs. Those miRNAs that could have been linked with the JAK/STAT signaling pathway via online target prediction were quantified in 52 tumor tissue samples. The same miRNAs were additionally quantified in 6 mesothelioma cell lines. Protein expression levels were assessed by immunohistochemistry (for tumor tissue samples) and Western Blot (for cell lines). Messenger RNA expression levels for STAT1, STAT3, SOCS1 and SOSC3 were detected in mesothelioma cell lines and the corresponding upregulated miRNAs were inhibited to answer the questions:

- Do the miRNAs investigated by now really target STATs, pSTATs and SOCS?
- Are SOCS1 and SOCS3 expressed when the corresponding miRNAs are downregulated?
- Can the STAT1/3 signaling cascade be restored to a physiological level by SOCS expression?

2. MATERIALS AND METHODS

2.1 Tissue fixation and histological staining

A total of 52 human malignant epithelioid mesothelioma samples were used for the investigation of the STAT signaling pathway. The patients gave informed consent and the study was approved by the local Ethics Committee of the Medical University of Graz (No. 24-135). All samples were routinely fixed in 4% neutral-buffered formalin, paraffin-embedded and afterwards dehydrated according to standard protocols. Four µm thick sections of the FFPE tissues were deparaffinized with xylol and dehydrated with graded ethanols before Hematoxylin-Eosin (H&E) staining was performed. The tissue fixation and the histological staining were carried out by collaborators of the laboratory of histology of the Institute of Pathology, Medical University of Graz. The stained reference sections were histologically verified by Prof. Dr. Helmut H. Popper and tumor areas with more than 85% tumor cells were indicated on the slide. These slides were used to locate the tumor on the tissue block for further RNA extraction and tissue microarray construction.

2.2 RNAs and microRNAs: extraction and quantification

2.2.1 RNA and miRNA extraction: FFPE tissue and tumor cells

RNA and miRNAs were extracted out of 52 FFPE tumor tissue samples as well as 6 mesothelioma cell lines and one liver cancer cell line. Therefore two different commercially available kits have been used: the RNeasy FFPE Kit (Qiagen, Hilden, Germany) and the miRNeasy Mini Kit (Qiagen).

The protocol for the RNeasy FFPE Kit has been optimized in a pilot study [73] and the main modifications were thickness of the sections, deparaffinization as well as Proteinase K digestion, which was elongated.

RNeasy FFPE Kit – optimized protocol:

1. Cut sections 20µm thick, using a microtome.
2. Place the sections in a 1,5ml tube.
3. Add 1ml xylene and vortex 10 seconds.
4. Incubate for 3min at 50°C (water bath).
5. Centrifuge at full speed (20817xg) for 2min at 20-25°C.
6. Remove the supernatant by pipetting.

7. Repeat steps 3-6.
8. Add 1ml of 100% ethanol to the pellet and mix by vortexing 10sec.
9. Centrifuge at full speed for 3min at 20-25°C.
10. Remove the supernatant by pipetting (carefully remove any residual ethanol).
11. Repeat steps 8-10.
12. Open the tube and incubate at room temperature for 10min or until all residual ethanol has evaporated.
13. Resuspend the pellet in 240µl Buffer PKD, add 10 µl Proteinase K and mix by vortexing 10sec.
14. Incubate at 55°C for 3h, then at 80°C for 15min.
15. Add 500µl Buffer RBC to adjust binding conditions.
16. Mix the lysate thoroughly and transfer it to a gDNA Eliminator spin column placed in a 2ml collection tube.
17. Centrifuge for 1min at 8000g (10000rpm).
18. Discard the column, save the flow-through and split the flow through (2x 350µl).
19. Add 875µl of 100% ethanol to the flow-through and mix well by pipetting.
20. Transfer 700µl of the sample to an RNeasy MinElute spin column placed in a 2ml collection tube.
21. Centrifuge for 1min at 8000g (10000rpm) and discard the flow through.
22. Repeat step 20 until the entire sample has passed through the column.
23. Add 500µl Buffer RPE to the RNeasy MinElute spin column.
24. Centrifuge for 1min at 8000g (10000rpm) and discard the flow through.
25. Add 500µl Buffer RPE to the RNeasy MinElute spin column.
26. Centrifuge for 2min at 8000g (10000rpm) and discard the flow through.
27. Place the RNeasy MinElute spin column in a new 2ml collection tube, open the lid of the spin column and centrifuge at full speed for 5min.
28. Place the RNeasy MinElute spin column in anew 1.5ml collection tube.
29. Add 20µl RNase free water directly to the spin column membrane. Close the lid and wait 5min.
30. Centrifuge for 1min at full speed to elute the RNA.
31. Place the eluate on the spin column again and centrifuge again for 1min at full speed.

miRNeasy Mini Kit – extraction protocol with on-column DNase digestion

1. Centrifuge cell lysate (300xg, 5min) and remove supernatant.
2. Resuspend the pellet in PBS, centrifuge again (300xg, 5min) and remove supernatant.
3. Add 700µl QIAzol Lysis Reagent to the sample and homogenize by vortexing for 1min (if $<3*10^6$ cells).
4. Incubate the homogenate at room temperature for 5min.
5. Add 140µl chloroform and cap the tube securely. Shake vigorously for 15s.
6. Incubate at room temperature for 2-3min.
7. Centrifuge for 15min at 12000xg at 4°C.
8. Transfer the upper aqueous phase to a new collection tube. Avoid transferring any interphase. Add 1.5 volumes (420µl) of 100% ethanol, and mix thoroughly by pipetting.
9. Pipet up to 700µl sample, including any precipitate, into an RNeasy Mini column in a 2ml collection tube. Close the lid and centrifuge at 8000xg (10000rpm) for 1min at room temperature. Discard the flow-through.
10. Repeat step 9 using the remainder of the sample.
11. Pipet 350µl Buffer RWT into the RNeasy Mini Spin Column and centrifuge for 1min at 8000xg to wash. Discard the flow-through.
12. Add 10µl DNase I stock solution to 70µl Buffer RDD. Mix gently by inverting the tube. DO NOT VORTEX!
13. Pipet the DNase I incubation mix (80µl) directly onto the RNeasy Mini Spin Column membrane and place on the bench top at 20-30°C for 15min.
14. Pipet 350µl Buffer RWT into the RNeasy Mini Spin Column and centrifuge for 1min at 8000xg. Discard the flow-through.
15. Pipet 500µl Buffer RPE onto the RNeasy Mini column. Close the lid, and centrifuge for 1min at 8000xg. Discard the flow-through.
16. Add 500µl Buffer RPE to the RNeasy Mini column. Close the lid, and centrifuge for 2min at 8000xg.
17. Place the RNeasy Mini column into a new 2ml collection tube (not supplied). Centrifuge at full speed for 1min to further dry the membrane.
18. Transfer the RNeasy Mini column to a new 1.5ml collection tube. Pipet 40µl RNase-free water directly onto the RNeasy Mini column membrane. Close the lid, wait 2min and centrifuge for 1min at 8000xg to elute. Collect the flow-through.

19. Repeat step 18 with eluate from step 18. Reuse the collection tube from step 18.

If this protocol has been performed with samples expected to contain less than 1µg total RNA, the buffer RWT has been prepared by adding 45ml of isopropanol to the concentrate (instead of 30ml ethanol as usually recommended). In this case 500µl Buffer RWT have been used to wash the column after the DNase digestion (see step 14). The flow-through was kept and reapplied to the RNeasy Mini Spin Column. After a centrifugation step, the protocol has been continued with step 15.
The RNase-Free DNase Set (Qiagen) was used for the recommended on column DNase digestion. Therefore 550µl RNase free water have been added to the lyophilized DNase to generate the stock solution.

2.2.2 Measurement of RNA concentration and purity

RNA concentration was measured by NanoDrop 1000 UV/Vis spectrophotometer (PEQLAB Biotechnologie GmbH, Erlangen, Germany). The ratios of A260/280 and A260/230 were used to indicate the purity of RNA samples. Nucleic acids and proteins have absorbance maxima at 260nm and 280 nm, respectively. A ratio of ~ 2.0 is generally accepted as pure for RNA and abnormal ratios usually indicate that the sample is contaminated by protein or a reagent such as phenol. Absorbance at 230nm is even an indicator for contamination and therefore even the ratio A260/230 is calculated and the expected values should be in the range between 2.0 and 2.2 (see www.nanodrop.com).

2.2.3 miRNA profiling

Due to the promising results of a pilot study a miRNA profiling has been performed to identify extremely up- or downregulated miRNAs in malignant mesothelioma. Therefore the TaqMan® Array Human MicroRNA Cards (Life Technologies, Carlsbad, USA) have been used with pooled RNA, extracted from 52 FFPE tumor tissue samples to detect the expression levels of 754 miRNAs. To identify extremely up-or downregulated miRNAs, the DeltaCq method was used with RNU44 as reference gene. Those miRNAs that could be linked to the STAT signaling pathway by using online target prediction tools were then quantified in every single sample as described below.
cDNA was generated using TaqMan® MicroRNA Reverse Transcription Kit (Life Technologies) and Megaplex™ RT Primers (Life Technologies) according to the

manufacturers' instructions. The reaction was performed on 900ng of total RNA (pooled RNA of about 12 samples). Megaplex^{TM}RT Primers are a mixture of miRNA specific stem-loop primers, which are specific for mature miRNAs.

Table 1: Components of the Mastermix for the Reverse Transcription (miRNA profiling)

component	volume in µl /reaction
Megaplex RT Primers (10X)	0.8
100mM dNTPs (with dTTP)	0.5
MultiScribe Reverse Transcriptase (50U/µl)	1.5
10X RT Buffer	0.8
$MgCl_2$(25mM)	0.9
RNase Inhibitor (20U/µl)	0.1
Nuclease Free Water	0.2
Total	**4.5**

4.5µl of Reverse Transcription Mix as well as 3µl RNA (300ng/µl) or water (= negative control) were mixed, incubated for 5min on ice and shortly centrifuged. Reactions were incubated for 40 cycles of 2min at 16°C, 1min at 42°C and 1sec at 50°C followed by 5min at 85°C and cooling down to 4°C.

6µl of the generated cDNA were then mixed with 450µl TaqMan® Universal PCR Master Mix, No AmpErase® UNG, 2X (Life Technologies) and 440µl nuclease-free water and loaded on the microRNA cards. Negative controls as well as endogenous controls, used for normalizing expression levels, are included on the cards. The real-time PCR was performed on the 7900HT Fast Real-time PCR system (Life Technologies). The SDS setup file was imported from the information CD, delivered with the TaqMan MicroRNA Array.

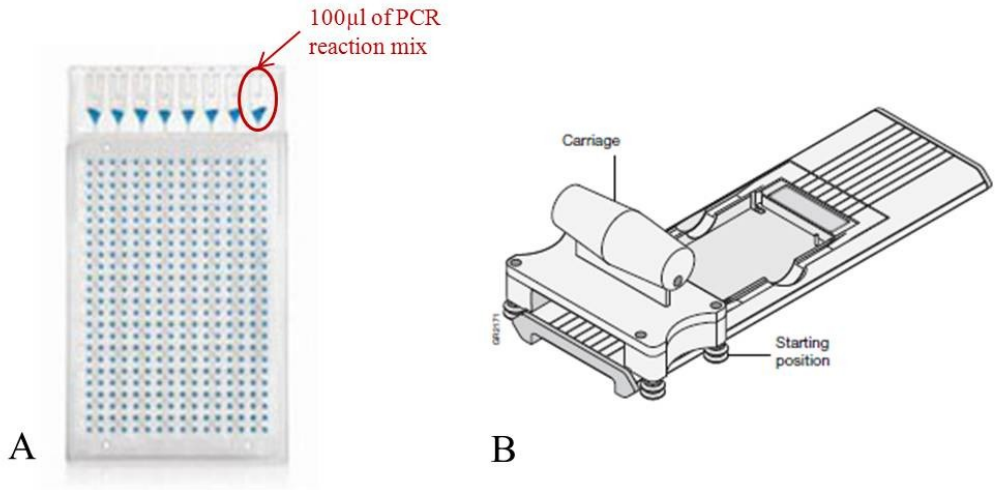

Figure 8: (A) TaqMan MicroRNA Array Card. 100µl of qPCR reaction mix are dispensed into each port. Cards are centrifuged twice before they are closed with a sealer (B).

2.2.4 miRNA quantification

2.2.4.1 In silico *target prediction*

One of the biggest challenges facing microRNA research is the identification of genes regulated by a specific microRNA. More and more tools are available to perform a target prediction. It is possible to search for the mRNA of interest or a special microRNA, which has for example a well-known cancer association. One big problem is that different databases provide different miRNA-mRNA interactions. And another problem is the possibility that microRNAs are not present in databases if you repeat the search weeks later. Therefore several different databases have been used; the results were compared and only accepted when at least two databases provided the same miRNA-mRNA interactions.
In order to identify miRNAs that are supposed to target components of the STAT signaling pathway, the following online target prediction tools have been used:

- TargetScanHuman (http://www.targetscan.org/)
- PicTar (http://pictar.mdc-berlin.de/)
- miRBase (http://www.mirbase.org/)
- microRNA.org (http://www.microrna.org/microrna/home.do)

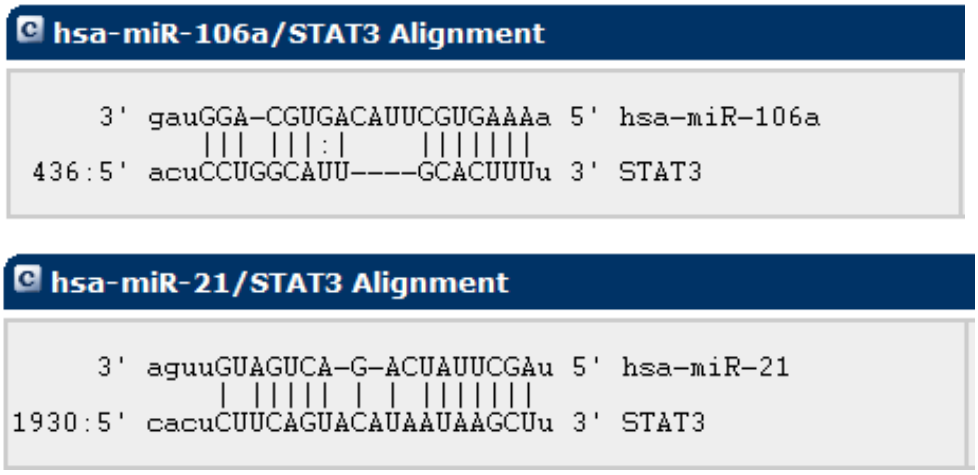

Figure 9: Alignment of miR-106a and STAT3 as well as miR-21 and STAT3 (from microRNA.org)

Figure 9 shows the imperfect base-pairing between the miRNAs, that have been successfully quantified and their target mRNA. Diana Lab (http://diana.cslab.ece.ntua.gr/pathways/) is a very helpful tool, when investigating the regulation of a signaling pathway. It is again possible to predict a miRNA-mRNA interaction but you do not only get the target gene name, you even get a list of pathways, where the target genes are involved.

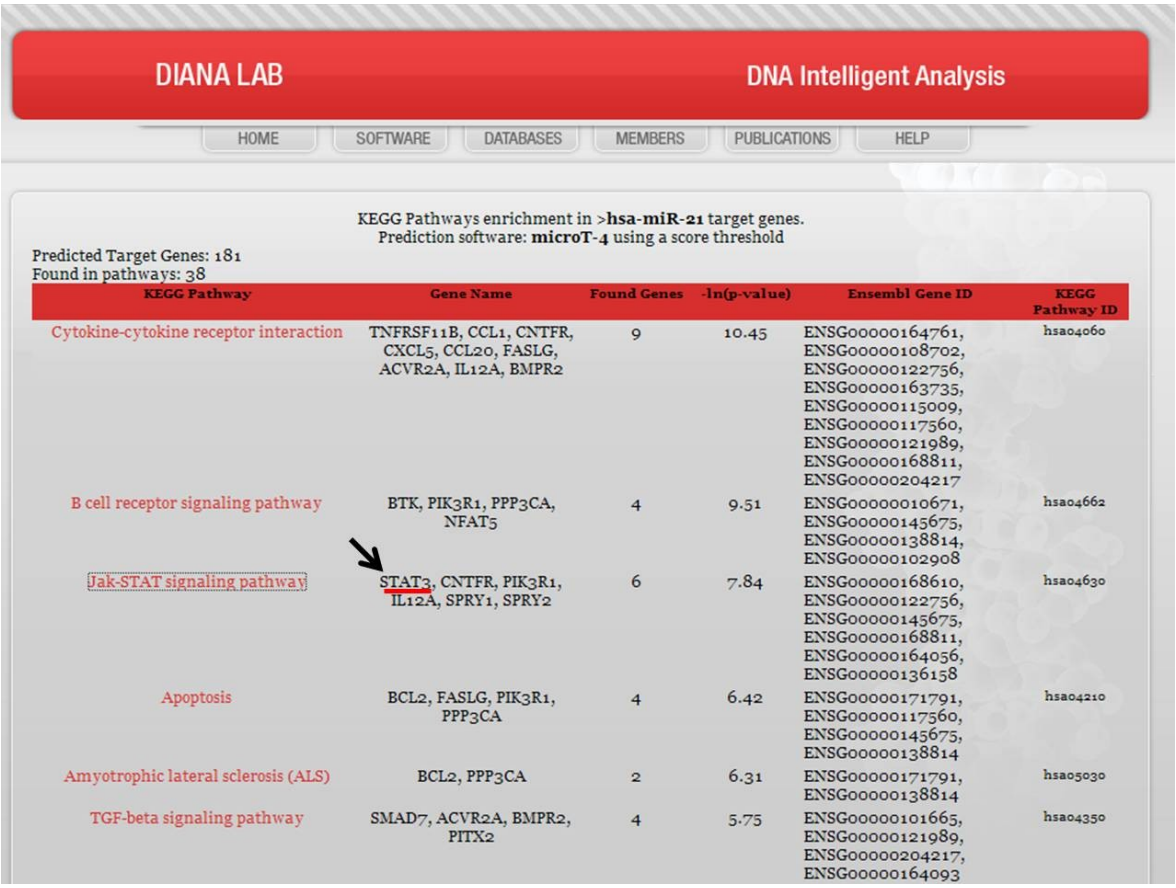

KEGG Pathway	Gene Name	Found Genes	-ln(p-value)	Ensembl Gene ID	KEGG Pathway ID
Cytokine-cytokine receptor interaction	TNFRSF11B, CCL1, CNTFR, CXCL5, CCL20, FASLG, ACVR2A, IL12A, BMPR2	9	10.45	ENSG00000164761, ENSG00000108702, ENSG00000122756, ENSG00000163735, ENSG00000115009, ENSG00000117560, ENSG00000121989, ENSG00000168811, ENSG00000204217	hsa04060
B cell receptor signaling pathway	BTK, PIK3R1, PPP3CA, NFAT5	4	9.51	ENSG00000010671, ENSG00000145675, ENSG00000138814, ENSG00000102908	hsa04662
Jak-STAT signaling pathway	STAT3, CNTFR, PIK3R1, IL12A, SPRY1, SPRY2	6	7.84	ENSG00000168610, ENSG00000122756, ENSG00000145675, ENSG00000168811, ENSG00000164056, ENSG00000136158	hsa04630
Apoptosis	BCL2, FASLG, PIK3R1, PPP3CA	4	6.42	ENSG00000171791, ENSG00000117560, ENSG00000145675, ENSG00000138814	hsa04210
Amyotrophic lateral sclerosis (ALS)	BCL2, PPP3CA	2	6.31	ENSG00000171791, ENSG00000138814	hsa05030
TGF-beta signaling pathway	SMAD7, ACVR2A, BMPR2, PITX2	4	5.75	ENSG00000101665, ENSG00000121989, ENSG00000204217, ENSG00000164093	hsa04350

Figure 10: Using Diana Lab for online target prediction (predicted target genes and corresponding signaling pathways.)With these prediction results you get the information that hsa-miR-21 plays a role in the JAK/STAT signaling pathway and that miR-21 most probably regulates STAT3, amongst others.

The miRNAs that have been selected via online target prediction tools are listed in table 2. They have been quantified in the 52 malignant mesothelioma tissue samples as well as in mesothelioma cell lines. The reference gene RNU6B was used to normalize the miRNA expression levels.

Table 2: List of miRNAs and their predicted targets in the STAT signaling pathway as well as TaqMan® MicroRNA Assay IDs (Life Technologies). # These miRNAs have only been quantified in 35 malignant mesothelioma samples of the pilot study; the other miRNAs have been quantified in all 52 tissue samples.

miRNA	predicted target	assay ID
hsa-miR-17	STAT3	002308
hsa-miR-19a#	SOCS1	000395
hsa-miR-19b	SOCS1, SOCS3	000396
hsa-miR-21	STAT3	000397
hsa-miR-30b	SOCS1, SOCS3	000602
hsa-miR-30c	SOCS1, SOCS3	000419
hsa-miR-30d-3p#	STAT1	002305
hsa-miR-106a#	STAT3	002169
hsa-miR-155#	SOCS1	002623
hsa-miR-222	SOCS3	002276
hsa-miR-223	STAT1	000526

2.2.4.2 Reverse Transcription and Assay validation

cDNA was generated using TaqMan® MicroRNA Reverse Transcription Kit (Life Technologies) according to the manufacturers' instructions. Stem loop primers are used in this kit, which are known for high efficiency and high specificity. High specificity means that there is discrimination among microRNAs that differ by only one nucleotide and the primers are specific for mature miRNAs. The reaction was performed on 10ng of total RNA in 96-well plates. To rule out any contamination, a "template-free" (RNAse free water instead of RNA) and a "RT-free" (no Reverse Transcriptase in the reaction) control were included.

Table 3: Components of the Mastermix for the Reverse Transcription (single miRNA Assays)

component	volume in µl /reaction
100mM dNTPs (with dTTP)	0.15
MultiScribeTM Reverse Transcriptase, 50U/µl	1.00
10X RT Buffer	1.50
RNase Inhibitor	0.19
Nuclease Free Water	4.16
Total	**7.00**

7µl Mastermix (see **Table3**) were used for each reaction, 5µl RNA Sample were added as well as 3µl of 5X TaqMan® MicroRNA RT Primer (Life Technologies).
The Reverse Transcription was performed using the following conditions: 16°C for 30min, 42°C for 30min, 85°C for 5min and cooling down to 4°C.

To make sure that the efficiency of the TaqMan® MicroRNA Assays (Life Technologies) is satisfying, an assay validation was performed for each miRNA and reference gene. Therefore, total RNA of 8 selected samples was mixed in same quantity and reverse transcribed. The generated cDNA was used for a dilution series with 6 dilutions (1:5 dilutions beginning with 0.1ng/µl). cDNA was even generated for each of the 8 selected samples and diluted to a concentration of 0.004ng/µl. QPCR was run in triplicates in FAST plates (MicroAmp® Fast Optical 96-well reaction plate with barcode, Life Technologies). After the qPCR a standard curve was generated with the SDS software 2.3. The standard curve plot displays a graph of threshold cycle versus starting copy number, as well as the calculated slope, the Y-intercept and the correlation coefficient of the standard curve. The slope should be between -3.2 and -3.6. Under ideal conditions, cDNA should be duplicated in every cycle. This is an efficiency of 100%. To calculate the efficiency of each miRNA assay, you have to use the formula: Efficiency $E = 10^{-1/slope}$

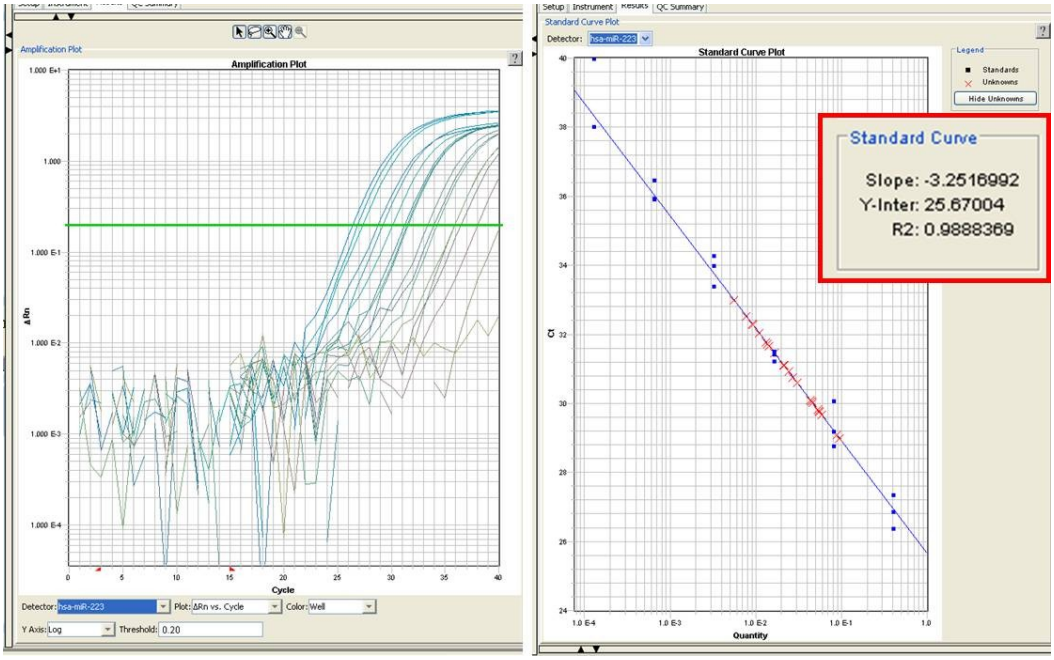

Figure 11: Amplification plot (left side) for miR-223 including the threshold (greenline) and standard plot (right side) with an ideal slope of -3.25 (assay validation)

2.2.4.3 Quantitative real-time PCR: TaqMan® MicroRNA Assays

The qPCR was performed in triplicates in 384-well plates (MicroAmp® Optical 384-well plate with barcode, Life Technologies). To avoid pipetting inaccuracy, a liquid handling workstation (Microlab Starlet, Hamilton Robotics, Reno, NV, USA) was used. Therefore a modified version relating to the volumes of cDNA and reagents had to be used: 5µl TaqMan® 2X universal Master Mix, No AmpErase UNG, 0.5µl TaqMan® MicroRNA Assay (20X) (both from Life Technologies), 0.5µl nuclease free water and 4µl cDNA in a concentration of 0.01478ng/µl. QPCR was performed using the 7900HT Fast real-time PCR System (Life Technologies). Reactions were incubated for 10min at 95°C, followed by 40 cycles of 15sec at 95°C and 1min at 60°C. The analysis of relative miRNA expression was performed using DeltaCq method with RNU6B as reference gene.

2.2.4.2 Quantification of miRNA expression

The Cq (quantification cycle) is the universal name for the fractional PCR cycle used for quantification. Cq levels are inversely proportional to the amount of target nucleic acid in the sample.

To normalize the microRNA expression level (Delta Cq), the average Cq-value for the reference gene of each patient was subtracted from the average Cq-value for the miRNA of each patient.

$$\Delta Cq = Cq_{miRNA} - Cq_{reference\ gene}$$

The values for the standard deviation (SD) have to be normalized (SD_{norm}) as well - "rg" means reference gene:

$$SD_{norm} = \sqrt{\frac{\left(SD_{miRNA}{}^{2} + SD_{rg}{}^{2} \right)}{3}}$$

To show the results in a bar-diagram, the $2^{-\Delta Cq}$ values are calculated – even for the standard deviation ($SD_{2^{\wedge}-\Delta Cq}$):

$$SD_{2^{-\Delta Cq}} = \ln(2) * 2^{-\Delta Cq} + SD_{norm}$$

2.2.5 mRNA quantification

RNA extracted out of six mesothelioma cell lines and one liver cancer cell line (with the RNeasy Mini Kit) has been used to analyze the expression of STAT1, STAT3, SOCS1, SOCS3 and the housekeeping gene GAPDH.

2.2.5.1 Reverse Transcription

cDNA was synthesized using RT² First Strand Kit (Qiagen) in a 96-well plates. The most accurate way to detect DNA contamination is the use of a "no-reverse-transcription" (NRT) control, in which reverse transcriptase is replaced by water in the cDNA synthesis reaction. If the difference in Cq values between the NRT control and a complete reaction for the same gene of interest is greater than 6, then any DNA contamination will not affect the reliability of the relative gene expression analysis. This is essential for optimal qPCR results.

cDNA synthesis using the RT^2 First Strand Kit:

1. Prepare the genomic DNA elimination mix for each RNA sample. Mix gently by pipetting up and down and then centrifuge briefly.

Table 4: Components of the genomic DNA elimination mix

component	amount /reaction
RNA	1000ng
Buffer GE	2.00µl
RNase-free water	variable
Total	**10.00µl**

2. Incubate the genomic DNA elimination mix for 5min at 42°C, then place immediately on ice for at least 1min.
3. Prepare the reverse-transcription mix.

Table 5: Components of the reverse-transcription mix

component	volume for 1 reaction	volume for 1 „NRT" reaction
5X Buffer BC3	4µl	4µl
Control P2	1µl	1µl
RE3 Reverse Transcriptase Mix	2µl	-
RNase-free water	3µl	5µl
Total	**10µl**	**10µl**

4. Add 10µl reverse-transcription mix to each tube containing genomic DNA elimination mix. Mix gently by pipetting up and down.
5. Incubate at 42°C for exactly 15min. Then immediately stop the reaction by incubating at 95°C for 5min.
6. Add 91µl RNase-free water to each reaction. Mix by pipetting up and down several times.
7. Generate a 1:10 dilution of each sample and place the reactions on ice and proceed with the real-time PCR protocol, or transfer them to a -20°C freezer for storage.

2.2.5.2 Quantitative real-time PCR: RT² qPCR Primer Assays

Real-time PCR using RT² qPCR Primer Assays and RT² SYBR Green Mastermixes (both from Qiagen). QPCR was performed in triplicates.

1. Prepare the PCR components mix in an Eppendorf tube.

Table 6: Components of the qPCR reaction

component	volume
RT² SYBR Green Mastermix	12.5µl
RT² qPCR Primer Assay (10µM stock)	1µl
RNase-free water	10.5µl
Total	**24µl**

2. Add 1µl of the 1:10 diluted cDNA to each reaction.
3. Seal the plate with an Optical Adhesive Film.
4. Briefly centrifuge the reaction plate and place it into the real-time cycler.

To control for DNA contamination introduced during reaction setup, a no-template-control (replacing template with water) has been prepared. To control for genomic DNA contamination, the "NRT-samples" from the cDNA synthesis reaction have been used for each gene of interest and each housekeeping gene.

QPCR was performed in Fast plates (Life Technologies) using the 7900HT Fast real-time PCR System (Life Technologies). Reactions were incubated for 10min at 95°C, followed by 40 cycles of 15sec at 95°C and 1min at 60°C. A dissociation curve analysis (SDS 2.3, Dissociation Stage: 95°C for 15sec, 60°C for 15sec, 95°C for 15sec) was performed as well to verify PCR specificity. A single peak should appear in each reaction at temperatures greater than 80°C.

The analysis of relative mRNA expression was performed using DeltaCq method with GAPDH as reference gene.

2.2.5.3 Quantitative real-time PCR: RT² Profiler PCR Array

cDNA was synthesized using RT² First Strand Kit (Qiagen) in 96-well plates (see **2.2.5.1**). For each cell line, two RT² Profiler PCR Arrays (Human JAK/STAT Signaling Pathway PCR Array, PAHS-039YC-2, Qiagen) were used. Therefore, two samples have been reversed transcribed: one sample, where cells have been transfected with STAT1 siRNA, and one sample, where the cells have been transfected with a control siRNA (see **2.4.6**).

1. Prepare the PCR components mix in a 5ml tube or a loading reservoir.

Table 7: Components of the qPCR reaction

component	volume
2x RT² SYBR Green Mastermix	1350µl
cDNA synthesis reaction	102µl
RNase-free water	1248µl
Total	**2700µl**

2. Carefully remove the RT² Profiler PCR Array from its sealed bag.
3. Add 25µl PCR components mix to each well of the RT² Profiler PCR Array.
4. Carefully, tightly seal the RT² Profiler PCR Array with an Optical Adhesive Film.
5. Centrifuge for 1min at 1000xg at room temperature to remove bubbles and place the RT² Profiler PCR Array in the real time cycler to start the run.

Table 7: Plate layout for real-time PCR. Line H contains 5 housekeeping genes (H1-H5), one control for genomic DNA contamination (H6), three reverse transcription controls (H7-9) and three positive PCR controls (H10-12).

	1	2	3	4	5	6	7	8	9	10	11	12
A	A2M	AKT1	BCL2L1	CCND1	CDKN1A	CEBPB	CEBPD	CRK	CRP	CSF1R	CXCL9	EGFR
B	EPOR	F2	F2R	FAS	FCER2	FCGR1A	GATA3	GHR	GRB2	HMGA1	IFNAR1	IFNG
C	IFNGR1	IL10RA	IL20	IL2RA	IL2RG	IL4	IL4R	IL6ST	INSR	IRF1	IRF9	ISG15
D	JAK1	JAK2	JAK3	JUN	JUNB	LRG1	MCL1	MPL	MYC	NFKB1	NOS2	NR3C1
E	OAS1	OSM	PDGFRA	PIAS1	PIAS2	PRL	PRLR	PTPN1	PTPN11	PTPRC	SH2B1	SMAD1
F	SMAD2	SMAD3	SMAD4	SMAD5	SOCS1	SOCS2	SOCS3	SOCS4	SOCS5	SP1	SPI1	SRC
G	STAM	STAT1	STAT2	STAT3	STAT4	STAT5A	STAT5B	STAT6	STUB1	TYK2	USF1	YY1
H	ACTB	B2M	GAPDH	HPRT1	RPLP0	HGDC	RTC	RTC	RTC	PPC	PPC	PPC

Each plate of the RT^2Profiler PCR Array includes 5 housekeeping genes: beta-Actin (ACTB), Beta-2-microglobulin (B2M), Glyceraldehyd-3-phosphate-dehydrogenase (GAPDH), Hypoxanthine-phosphoribosyltransferase 1 (HPRT1) and Ribosomal protein, large, P0 (RPLP0).

The Cq value for the human genomic DNA control wells (HGDC) should be greater than 35. If this is the case, the level of genomic DNA contamination is too low to affect gene expression profiling results.

The average (AVG) Cq values for the reverse transcription control (RTC) and the positive PCR control (PPC) as well as the ΔCq value have been calculated:

$$\Delta Cq = AVG\ Cq^{RTC} - AVG\ Cq^{PPC}$$

If this value is less than 5, then no inhibition of the reverse transcription reaction is apparent.

The average Cq^{PPC} value should be 20 +/- 2 on each RT^2 Profiler PCR Array and should not vary by more than 2 cycles between RT^2 profiler PCR Arrays being compared. Larger values indicate the presence of PCR amplification inhibitors.

The ΔCq value for each pathway-focused gene in each plate was calculated using the Cq values for the gene of interest (GOI) and the housekeeping genes (HKG) used for normalization:

$$\Delta Cq = Cq^{GOI} - Cq^{AVG\ HKG}$$

Since the Cq values for the 5 housekeeping genes were nearly the same, the average Cq value for all housekeeping genes was calculated and used for normalization.

The results of two RT^2 Profiler PCR Arrays had to be compared. Therefore the ΔΔCq values for all genes have been calculated:

$$\Delta\Delta Cq = \Delta Cq\ (experimental\ samples) - \Delta Cq\ (control\ samples)$$

Experimental samples: cells treated with STAT1 siRNA

Control samples: cells treated with control siRNA

2.3 Proteins: extraction and quantification

2.3.1 Protein extraction

In order to determine via Western Blot whether IFNγ stimulation or the inhibition of a miRNA has an influence on protein expression, cells have to be lysed to extract the proteins. To avoid enzymatic protein degradation, protease inhibitors need to be included during the protein isolation process. Since phosphorylation of proteins means activation of those proteins in the STAT signaling pathway, even the phosphorylation status of e.g. STAT1 and STAT3 should be detected by Western Blot – therefore phosphatase inhibitors are used to avoid dephosphorylation during protein extraction and storage of protein lysates.

1. Prepare RIPA buffer + Protease and Phosphatase Inhibitors (for each ml of RIPA buffer, add 10µl Protease and 10µl Phosphatase Inhibitor: Calbiochem® Protease Inhibitor Cocktail Set 1, Calbiochem® Phosphatase Inhibitor Cocktail Set II, Merck KGaA, Darmstadt, Germany)
2. Wash cells twice with ice-cold PBS.
3. Add 400µl RIPA buffer per well (6-well plate) or 1000µl per flask (25cm²).
4. Incubate plate/flask for 10min on ice.
5. Scrape cells and transfer lysate to Eppendorf tube.
6. Incubate 15min on ice, vortex every 5 minutes.
7. Centrifuge 15min at 4°C and 20000xg.
8. Transfer supernatant to new Eppendorf tube.
9. Store at -20°C.

2.3.2 Protein quantification

Protein concentration was determined by Lowry Method (BioRad DC Protein Assay, Bio-Rad, Hercules, USA) to make sure that the same amount (usually 20µg) is used of each sample to be able to detect expression differences among different samples (e.g. IFNγ stimulated vs. unstimulated samples).

1. Dissolve 0.1g of BSA in 10ml Aqua dest. to generate a standard curve.
2. Use 500µl of this solution and mix them with 500µl Aqua dest. – this is the starting dilution.
3. Make a dilution series with 5 dilutions (1:2 dilutions starting with 5mg/ml).

4. Mix 5µl Aqua dest., 5µl BSA dilution (or sample of interest), 100µl reagent A' (=1ml reagent A + 20µl reagent S) and 800µl reagent B in disposable cuvettes. For the blank use 5µl water instead of sample or BSA dilution.
5. Vortex and incubate mixture at room temperature for 15min.
6. Measure the absorption of each sample at 750nm.
7. The absorptions of the BSA dilutions are used to generate a standard curve.
8. The automatically calculated regression line is then used to calculate the protein concentrations of the samples of interest.

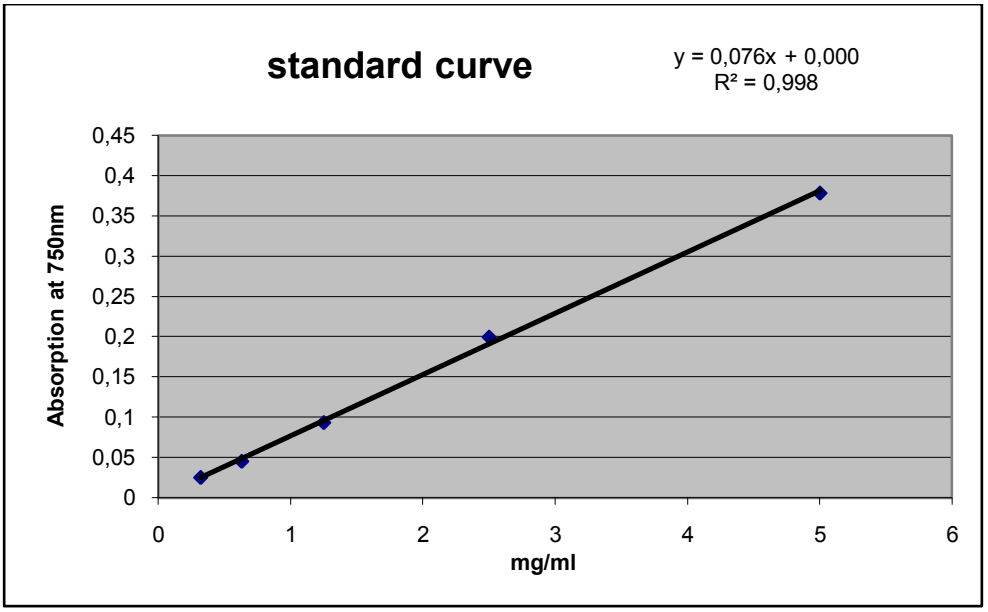

Figure 12: Standard curve generated with dilutions of BSA and calculated regression line. X-Axis: BSA concentrations in mg/ml, Y-Axis: Absorption at 750nm

The formula y=0.0761x + 0.0008 is used to calculate the concentration of the sample of interest, being y the absorption of the sample of interest.

2.3.2.1 Increasing the protein concentration

All protein samples with a concentration lower than 1mg/ml were concentrated with the Amicon Ultra-0.5 ml Centrifugal Filters (10K) for Protein Purification and Concentration (Amicon® Ultra, Millipore, Billerica, USA).

1. Load 400µl of protein lysate on the filter device and centrifuge for 15min at 14000xg and 7°C.
2. Discard the flow through.
3. Separate device from tube and turn device upside down in clean tube.

4. Centrifuge for 2min at 1000xg and 7°C.
5. Collect the flow-through in clean Eppendorf tube and repeat the protocol with the remaining lysate using the same device.
6. Pool the samples, place them on ice to use them immediately for protein quantification or store the samples at -20°C.

2.3.3 SDS-Polyacrylamide-Gelelectrophoresis (SDS-PAGE) and Western Blot

The SDS-PAGE is used to separate proteins by molecular weight in a polyacrylamide-gel (omniPAGE, Cleaver Scientific, Rugby, UK). An electric field is applied across the gel, causing the negatively charged proteins to migrate towards the anode. Small molecules more easily fit through the pores of the gel and therefore migrate a longer distance through the gel. The gel was run usually for 2.5 hours (110Volt). A prestained protein ladder (Page Ruler^{TM} Prestained Protein Ladder, #26616, Thermo Scientific, Waltham, USA) has been used as molecular-weight-marker. Following electrophoresis the gels have been processed further for Western Blot analysis.

Western Blot analysis is used to detect specific proteins with specific antibodies in a tissue homogenate or protein lysate. The protein lysate is separated by SDS-PAGE and proteins are then transferred to a membrane (nitrocellulose (NC) (Bio-Rad) or polyvinylidene fluoride (PVDF)). Dry PVDF membranes (Hybond-P, GE Healthcare Europe GmbH, Freiburg, Germany) have to be activated with methanol for 10sec. To transfer the proteins from the gel to the membrane, a semidry-blotting-system (PerfectBlue^{TM} Semi-Dry-Electroblotter, PEQLAB) was used. The membrane is incubated with the primary antibody against the protein of interest. This antibody is then detected via a secondary antibody, which is conjugated with an alkaline peroxidase (horseradish peroxidase). The principle of the detection is chemiluminescence: luminol (= part of the detection reagent, e.g. ECL Western Blotting Products, Amersham, GE Healthcare) is oxygenated by the horseradish peroxidase and this leads to emission of light which is detected by a film (T-MAT G/R film, Eastman Kodak Company, Rochester, New York, USA).

For each antibody used, the Western Blot protocol has to be optimized: if you are using a 8% or 12% SDS gel depends on the molecular weight of the protein of interest. The higher the molecular weight, the lower the percentage of the SDS gel. If one should use NC or PVDF membranes is sometimes given by the datasheet of the primary antibody. Either milk powder or BSA dissolved in 1X TBS-T can be used as blocking reagent. For primary

antibody incubation one should strictly follow the recommendations of the manufacturer. If the protein of interest is very low expressed, ECL Plus - instead of ECL - can be used as detection reagent.

SDS-PAGE and Western Blot protocol:

1. Remove combs out of SDS gel and wash the slots twice with running buffer. Dry the slots with filter paper.
2. Prepare the samples by adding Sample buffer and if necessary additional RIPA buffer. Incubate the samples for 10min at 99°C, place them on ice for 1min and centrifuge the samples for 10min at 11000xg and 18°C.
3. Transfer the samples in the slots of the SDS gel and don't forget to use a protein ladder. Then cover the samples in the slots with running buffer.
4. Perform the SDS-gel electrophoresis at 110V for about 2.5 hours.
5. In the meantime prepare the transfer buffer and store it at -20°C.
6. Equilibrate filter paper, membranes and SDS gel for 10min in transfer buffer. When using a PVDF membrane, you have to activate it with methanol.
7. For the semidry blotting system, use 3 filter papers; put the NC or PVDF membrane on it, then the SDS-gel and again 3 filter papers. Remove all air bubbles.
8. Perform the blotting at 14V and 440mA for 90min.
9. Stain the membranes for 1min with Ponceau S. Perform the de-staining with Aqua dest. and incubate the membranes afterwards in 1X TBS for 15min.
10. Dry the membrane on a filter paper for 30min.
11. Moisturize the membrane with 1X TBS-T and incubate the membrane for 2hours at room temperature either with milk-powder dissolved in 1X TBS-T or BSA dissolved in 1X TBS-T.
12. Incubate the membrane with the primary antibody over night at 4°C on a shaker. Follow the recommendations of the manufacturer of the antibody. Use 0.25ml dilution reagent per cm^2 of membrane.
13. Wash the membranes with 1X TBS-T - once for 5min and 3 times for 10min.
14. Incubate the membranes with the appropriate secondary antibody at room temperature for 90min on a shaker. Use 0.25ml dilution reagent per cm^2 of membrane.
15. Wash the membranes with 1X TBS-T - once for 5min and 3 times for 10min.
16. Develop the membranes by using ECL (mix 1:1, 0.125ml/cm^2 membrane) or ECL Plus (mix 40:1, 0.1ml/cm^2 membrane) and Kodak film.

Table 8: List of antibodies, used for Western Blot. All antibodies were validated for specificity by Western Blot analysis.

antibody	membrane	dilution	detection reagent
STAT1 (M-22) sc-592 Santa Cruz[1]	NC	1:500	ECL
pSTAT1 Tyr701 (58D6) #9167 Cell Signaling[2]	NC	1:1000	ECL
STAT3 (79D7) #4904 Cell Signaling[2]	NC	1:2000	ECL
pSTAT3 Tyr705 (D3A7) #9145 Cell Signaling[2]	NC	1:1000	ECL
SOCS1 (38-5200) Invitrogen[3]	PVDF	1:250	ECL
GAPDH (FL-335) sc-25778 Santa Cruz[1]	NC + PVDF	1:500	ECL

Secondary antibody for all antibodies: Swine Anti-Rabbit (#P0217), 1:1000, Dako[4]

1: Santa Cruz Biotechnology, Santa Cruz, USA

2: Cell Signaling, Danvers, USA

3:Invitrogen, Carlsbad, USA

4: Dako, An Agilent Technologies Company, Santa Clara, USA

2.3.3.1 Reagents and buffers

Acrylamide/Bis, 37.5:1

Separating gel buffer: 18.2g Tris (100ml)
Dissolve in Aqua dest., pH 8.8 (with 32% HCl)

Stacking gel buffer: 6.1g Tris (100ml)
Dissolve in Aqua dest., pH 6.8 (with 32% HCl)

Separating gel (12%): 6.7ml Acrylamide
4ml separating gel buffer
5.3ml Aqua dest.
160µl SDS solution (10%)
75µl APS (10%)
30µl TEMED

Separating gel (8%):	4.5ml Acrylamide
	4ml separating gel buffer
	7.5ml Aqua dest.
	160µl SDS solution (10%)
	75µl APS (10%)
	30µl TEMED
Stacking gel (5%):	1.7ml Acrylamide
	4ml separating gel buffer
	7.5ml Aqua dest.
	100µl SDS solution (10%)
	30µl APS (10%)
	15µl TEMED
Sample buffer:	10mM NaH_2PO_4 (pH7.4)
	5% SDS
	10% 2-Mercaptoethanol
	10% Glycerol
Running buffer:	15g Tris
	5g SDS
	72g Glycine
	Dissolve in 5l Aqua dest.
Transfer buffer (stock):	28g Tris
	143g Glycine
	Dissolve in 1l Aqua dest.
Transfer buffer:	100ml Transfer buffer (stock)
	200ml methanol
	700ml Aqua dest.

Ponceau S staining solution:	2.5g Ponceau S 5ml glacial acetic acid Add 500ml Aqua dest.
10X TBS stock solution:	60.55g Tris 87.66g NaCl Dissolve in 1l Aqua dest., pH 7.4 (with 32% HCl)
1X TBS-T:	100ml 10X TBS stock solution 900ml Aqua dest. 1ml Tween 20
5% milk powder solution:	5g nonfat dry-milk powder Dissolve in 100ml 1X TBS-T
5% BSA solution:	5g BSA Dissolve in 100ml 1X TBS-T

2.3.4 Tissue microarray (TMA) construction and immunohistochemistry

For each case, 3 to 5 tissue cylinders (depending on the availability of tumor tissue samples) with a diameter of 0.6mm were punched from the marked tumor areas and assembled into a new paraffin block by using a manual instrument (Beecher Instruments, Sun Prairie, Wisconsin, USA). Normal adjacent pleura was used for comparison and punched parenchyma was used as staining control. Four µm thick sections were cut from the TMA block and used for immunohistochemical staining according to standard methods.

Protein expression levels were recorded semi-quantitatively (done by Prof. Dr. Helmut H. Popper) and the staining scores were calculated by multiplying the staining intensity (from 0 to 3+, no staining to strong staining) by percentage (0-100%) of positive cells.

The tissue microarray construction was done by BMA Iris Halbwedl, sections were cut by BMA Mohammed Al-Effah and the immunohistochemical staining was performed by

BMA Margit Gogg-Kamerer as well as BMA Elisabeth Grygar from the Institute of Pathology.

Table 9: List of antibodies used for immunohistochemistry. All antibodies were validated for specificity by Western Blot analysis and immunohistochemistry in test-TMAs.

antibody	dilution	antigen retrieval	detection
STAT1 (M-22) sc-592 Santa Cruz[1]	1:1000	Ventana	CC1/View
pSTAT1 Ser727 sc-16570 Santa Cruz[1]	1:50	MW 9.0	743/EnV+
STAT3 (H-190) sc-7179 Santa Cruz[1]	1:100	Ventana	CC1/View
pSTAT3 Tyr705 (D3A7) #9145 Cell Signaling[2]	1:400	MW 9.0	EnV DAB
SOCS1 (38-5200) Invitrogen[3]	1:200	Ventana	CC1/View
SOCS3 (SO1) sc-51699 Santa Cruz[1]	1:50	MW 9.0	CM DAB
Survivin RB-9245 Fisher Scientific[4]	1:50	MW 6.0	EnV DAB
PIAS1 ab77231 Abcam[5]	1:100	WB	EnV DAB
PIAS3 ab22856 Abcam[5]	1:500	MW 9.0	EnV DAB
BAP1 (C-4) sc-28383 Santa Cruz[1]	1:100	MW 9.0	EnV DAB

1: Santa Cruz Biotechnology, Santa Cruz, USA

2: Cell Signaling, Danvers, USA

3:Invitrogen, Carlsbad, USA

4: Fisher Scientific, Waltham, USA

5: Abcam, Cambridge, United Kingdom

CC1: Cell conditioning 1, Ventana (Ventana, A Member of the Roche Group, Tucson, USA)

CM: ChemoMate Dako (Dako, An Agilent Technologies Company, Santa Clara, USA)

CM DAB: ChemoMate Detection Kit Peroxidase/ DAB rabbit/ mouse chromogen

DAB: 3,3'- Diaminobenzidine

EnV DAB: ChemoMate Envision, HRP, rabbit/mouse

MW: microwave

WB: water bath

9.0: target retrieval solution, pH 9.0, Dako

2.4 Cell culture

Cell culture medium is not only the ideal culture medium for eukaryotic cells but even for bacteria and fungi. Most of these microorganisms grow faster than the eukaryotic cells and may even produce toxic metabolites that can harm the cultured cells irreversible. Therefore, avoiding contamination is the most important point in cell culture experiments.
To guarantee this, all laboratory equipment (bottles, forceps, Eppendorf tubes etc.) is sterilized in an autoclave (20min, 121°C, 2bar). An activation of the UV lamp of the laminar-flow-work bench for at least 20min even reduces the microbial count. All surfaces, as well as hands, were cleaned with 70% ethanol. All disposable plastic ware used (tissue culture flasks, 6-well plates, pipettes etc.) was purchased as sterile plastic ware. Due to this precautionarymeasures, all known microorganisms should be destroyed.
The addition of fetal bovine serum (FBS) to cell culture medium is essential for optimal growth of the cultured cells. The serum provides hormones, binding proteins and lots of essential amino acids, micronutrients as well as buffer- and neutralizing systems such as albumins and immunoglobulins. However, the exact composition is still not fully known and differs from bottle to bottle. Furthermore it is possible that FBS contains toxic substances and unwanted microorganisms like viruses, bacteria or fungi. To avoid a contamination, antibiotics and antimycotics (penicillin/streptomycin) have been added to the cell culture media.

2.4.1 Cultivation of cell lines

Two mesothelioma cell lines were purchased from ATCC (American Type Cancer Collection, via LGC, Germany):

- NCI-H2052 (ATCC® CRL-5915™)
- MSTO-211H (ATCC® CRL-2081™)

These cell lines were cultured in RPMI-1640 supplemented with 10% FBS and 1% penicillin/streptomycin. Four additional mesothelioma cell lines were kindly provided by Arti Shukla, PhD from the Department of Pathology of the University of Vermont, Burlington, USA:

- Hmeso (originally designated H-MESO-1)[74]
- PPM Mill (H2373)
- PPM Gar (H2461)
- PPM Rob (H2595)

These cell lines were cultured in special medium as reported previously [75].
The HepG2 cell line was purchased from ATCC and is known for high SOCS1 expression. Therefore this cell line was used as a control cell line in all cell culture experiments. The HepG2 cell line was cultured in Opti-MEM supplemented with 10% FBS as well as 1% penicillin/streptomycin.
All cell lines are stored in special cryomedium in liquid nitrogen. To thaw the samples, vials were incubated in a water bath (37°C) for 90sec. The cells have then been transferred to tissue culture flasks with pre-warmed medium and were maintained in a humidified atmosphere at 37°C with 5% CO_2.

2.4.2 Trypsinization

Adherent cells have to be detached from tissue culture flasks before they can be counted and seeded again in e.g. 6-well plates. All the mesothelioma cell lines as well as the HepG2 cell line are adherent cells. Detachment has been done with trypsin/EDTA. The following protocol is for detaching cells in 75cm² tissue culture flasks:

1. Totally remove the medium.
2. Wash cells twice with 10ml of pre-warmed (37°C) PBS buffer.
3. Add 4ml of pre-warmed trypsin/EDTA and incubate the flask in the incubator for max. 3min until single cells are present (control under microscope).
4. Add 8ml medium (complete, with FBS) to stop the reaction.
5. Transfer cell suspension to a 15ml falcon and centrifuge for 10min at 980rpm.
6. Remove supernatant and resuspend the pellet in 6ml fresh medium.
7. Perform the cell counting and determination of viability as described below.
8. Transfer the appropriate amount of cell suspension to a new tissue culture flask.

2.4.3 Cell counting and determination of viability

To detect the number of cells, a "Neubauer" counting chamber (see **Figure 13**) has been used. The chamber was a double-chamber meaning that the chamber has two counting areas (two grids) which can be loaded independently. Every grid has 9 square subdivisions. The squares placed in the corners were used for counting mesothelioma cells.

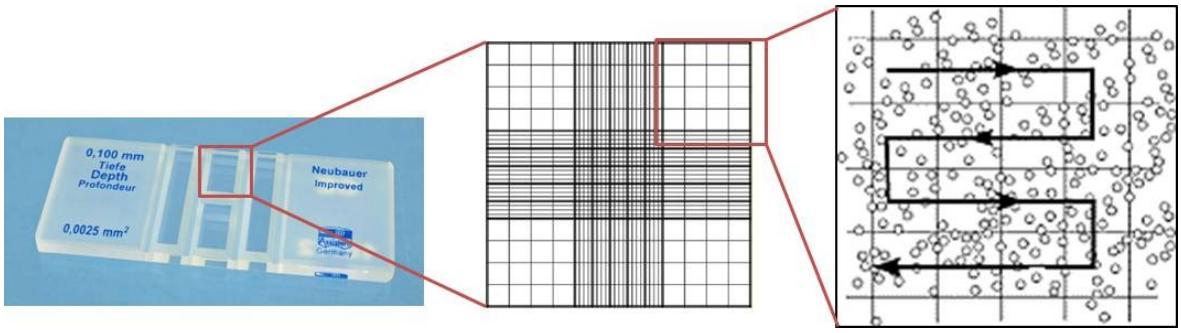

Figure 13: Neubauer counting chamber (left side) with two counting areas. Every grid has 9 square subdivisions (middle) and the squares in the corners have been used for counting cells in a special manner (right side).

The viability has been tested with trypan blue staining. Trypan blue is an acetic dye, which easily binds proteins. The principle of the test is that only dead cells can absorb trypan blue while the cytoplasm and the nucleus are not stained in living cells.
The number of cells (total cell number) is the sum of all counted cells (dead or alive) in all squares counted. The number of living cells is the sum of all unstained cells counted in all squares counted.

Formula for determination of viability:

$$\frac{number\ of\ living\ cells}{total\ cell\ number} \times 100 = \%\ vital\ cells$$

Formula for cell counting (cells/ml):

$$\frac{number\ of\ living\ cells}{number\ of\ squares\ enumerated * 10\text{^}4 * dilution\ factor} = cells/ml$$

2.4.4 Serum starvation and Interferon-gamma stimulation

For the interferon-gamma stimulation experiments $5x10^6$ cells have been seeded in 25cm² tissue culture flasks. Twenty four hours after seeding the cells, serum starvation was started over night. Therefore the medium containing FBS has been totally removed and has been replaced by medium, not containing FBS. Serum starvation has been carried out for 24h and afterwards cells were either left untreated or have been stimulated with 50ng/ml of INFγ (human recombinant, Sigma Aldrich, St.Louis, USA) for 15min, 1h and 4h. After the

incubation time, medium was removed completely and cells were washed twice with ice-cold PBS, before protein extraction was started (see **2.3.1**).

2.4.5 miRNA inhibition

The transfection with miRNA inhibitors was optimized for each cell line used regarding cell number, concentration of miR-inhibitors and final incubation time (post-transfection).
Cell line used: CRL-5915
Transfection reagent: Lipofectamine RNAiMAX (Life Technologies, #13778-075)
miRCURY LNA inhibitors (Exiqon, Vedbaek, Denmark) : hsa-miR-19b (#410119-00), hsa-miR-21 (#410135-00), hsa-miR-30b (#4410189-00), hsa-miR-30c (#411548-00), microRNA antisense control A (#199004-00), stock solution: 50nM, working solution: 10nM

150000 - 300000 cells were seeded in 2ml media (RPMI-1640 + 10% FBS, without antibiotics) on the day before transfection in a 6-well plate. Right before transfection, the old media was removed and replaced by 2ml fresh media.
Example for a transfection process with a miRNA-inhibitor concentration of 50nM (see **Figure 14**) - for each well:

1. 150µl Opti-MEM and 12µl Lipofectamine RNAiMAx were carefully mixed.
2. 150µl Opti-MEM and 12µl siRNA (working solution - either miRNA-inhibitor or a combination of miRNA-inhibitors or miRNA antisense control A) were carefully mixed.
3. The mixtures of 1. and 2. were combined in an Eppendorf tube, carefully mixed by pipetting up and down and incubated for 5min at room temperature.
4. 250µl of the miRNA-inhibitor-Lipofectamine-complex was added drop by drop to the cultured cells in the 6-well plates and plates were rotated extremely carefully for optimal mixing.
5. Cells were examined under microscope for morphological changings and cells were harvested for RNA or protein extraction 24h post-transfection.

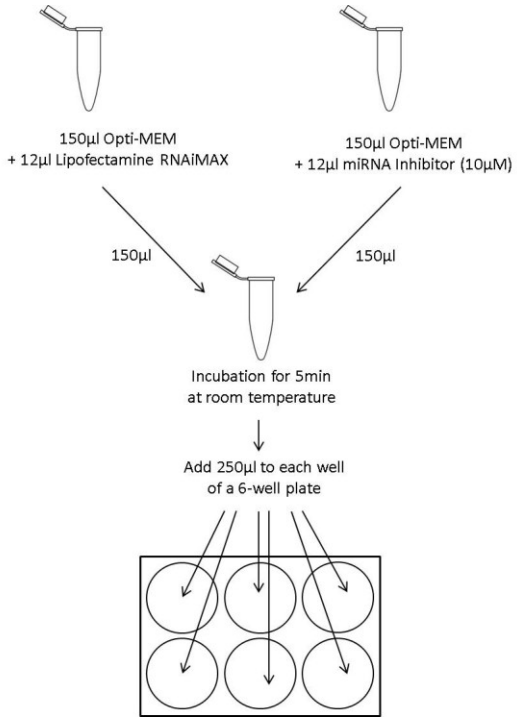

Figure 14: Transfection procedure using microRNA inhibitors. The amount of reagents is enough forthe transfection of one well (50nM miRNA-inhibitor).

2.4.6 siRNA

The transfection with siRNA was optimized for each cell line used regarding cell number, concentration of siRNA (see **Table 10**) and final incubation time (post-transfection).
Cell lines used: CRL-5915 and MSTO-211H
Transfection reagent: Lipofectamine RNAiMAX (Life Technologies, #13778-075)
siRNAs: SignalSilence® Stat1 siRNA II (Cell Signaling, #6544) and SignalSilence® Control siRNA (Cell Signaling, #6568), stock solution: 10µM

150000 (CRL-5915) or 200000 (MSTO-211H and Hmeso) cells were seeded in 3ml media (without antibiotics) on the day before transfection in a 6-well plate. Five hours before transfection, the old media was removed and replaced by 2ml fresh media.
Example for a transfection process with a siRNA concentration of 100nM (see **Figure 15**) - for each well:

1. 78µl Opti-MEM and 22µl Lipofectamine RNAiMAx were carefully mixed and incubated for 5min at room temperature.
2. 78µl Opti-MEM and 22µl siRNA (either STAT1 siRNA or control siRNA) were carefully mixed.

3. The mixtures of 1. and 2. were combined in an Eppendorf tube, carefully mixed by pipetting up and down and incubated for 20min at room temperature.
4. 200µl of the siRNA-Lipofectamine-complex was added drop by drop to the cultured cells in the 6-well plates and plates were rotated extremely carefully for optimal mixing.
5. Cells were examined under microscope for morphological changings and cells were harvested for RNA or protein extraction 24h post-transfection (time-point of optimal, decreased STAT1 expression).

Table 10: Composition of transfection-solution at different concentrations. The amount of reagents is enough for the transfections of cells in one well of a 6-well plate.

	amount/reaction	
concentration	**Opti-MEM**	**Lipofectamine or siRNA**
100nM	78µl	22µl
70nM	84.6µl	15.4µl
50nM	89µl	11µl
30nM	93.4µl	6.6µl

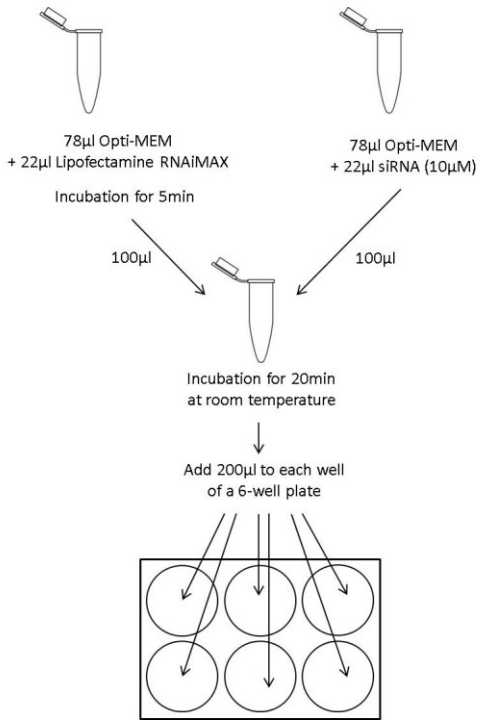

Figure 15: Transfection procedure using siRNA: STAT1 siRNA or control siRNA. The amount of reagents is enough forthe transfection of one well (concentration: 100nM).

2.5 Statistics

Statistical analyses have been discussed with collaborators of the Institute for Medical Informatics, Statistics and Documentation of the Medical University of Graz and the analyses have been performed by Dr. Franz Quehenberger.

2.5.1 The role of BAP1 in malignant pleural mesothelioma

It was tested whether BAP1 expression has an influence on survival time and if BAP1 expression can be correlated with asbestos exposure and used as a prognostic factor of outcome.

Statistical tests were performed two-sided. For group comparisons, the Wilcoxon-Mann-Whitney test was used. Survival rates were estimated by Kaplan-Meier method. Cox proportional hazards regression with score criterion was used to test for continuous and categorical risk factors. If two groups are compared, this procedure is the log-rank test. In multivariate Cox proportional hazards regression marginal (type-II) likelihood ratio test were calculated with R-package aov version 2.0-16. [76]

2.5.2 MicroRNAs and STAT signaling in malignant pleural mesothelioma

To correlate the results of the immunohistochemistry with the miRNA expression levels, a descriptive statistical analysis has been performed. Scatter plots were generated: in these diagrams, Spearmans' correlation coefficient (r) and p-values of the hypothesis $r = 0$ are shown. [26]

P-values below 0.05 were considered statistically significant. R 2.15.1 (http://www.r-project.org) was used for calculations.

3. RESULTS

3.1 The role of BAP1 in malignant pleural mesothelioma

The results of this study were published in *Pathology and Oncology Research*. [76]

A total of 123 human malignant mesothelioma samples were used for the present study.Two tissue microarrays have been constructed: one with the samples from the Medical University of Graz (named "Graz") and another with 57 samples kindly provided by Dr. Thomas Mairinger, Berlin (named "Berlin") and an immunohistochemical staining was performed. Survival data were available for all 123 patients. In 52 patients exposure data for asbestos fibers were available – 21 of them had a history of asbestos exposure. For major clinicopathological characteristics (gender, histological subtype and treatment) see **Table 11**.

Table 11: Patient characteristics; n = 123 human malignant mesothelioma samples

Characteristic	n (%)
Gender	
male	89 (72%)
female	34 (28%)
Histology	
epithelioid	108 (88%)
sarcomatoid	1 (1%)
biphasic	14 (11%)
Treatment	
operation	123 (100%)
chemotherapy (cisplatin+pemetrexed)	39 (32%)
chemotherapy (carboplatin+pemetrexed)	20 (16%)
chemotherapy (platin+pemetrexed)	5 (4%)
chemotherapy (pemetrexed)	4 (3%)
no chemotherapy	11 (9%)
no data concerning chemotherapy	44 (36%)

3.1.1 Immunohistochemical analysis

The immunohistochemical analysis was carried out by Prof. Dr. Helmut H. Popper. Sixty percent ofthe MPM cases used in the present study were not positively stained by the anti-BAP1 antibody. No nuclear staining (see **Figure 16A**) indicates epigenetic downregulation of BAP1 or BAP1 mutation-positive tumors whereas specific nuclear staining (see **Figure 16B**) is achieved for BAP1 mutation-negative tumor samples. If negative staining is equivalent to real *BAP1* mutations needs to be clarified. Antibody staining was also seen in all normal mesothelial cells adjacent to the tumor (internal positive control).

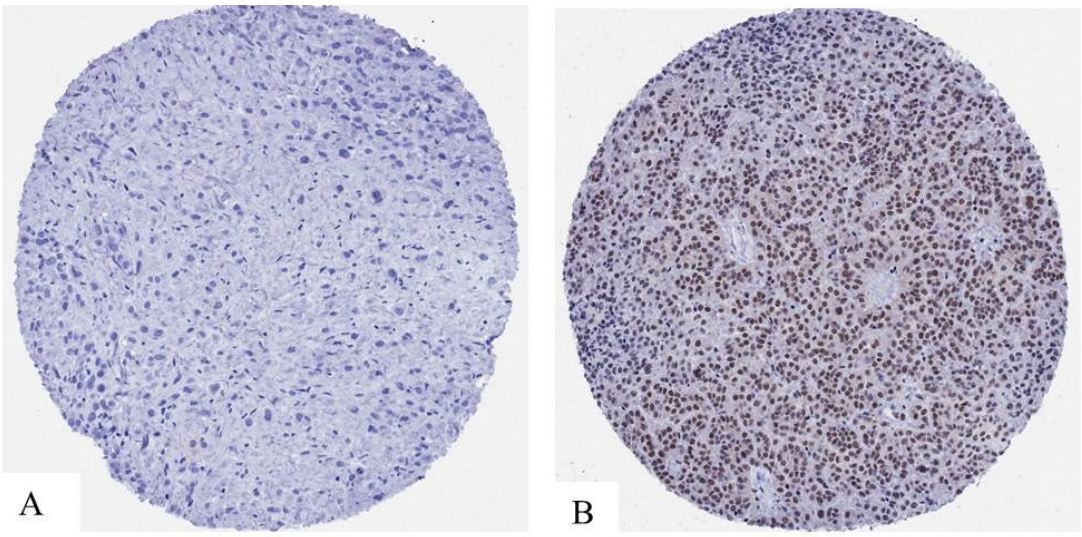

Figure 16: Immunohistochemical staining of tissue microarray sections with anti-BAP1 antibody (40x magnification). No nuclear staining was observed among tumor samples with epigenetic downregulation of BAP1 or BAP1 mutation positive samples (A) whereas specific, nuclear staining was observed among BAP1 mutation-negative tumor samples (B).

3.1.2 Asbestos exposure and BAP1 expression

One aim was to clarify if asbestos exposure has an influence on BAP1 expression.Fifty-two samples were used for this analysis and it was found that it has no statistically significant effect on the BAP1 expression whether the patient has been exposed to asbestos or not (p=0.93) (see **Figure 17**).

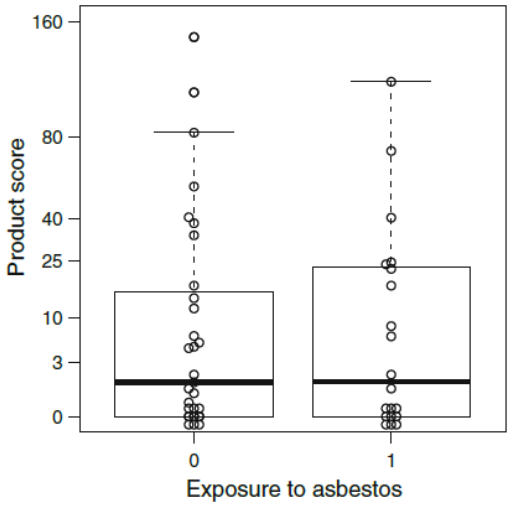

Figure 17: Dot plot with overlayed box and whiskers plot for the influence of asbestos exposure on BAP1 expression (product scores of immunohistochemistry).

3.1.3 Overall survival and BAP1 expression

As mentioned above, due to the number of MPM cases available for the BAP1 study, two tissue microarrays have been constructed. They were analyzed separatelywith respect to overall survival time (see **Figure 18**). No statistically significant difference in survival time was found (p=0.57) between the two tissue microarrays. Therefore all samples have been combined for further analyses.

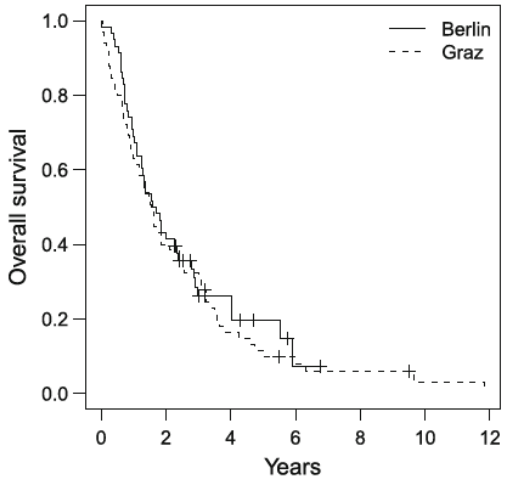

Figure 18: Comparison of overall survival time between the two tissue microarrays (Berlin = 57 samples from Berlin, Graz = 66 samples from the Medical University of Graz).

A significant effect of BAP1 expression score on overall survival time (p=0.0014, score test of Cox regression) was detected. None of the additional clinical risk factors age, sex and subtype was significant. To visualize the effect, patients were split into two groups at BAP1 score 50 (see **Figure 19**). This cutoff was chosen to make sure that only samples with an intense staining and an average or high percentage of stained cells are assessed as positive. Survival times differed significantly between the two groups (p=0.048). The higher the BAP1 expression and therefore the expression of non-mutated BAP1, the shorter the overall survival.

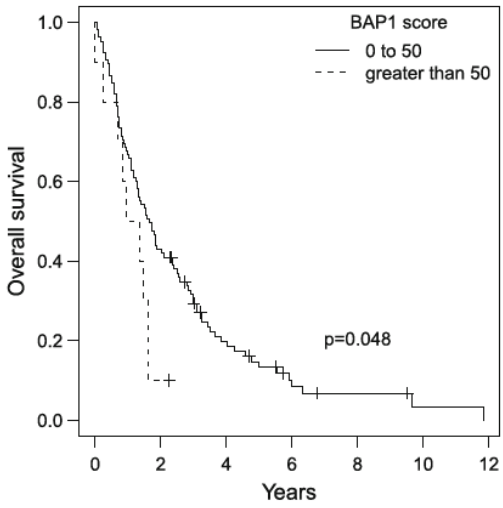

Figure 19: Dependence of overall survival time on BAP1 expression. Mortality is lower at higher BAP1 expression (p=0.0014).

3.2 STAT signaling in malignant pleural mesothelioma

3.2.1 Expression of STATs and their negative regulators in tumor tissue samples

The immunohistochemical analysis was again performedby Prof. Dr. Helmut H. Popper. A positive staining was achieved for seven antibodies (see **Figure 20**): the expression levels of STAT1 and PIAS1 were nearly the same, STAT3 was lower expressed than STAT1 and a very low positive staining was detected for STAT1 phosphorylated on serine 727 (pSTAT1-S727). A weak-positive but specific staining for STAT3 phosphorylated on tyrosine 705 (pSTAT3-Y705) was detected in a few cases. PIAS1 was higher expressed than PIAS3. SOCS1 and SOCS3 expression was not detected by immunohistochemistry. Survivin was found to be highly expressed.

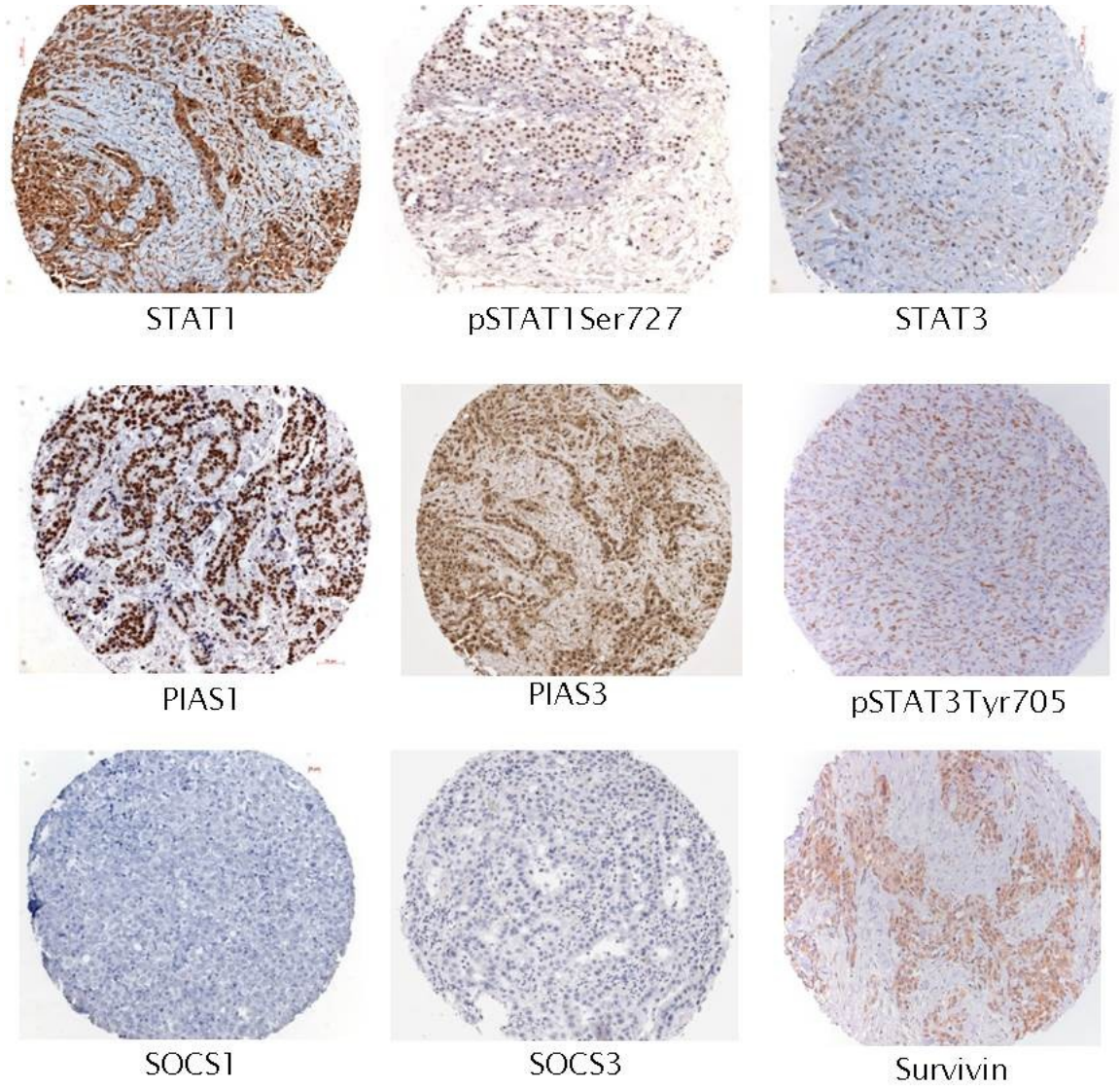

Figure 20: Immunohistochemical staining of tissue microarray sections and Box Plot for the results of the IHC staining (product scores are shown on the vertical axis). Positive staining was achieved for STAT1, pSTAT1-S727, STAT3, pSTAT3-Y705, PIAS1, PIAS3 and Survivin.

PIAS proteins sumoylate STATs, which leads to an inhibition of the transcriptional activation. [32] Since these proteins are constitutively expressed in many cell lines and since they do not only target STATs, further experiments focused on SOCS proteins, which are induced in a classical negative feedback-loop.

3.2.2 IFN-γ stimulation

STAT1 was higher expressed than STAT3 in all six mesothelioma cell lines. SOCS1 expression was absent in MPM cell lines but detected in the control cell line HepG2. IFN-γ had no effect on STAT1, STAT3 or SOCS1 expression; however, phosphorylation of STAT1 on tyrosine 701 (Y701) increased as early as 15min after IFN-γ treatment.

Phosphorylation of STAT1 on serine 727 was not detected by Western Blot, neither in stimulated nor in unstimulated samples. GAPDH was used as control and was equally expressed in all samples (see **Figure 21**).[33]

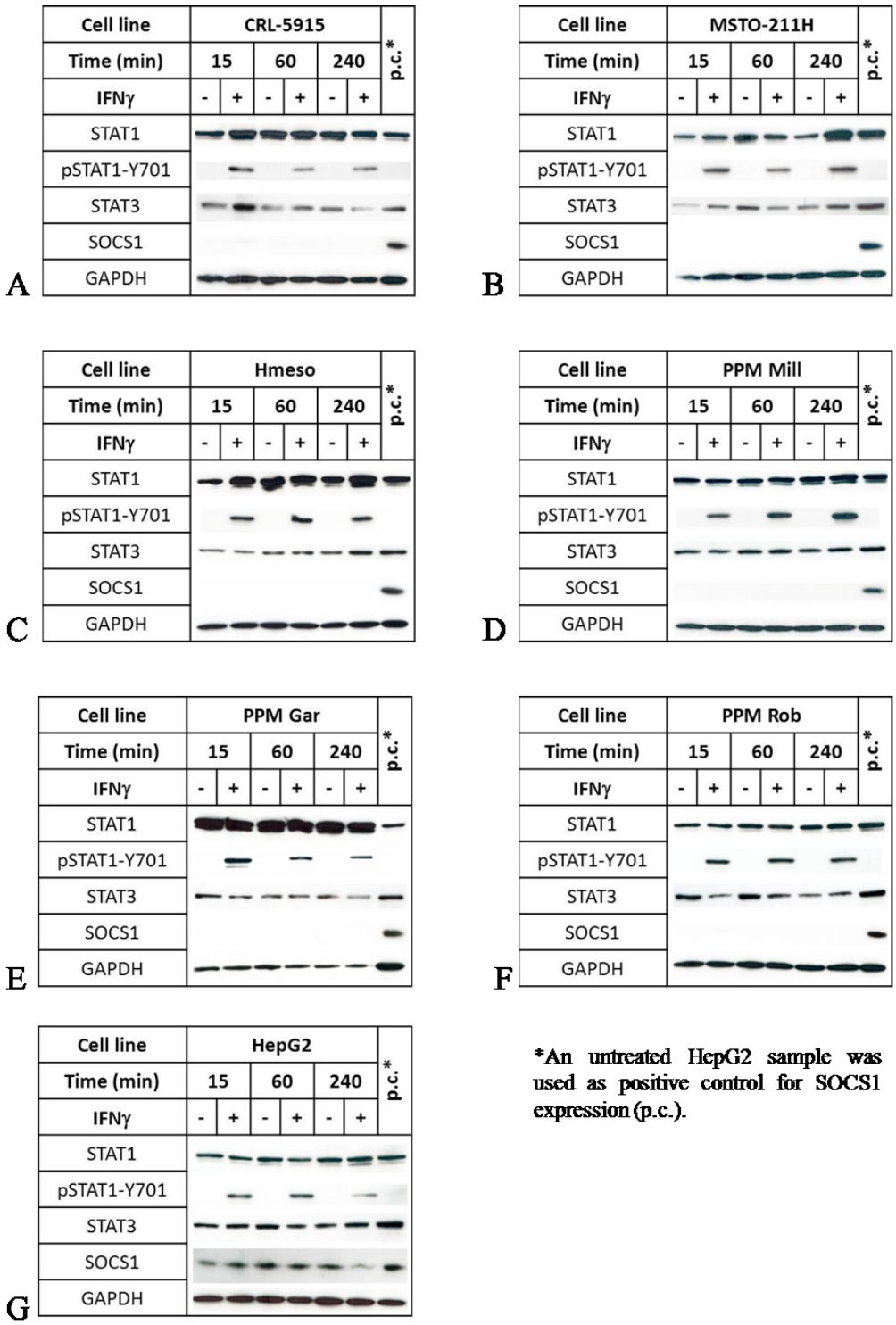

Figure 21: Effect of IFN-γ treatment on protein expression in six mesothelioma cell lines (CRL-5915 (A), MSTO-211H (B), Hmeso (C), PPM Mill (D), PPM Gar (E) and PPM Rob (F)) and one control cell line (HepG2 (G)). Cells were incubated in the absence (-) or presence (+) of INF-γ for the indicated time.[33]

3.2.3 mRNA expression in MPM cell lines

The results for the expression of STAT1, STAT3, SOCS1 and SOCS3 on mRNA level (see **Figure 22**) differ from the expression pattern on protein level: STAT1 and STAT3 mRNA is downregulated compared to GAPDH, SOCS1 and SOCS3 mRNA is downregulated as well. Therefore it is possible to detect SOCS mRNA but there is no SOCS protein in mesothelioma cell lines. This means that the translation process is probably inhibited or affected by miRNAs.

What has to be pointed out is that there is no difference between the mesothelioma cell lines and the control cell line HepG2.

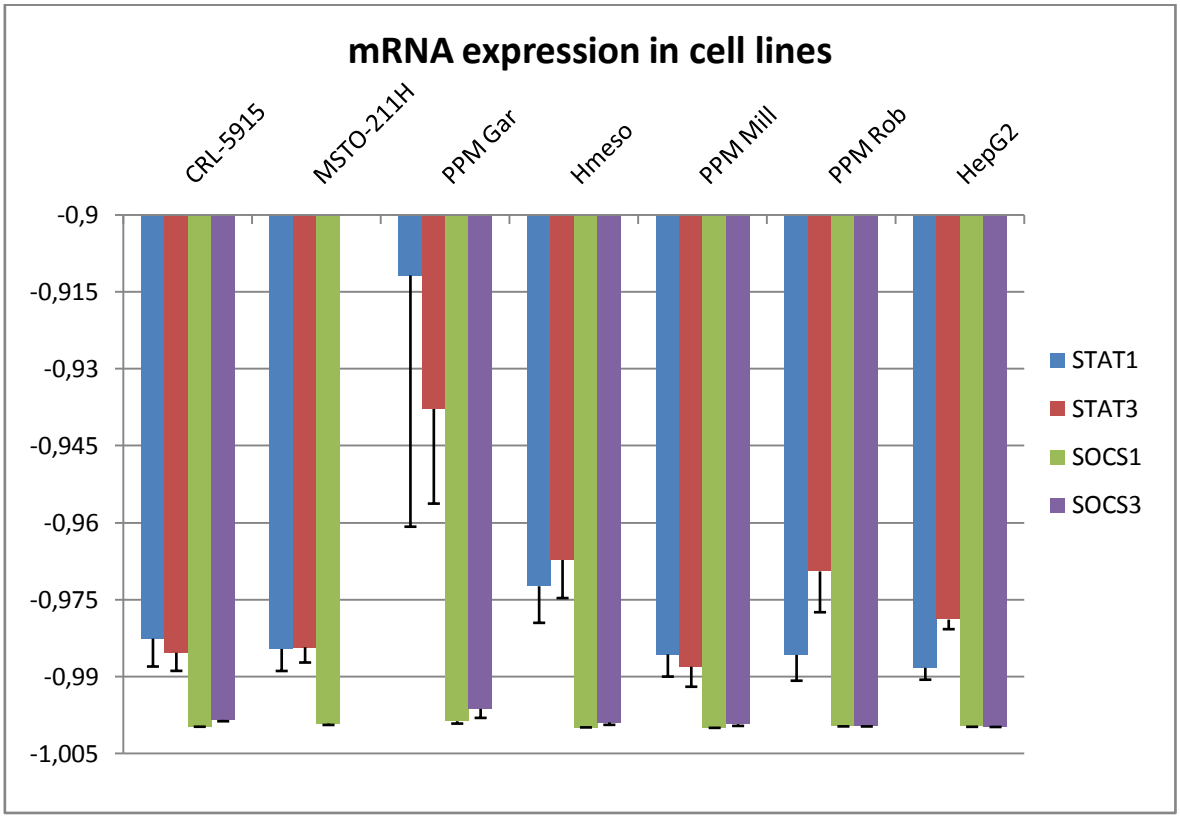

Figure 22: STAT1, STAT3, SOCS1 and SOCS3-mRNA expression levels in all six mesothelioma cell lines and the control cell line HepG2. Expression levels are normalized to the housekeeping gene GAPDH. $2^{-\Delta Cq}$ values are shown; error bars indicate the standard deviation.

3.3 STAT1 knock-down

The mesothelioma cell lines CRL-5915, MSTO-211H and Hmeso have been used for STAT1 knock-down experiments. Transfection conditions (cell density, concentration of siRNA or incubation time) have been optimized for each cell line. Western Blot analysis has been used to detect the optimal conditions.

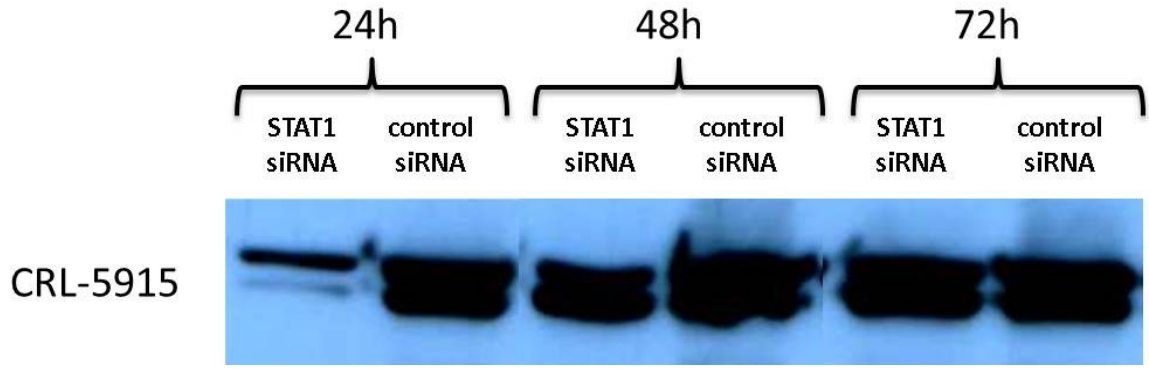

Figure 23: Western blot analysis (STAT1 antibody) of extracts from CRL-5915 cells - transfected with 100nM STAT1 siRNA or 100nM control siRNA - 24h, 48h and 72h post-transfection.STAT1 expression is silenced 24h post-transfection. If the incubation time is longer than 24h, STAT1 expression increases.

CRL-5915 have been treated either with 100nm STAT1 siRNA or control siRNA for 24h, 48h or 72h. Optimal STAT1 knock-down has been achieved after an incubation time of 24h (see **Figure 23**). Afterwards, STAT1 expression increased again and was equally expressed in all samples (STAT1 and control siRNA).

Treating MSTO-211H cells with 100nM of siRNA resulted in a detachment of nearly all cells already after 24h of incubation. It was possible to extract enough protein to perform a Western Blot analysis, but it was not possible to extract enough RNA for further qPCR analysis. Therefore, the amount of siRNA was decreased (70nM, 50nM and 30nM) while the incubation time has not been changed.

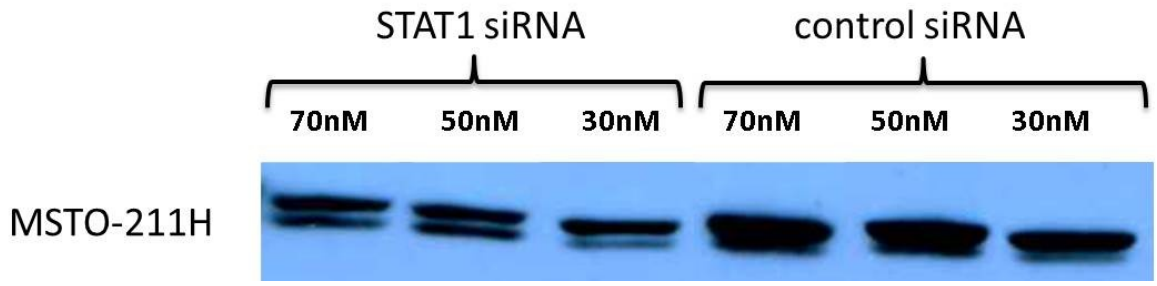

Figure 24: Western Blot analysis (STAT1 antibody) of extracts from MSTO-211H cells – transfected with 70nM, 50nM or 30nM STAT1 siRNA or control siRNA – 24h post-transfection. In general, STAT1 is lower expressed than in CRL-5915 cells. However STAT1 expression is silenced, not depending on the concentration of siRNA.

In MSTO-211H, STAT1 is in general lower expressed than in CRL-5915 (see also **Figure 21**). However, STAT1 was successfully knocked-down by using STAT1 siRNA, not depending on the concentration of siRNA. For further experiments, 70nM STAT1 or control siRNA have been used to treat MSTO-211H.

STAT1 was found to be highly expressed in the cell line Hmeso in previous investigations (see also **Figure 21**). Therefore this cell line has even been used for the STAT1-knock-down experiments.

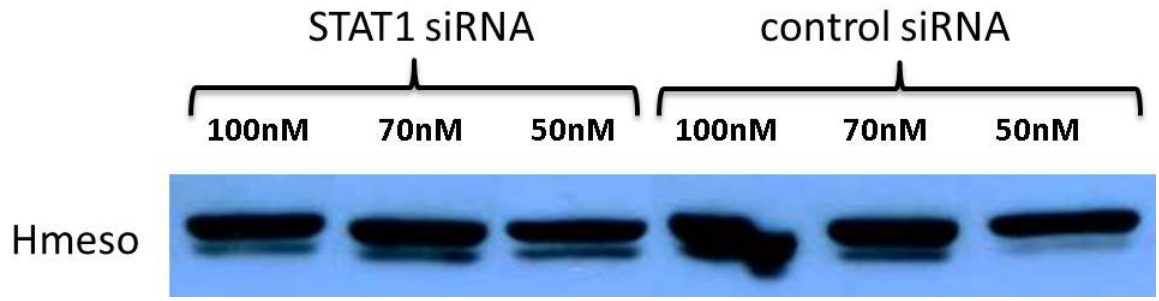

Figure 25: Western Blot analysis (STAT1 antibody) for extracts from Hmeso cells – transfected with 100nM, 70nM or 50nM STAT1 siRNA or control siRNA – 24h post-transfection. If STAT1 expression is silenced at any concentration is not clear after this Western Blot analysis.

The siRNAs have been used in three different concentrations. However, if STAT1 expression was successfully knocked-down in Hmeso, is not clear after Western Blot analysis (see **Figure 25**) since all bands have the same thickness.

Since it was expected that STAT1 expression was decreased at least at the highest siRNA concentration (100nM), mRNA expression levels of STAT1 and GAPDH have been detected in triplicates by using RT^2 qPCR Primer Assays as mentioned before.

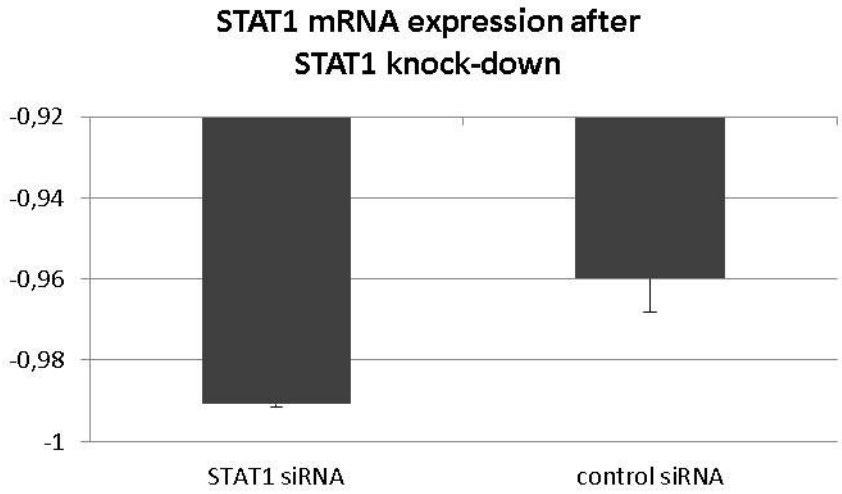

Figure 26: STAT1-mRNA expression levelsafter STAT1 knock-down using siRNA in the cell line Hmeso. STAT1 is lower expressed when 100nM STAT1 siRNA were used compared to100nM control siRNA. $2^{-\Delta Cq}$ values are shown and the expression levels were normalized to GAPDH. Error bars indicate the standard deviation.

STAT1-mRNA expression was found to be successfully knocked-down in Hmeso by using 100nM STAT1 siRNA (see **Figure 26**). As mentioned previously, STAT1-mRNA is downregulated compared to GAPDH-mRNA (see also **Figure 22**). Therefore a downregulation was even detected, when the control siRNA was used.
For further experiments, 100nM STAT1 or control siRNA have been used to treat Hmeso.

QPCR (RT^2 Profiler PCR Array) was used to detect mRNA expression levels of all known JAK and STAT family members, the receptors that activate them, STAT-inducible genes, negative regulators of the pathway and apoptosis an cell cycle related genes (see **Table 7**) in order to investigate the consequences of STAT1 knock-down. For each sample, only one RT^2 Profiler PCR Array has been performed meaning that the results are based on single assessments.
For quantitative PCR analysis it is important to use RNA of highest quality and samples should not be contaminated with genomic DNA. While RNA quality can be checked before performing the reverse transcription, other tests (e.g. DNA contamination) are included during real time PCR.
Several quality control tests (explanations on page 40) are included on the RT^2 Profiler PCR Array and all cell lines have passed all tests (see **Table12**).

Table 12: Data analysis for CRL-5915 (blue), MSTO-211H (red) and Hmeso (green). Several quality-control tests are included on the RT^2 Profiler PCR Array. All samples (either treated with STAT1 siRNA or with the control siRNA) passed all test

	Control siRNA	STAT1 siRNA	Specified value
Cq value for the human genomic DNA control (HDGC)	37.56 Undetermined Undetermined	Undetermined Undetermined Undetermined	>35
$\Delta Cq = AVG\ Cq^{RTC} - AVG\ Cq^{PPC}$	2.1 3.2 3.1	2.2 2.6 2.7	<5
average Cq^{PPC}	21.09 20.40 20.58	21.30 20.59 20.68	20 +/- 2
difference between average Cq^{PPC} of control siRNA and STAT1 siRNA	0.21 0.56 0.10		<2

As mentioned previously, the Cq values for the 5 housekeeping genes included on the RT^2 Profiler PCR Array were nearly the same. Therefore the average Cq value for all housekeeping genes was calculated and used for normalization.

STAT1-mRNA was successfully knocked-down by using STAT1 siRNA in all three mesothelioma cell lines. The effect of STAT1 knock-down on the other components of the STAT signaling pathway differs between the cell lines (see **Figure 27**). While CRL-5915 seems to compensate STAT1 knock-down by an upregulation of STAT5a, MSTO-211H and Hmeso show slightly upregulated expression levels of STAT3. SOCS1/2/3-mRNA as well as PIAS3 are upreglated in CRL-5915 while these mRNAs are only slightly upregulated or even downregulated in the other two cell lines.

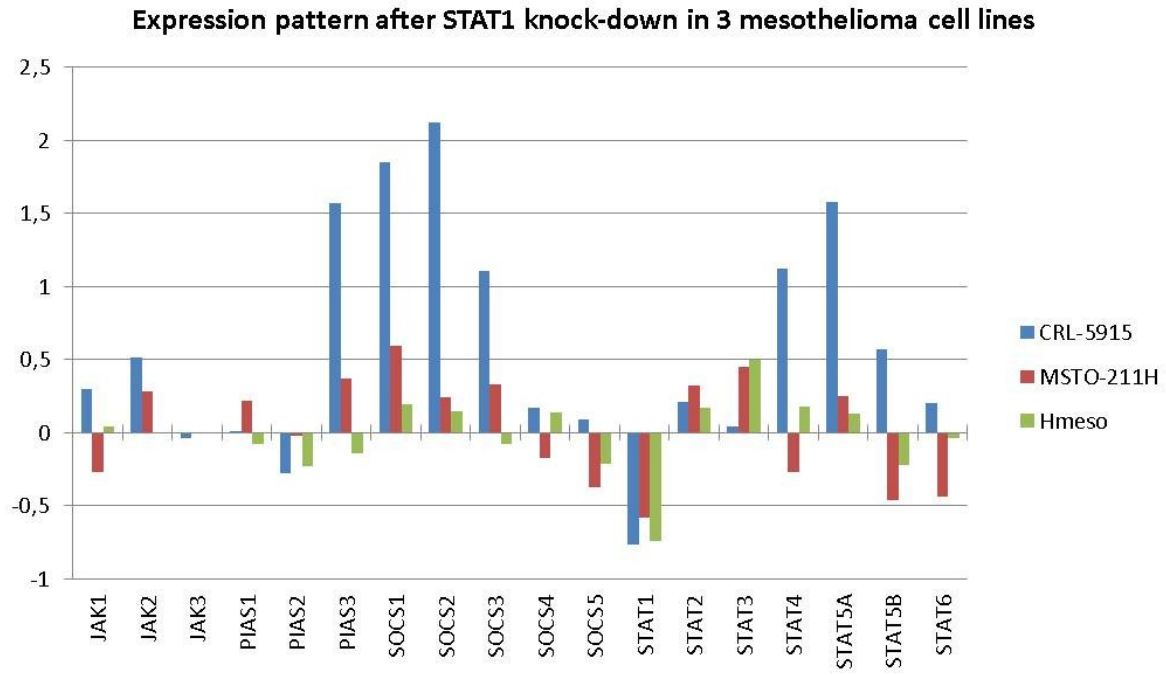

Figure 27: mRNA-expression levels of components of the STAT signaling pathway after STAT1 knock-down in CRL-5915, MSTO-211H and Hmeso. The Cq values for all 5 housekeeping genes was nearly the same, therefore an average Cq value has been calculated and was used for normalization. $2^{-\Delta\Delta Cq}$ values are shown (STAT1-siRNA samples compared to control-siRNA samples).

Most of the genes included on the RT^2 Profiler PCR Array are differentially expressed in the mesothelioma cell lines investigated (see **Figure 28**). Three genes (indicated by red arrows) were found to be either up- or downregulated in all cell lines (with $2^{-\Delta\Delta Cq}$ values of at least 0.5):

- CDKN1A: cyclin-dependent kinase inhibitor 1A (also known as p21)
- F2R: coagulation factor II (thrombin) receptor
- IL10RA: interleukin 10 receptor, alpha

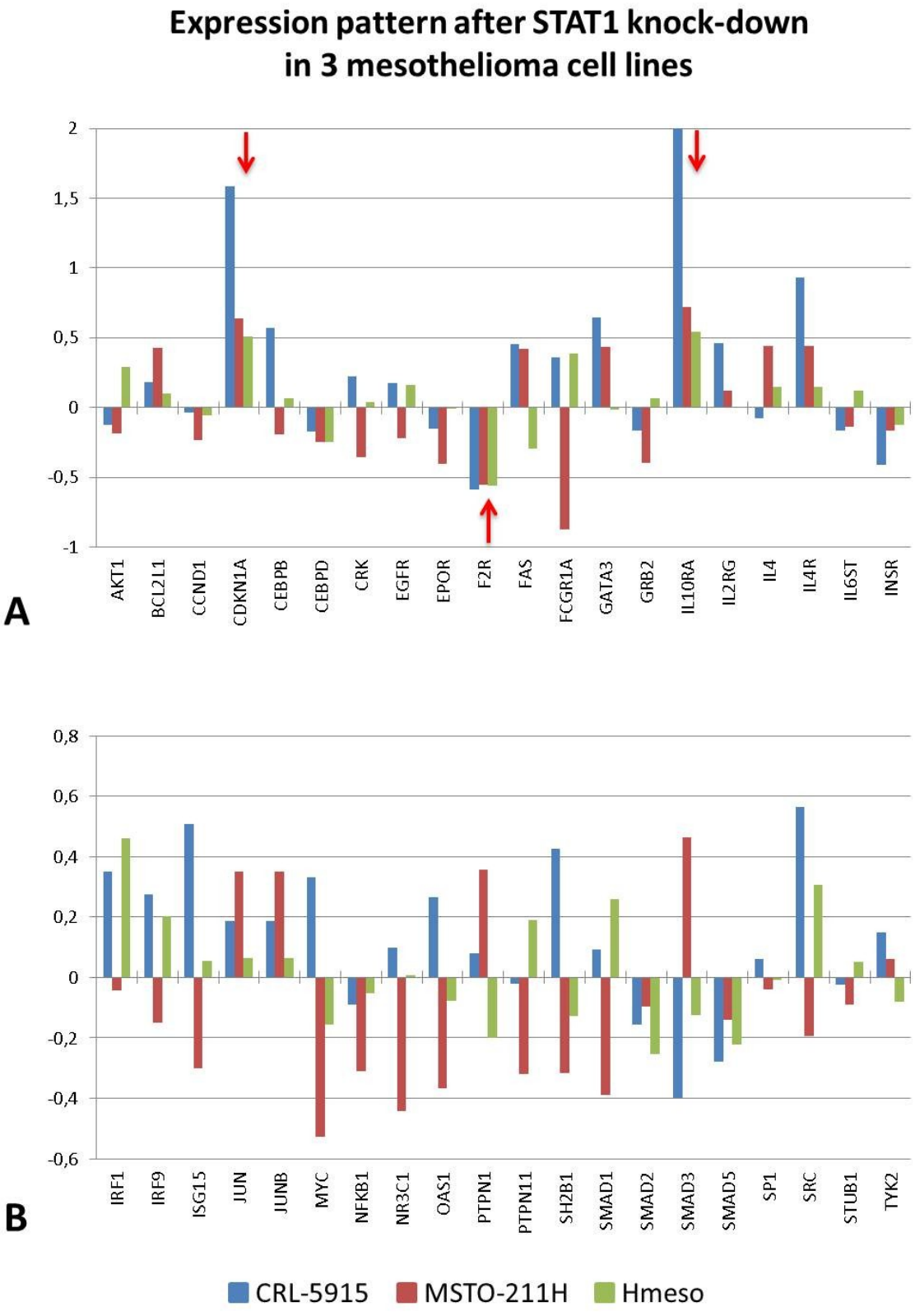

Figure 28: mRNA-expression levels of genes associated with the STAT signaling pathway after STAT1 knock-down in three mesothelioma cell lines. The Cq values for all 5 housekeeping genes was nearly the same, therefore an average Cq value has been calculated and was used for normalization. $2^{-\Delta\Delta Cq}$ values are shown (STAT1-siRNA samples compared to control-siRNA samples). Three genes (indicated with red arrows) are either up- or downregulated in all three cell lines ($2^{-\Delta\Delta Cq}$ values are at least 0.5). Figure (A) and (B) only differ in scaling of the y-axis.

3.4 miRNAs as possible regulators of STAT signaling in MPM

3.4.1 miRNA profiling in tumor tissue samples

By performing the miRNA profiling it was possible to identify 29 miRNAs, which possibly play a role in malignant mesothelioma. Twelve of them were predicted to target components of the STAT signaling pathway (see **Table 13**) and the miRNAs found to upregulated were quantified in every single sample.

Table 13: Results of themiRNA profiling in MPM tumor tissue samples. Pooled RNA samples (~ 8 tumor tissue samples) have been used for this analysis.

microRNA	expression compared to RNU44	predicted targets
hsa-let-7b	slightly downregulated	SOCS1
hsa-miR-106a	upregulated	STAT3
hsa-miR-126	highly upregulated	
hsa-miR-145	upregulated	
hsa-miR-146a	upregulated	
hsa-miR-146b	upregulated	
hsa-miR-150	slightly downregulated	
hsa-miR-155	slightly downregulated	SOCS1
hsa-miR-16	highly upregulated	
hsa-miR-17	upregulated	STAT3
hsa-miR-191	upregulated	
hsa-miR-193b	slightly downregulated	
hsa-miR-199a-3p	slightly downregulated	
hsa-miR-19b	upregulated	SOCS1, SOCS3
hsa-miR-21	upregulated	STAT3
hsa-miR-210	slightly downregulated	
hsa-miR-214	slightly downregulated	SOCS1
hsa-miR-218	slightly downregulated	SOCS3
hsa-miR-222	upregulated	SOCS3
hsa-miR-223	highly upregulated	STAT1
hsa-miR-24	extremely upregulated	
hsa-miR-26a	slightly upregulated	
hsa-miR-29a	upregulated	
hsa-miR-30b	expressed as control	SOCS1, SOCS3
hsa-miR-30c	slightly upregulated	SOCS1, SOCS3
hsa-miR-31	slightly downregulated	
hsa-miR-320	slightly upregulated	
hsa-miR-342-3p	slightly upregulated	
hsa-miR-484	upregulated	

MicroRNA quantification experiments were performed only in 45 of 52 tumor tissue samples (not enough RNA in 7 tumor samples). MiR-223 was found to be highly upregulated in the miRNA profiling experiment. When this miRNA was quantified in 45 tumor samples, it was found to be upregulated only in 50% of samples, and slightly downregulated in the rest of the samples compared to RNU6B. Even though two different endogenous controls have been used to normalize the expression levels (RNU44 for miRNA profiling, RNU6B for single miRNA assays), the difference in the expression pattern should not be that huge. It is more likely that this discrepancy is caused by the fact that the miRNA profiling was a single analysis of pooled samples while all 45 tumor samples have been used in triplicates for the single miRNA assays. However, the results have been correlated with the STAT1 expression levels, detected by immunohistochemistry but the influence of miR-223 on STAT1 expression is not statistically significant for the tested sample group (see **Figure 29**).

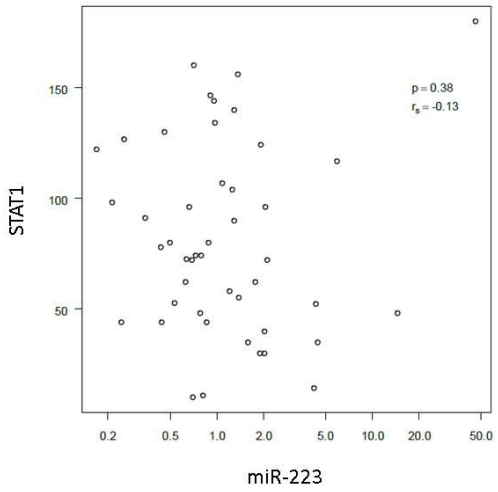

Figure 29: Scatter plot for $2^{-\Delta Cq}$ values of miR-223 in relation to product scores of immunohistochemistry of STAT1. The expected influence is not statistically significant for the tested sample group (p=0.38).

MiR-17 was upregulated in nearly all 45 tumor tissue samples whereas miR-21 was found to be extremely upregulated in all samples. These miRNA expression levels have been correlated with STAT3 expression levels but both miRNAsdo not have a statistically significant influence on STAT3 expression in malignant pleural mesothelioma (see **Figure30**).

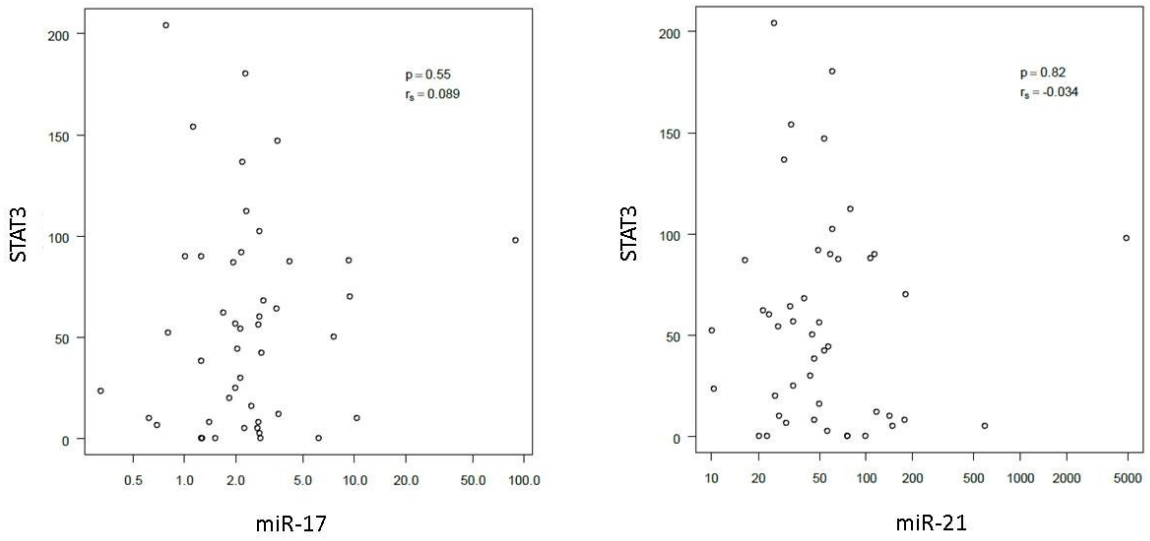

Figure 30: The scatter plots show the $2^{-\Delta Cq}$ values of miR-17 and miR-21 in relation to product scores of immunohistochemistry of STAT3. Neither miR-17 (p=0.55) nor miR-21 (p=0.82) have a statistically significant influence on STAT3 expression.

Since miR-106a was found to be upregulated in a previous study and the correlation between miR-106 and STAT3 was not statistically significant, this analysis has not been performed a second time.

MiR-19b, miR-30b, miR-30c and miR-222 (all targeting SOCS1 and SOCS3), were found to be upregulated in nearly all samples (see **Figure 31 and 32**)

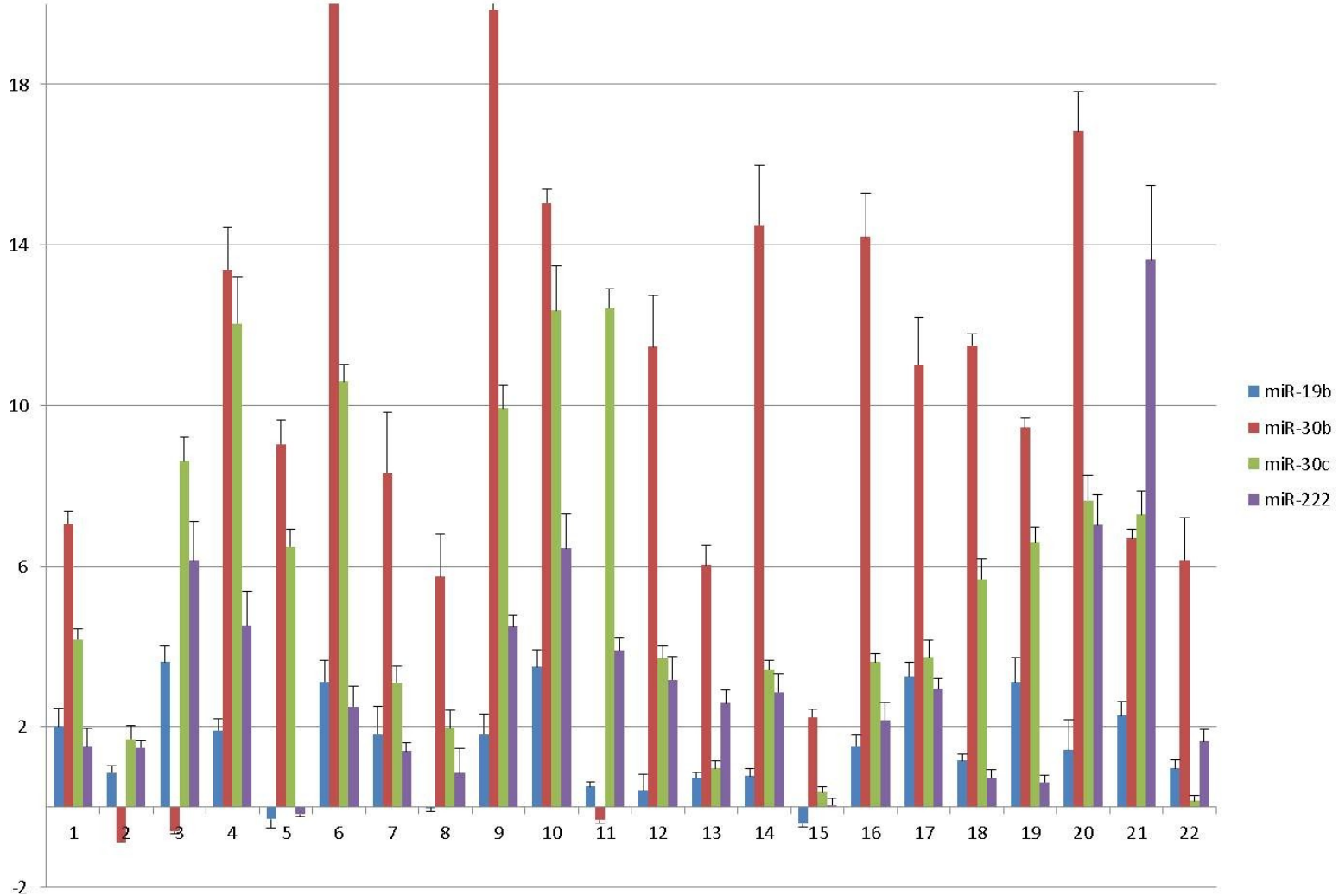

Figure 31: miRNA expression levels in MPM tumor tissue samples. RNU6B was used for normalization. $2^{-\Delta Cq}$ values are shown; error bars indicate the standard deviation.

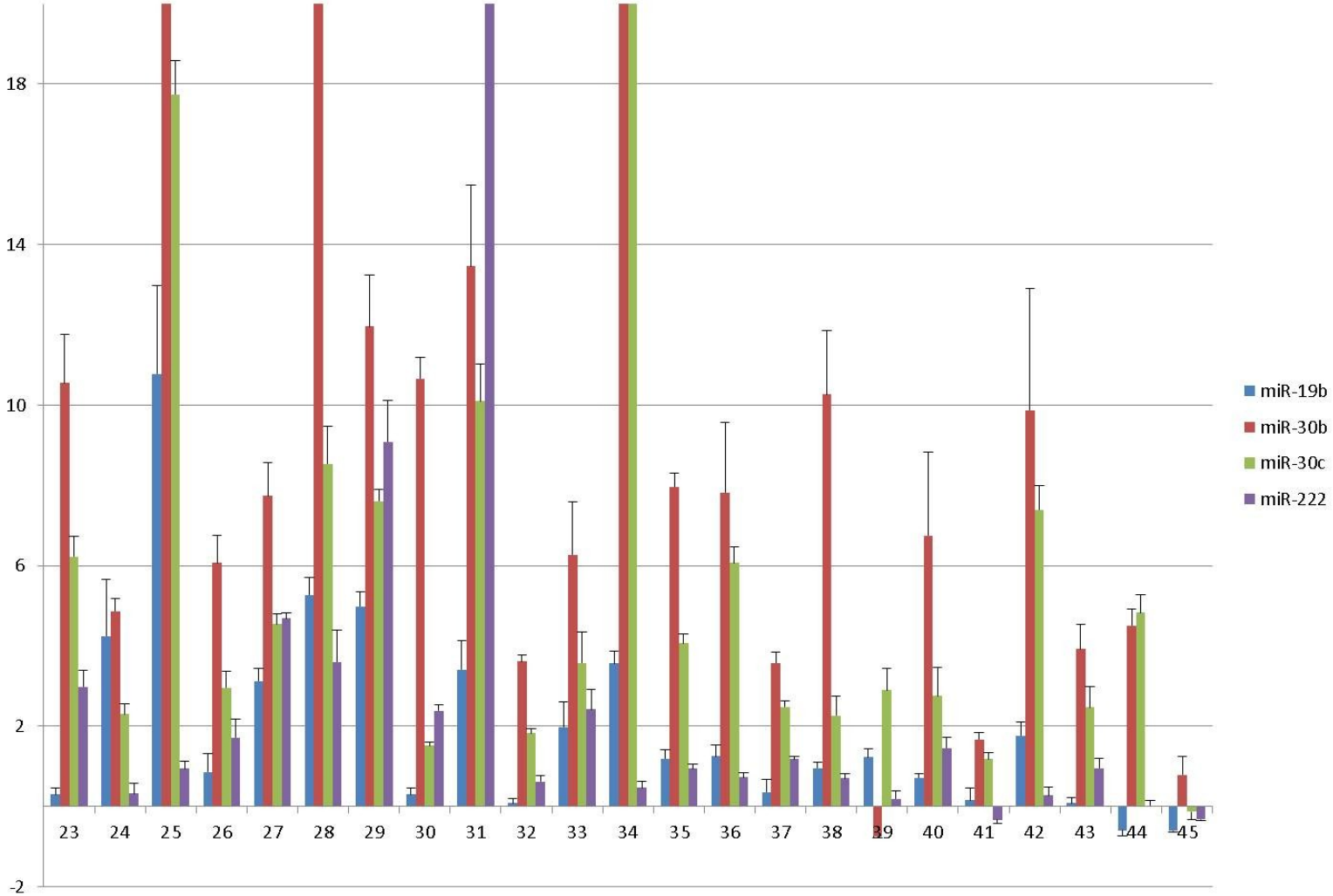

Figure 32: miRNA expression levels in MPM tumor tissue samples. RNU6B was used for normalization. $2^{-\Delta Cq}$ values are shown; error bars indicate the standard deviation.

3.4.2 miRNAs in MPM cell lines

The miRNA quantification data for the mesothelioma cell lines (see **Figure 33**), confirmed the results of the FFPE tumor tissue samples: Three miRNAs (miR-17, miR-106a and miR-21) – targeting STAT3 – were even upregulated, whereas miR-21 was extremely upregulated in FFPE tumor tissue samples and mesothelioma cell lines. This miRNA has a well-known cancer association in a wide variety of human tumors.

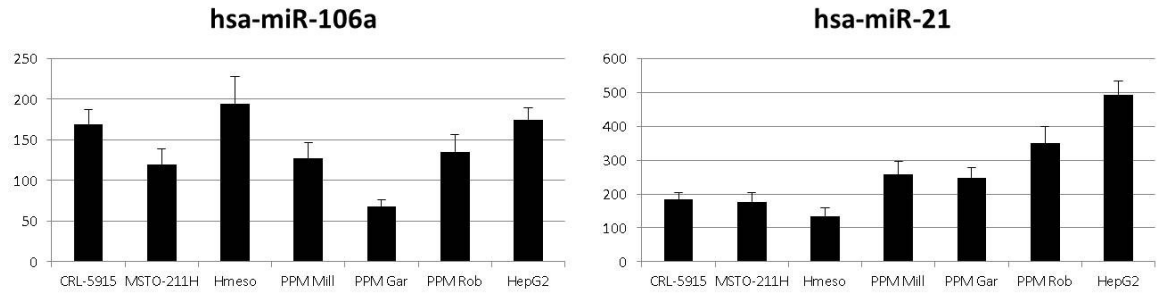

Figure 33: Expression of miRNAs possibly targeting STAT3 in all 6 mesothelioma cell lines and the control cell line HepG2. RNU6B was used for normalization.$2^{-\Delta Cq}$ values are shown; error bars indicate the standard deviation.

Four miRNAs (miR-19b, -30b, -30c and -222) which are predicted to target SOCS1 and SOCS3, were found to be upregulated as well (see **Figure 34)**

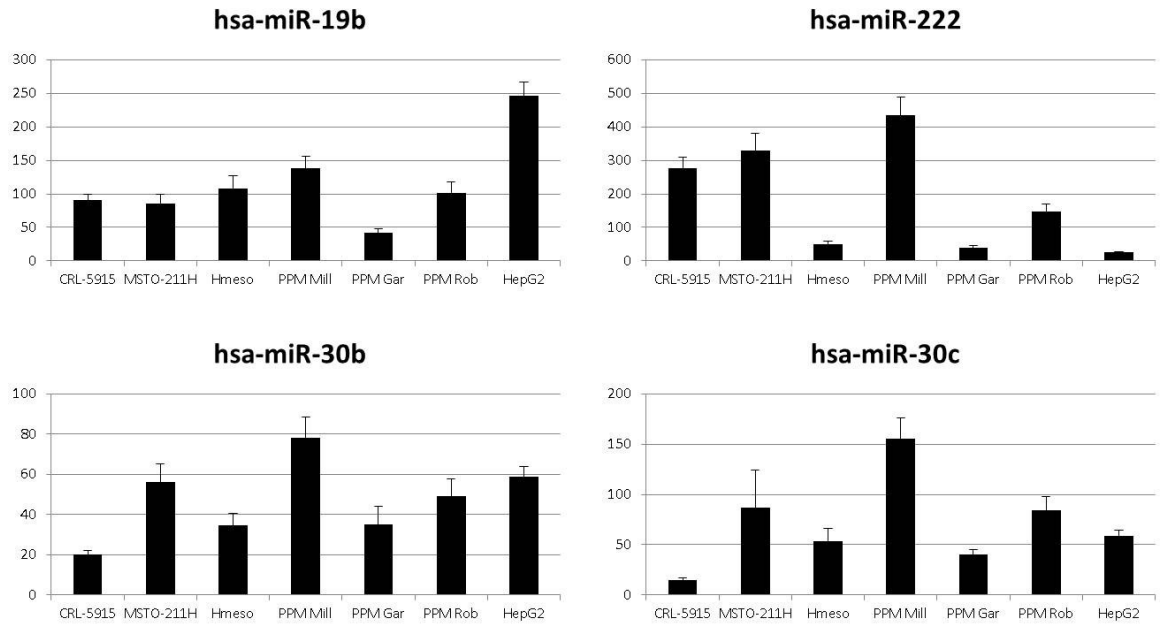

Figure 34: Expression of miRNAs possibly targeting SOCS1 and SOCS3 in all 6 mesothelioma cell lines and the control cell line HepG2. RNU6B was used for normalization.$2^{-\Delta Cq}$ values are shown; error bars indicate the standard deviation.

The expression of all six miRNAs is upregulated compared to the reference gene RNU6B; however the amount of each miRNA differs between the different cell lines. What has to be pointed out is that there is no difference between the mesothelioma cell lines and the control cell line HepG2. Compared to HepG2, miR-21 and miR-19b are lower expressed in mesothelioma cell lines.

3.4.3 miRNA inhibition

The hypothesis was that high miRNA expression levels are responsible for the downregulation of STAT3 or the missing expression of SOCS1/SOCS3. The knock-down of these miRNAs should therefore result in increased STAT3 or SOCS1/SOCS3 expression.Since it was reported that SOCS1 expression levels could have been increased after the knock-down of miR-19a and miR-19b (which is highly expressed in MPM) or a combination of both inhibitors in multiple myeloma, [77] it was also investigated if a combination of miRNA inhibitors leads to SOCS1/3 expression in MPM.

Detecting miRNA expression after a knock-down experiment is definitely not the Gold-standard to control for efficient inhibition. If transfection is inefficient, it is often because knockdown oligonucleotides are retained on the outside of the cell membrane or are sequestered in internal vesicles, physically separated from their miRNA targets in the cytoplasm. However, during cell lysis these oligonucleotides are released and will interact with miRNAs in the lysate. Real-time PCR can therefore not distinguish between biologically relevant complexes that formed in the cytoplasm of transfected cells and complexes that formed following cell lysis.
However, to check whether the miRNA inhibitors were working or not, miRNA quantification by real-time PCR has been performed. In all experiments, miRNAs have been knocked down by their specific inhibitors compared to the negative control A (see **Figure 35 and 36**).

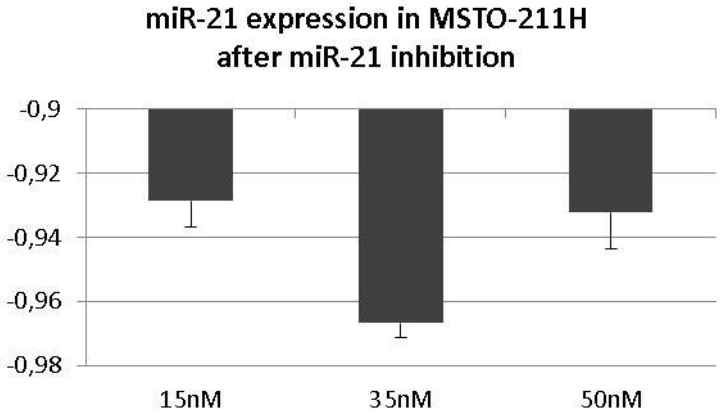

Figure 35: Reducedexpression ofmiR-21 in MSTO-211H after inhibition of miR-21. Different concentrations (15nM, 35nM and 50nM) of the miR-inhibitor have been used. $2^{-\Delta Cq}$ values are shown and the expression levels were normalized to "miRNA antisense control A". Error bars indicate the standard deviation.

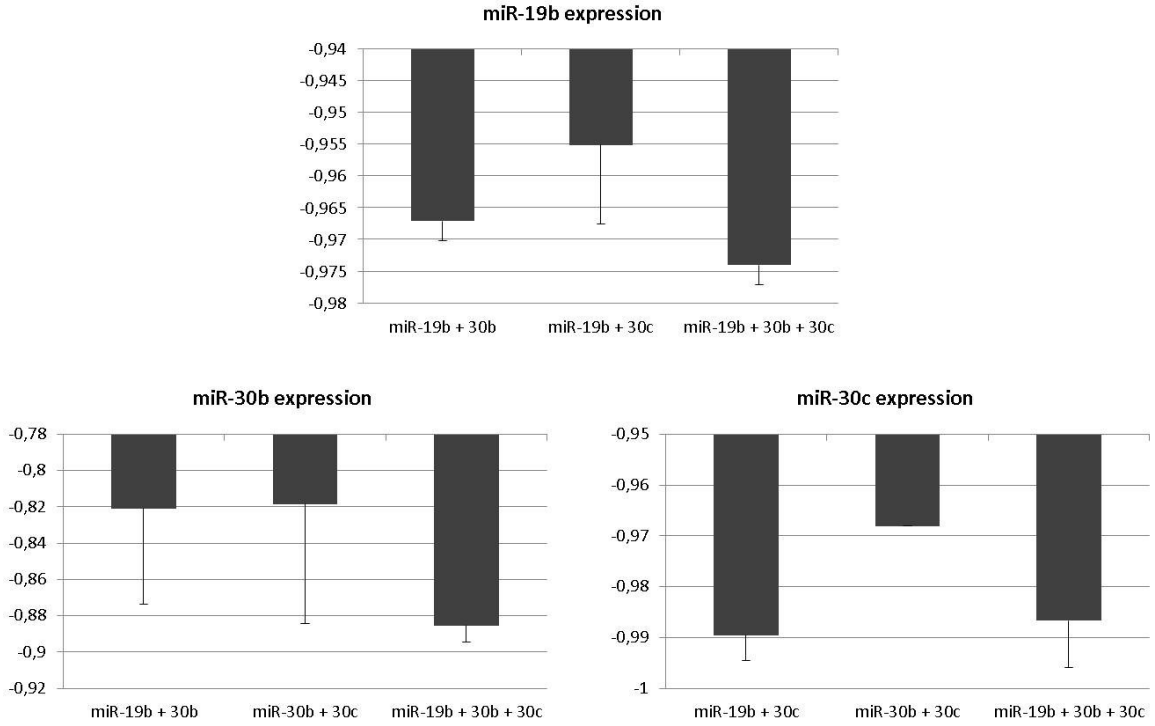

Figure 36: Expression of miR-19, miR-30b and miR-30c after using two or three miR-inhibitors at the same time.The concentration of the miR-inhibitor-combinations was 100nM. $2^{-\Delta Cq}$ values are shown and the expression levels were normalized to "miRNA antisense control A". Error bars indicate the standard deviation.

mRNA expression levels (STAT3 or SOCS1) have been quantified by real-time PCR. It was expected that, the higher the concentration of the miRNA inhibitor, the higher the expression of the target mRNA. This hypothesis was not true for STAT3-mRNA

expression after miR-21 inhibitionin two malignant mesothelioma cell lines (see **Figure 37**): STAT3 expression is a little bit increased but the effect cannot be correlated with the concentration of the inhibitor and the effect is not the same in MSTO-211H and CRL-5915.

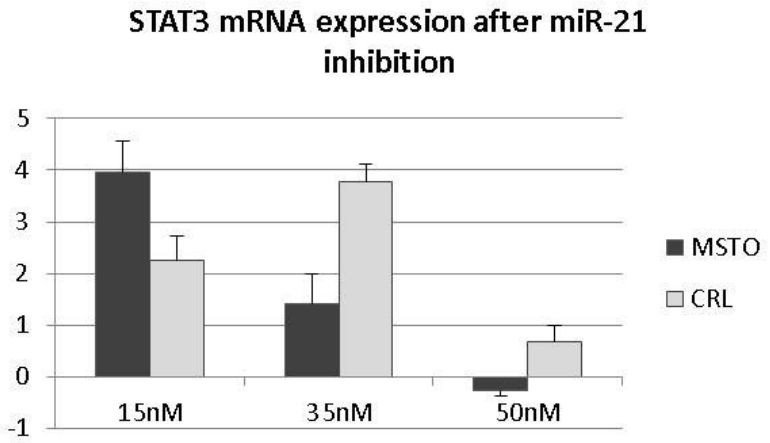

Figure 37: STAT3-mRNA expression levels in two mesothelioma cell lines (MSTO-211H and CRL-5915) after miR-21 inhibition. Different concentrations (15nM, 35nM and 50nM) of the miR-inhibitor have been used. $2^{-\Delta Cq}$ values are shown and the expression levels were normalized to "miRNA antisense control A". Error bars indicate the standard deviation.

SOCS1 mRNA expression is slightly upregulated when a combination of two (miR-19b and miR-30b) or three miRNA inhibitors (miR-19b, miR-30b and miR-30c) was used (compared to untreated samples) (see **Figure 38**). But the $2^{-\Delta Cq}$ values are definitely too low and the standard deviations are too high, to assume that this is a real effect, caused by knocking-down miRNAs.

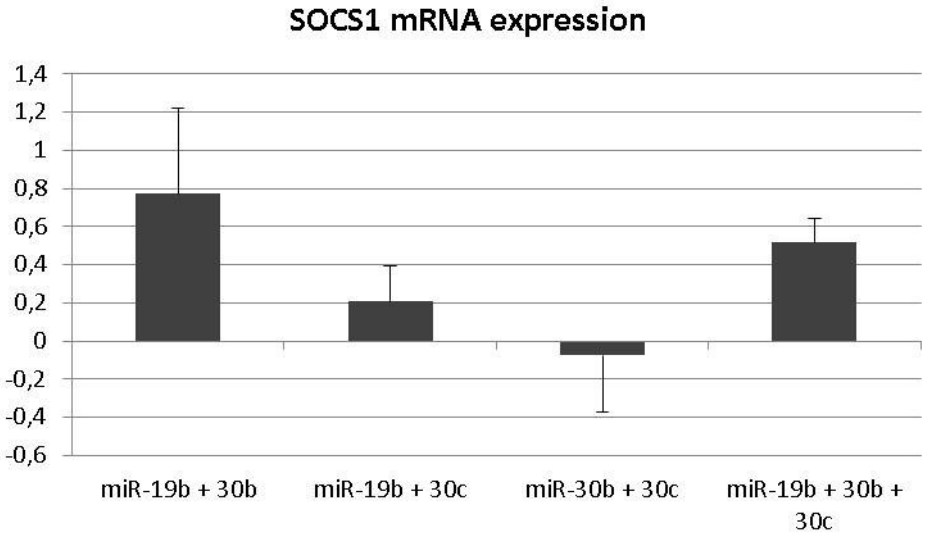

Figure 38: SOCS1-mRNA expression levels in CRL-5915 after using a combination of two or three miR-inhibitors. $2^{-\Delta Cq}$ values are shown and the expression levels were normalized to "miRNA antisense control A". Error bars indicate the standard deviation.

Since real-time PCR is a sensitive method and the changes observed were very small, it was no big surprise that it was not possible to detect a change in STAT3 (see **Figure 39**) protein expression by Western Blot. STAT3 was equally expressed in treated and untreated samples.

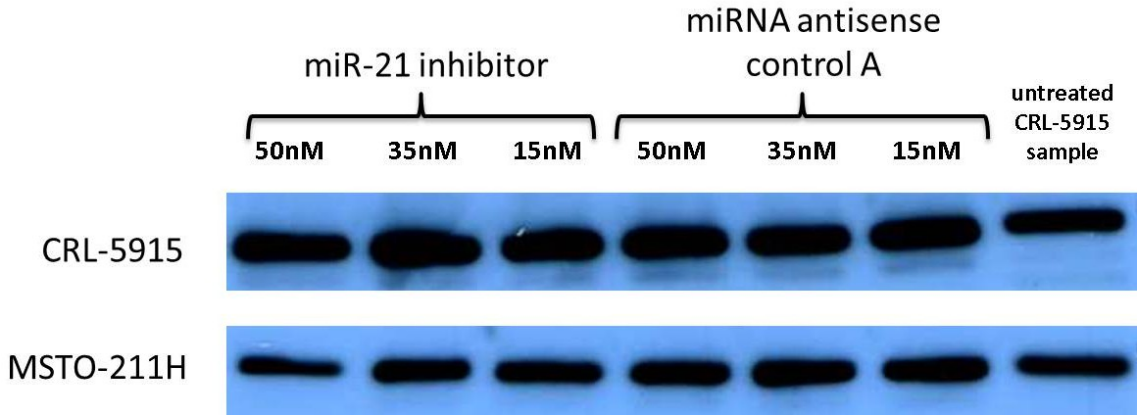

Figure 39: Western Blot analysis showing the effect of miR-21 inhibition on STAT3 expression on protein level in two mesothelioma cell lines (MSTO-211H and CRL-5915). Different concentrations (15nM, 35nM and 50nM) of the miR-inhibitor have been used. An untreated CRL-5915 sample has been used as control.

Using single miR-inhibitors or a combination of inhibitors that are supposed to target SOCS1 had no effect on SOCS1 protein expression. SOCS1 expression was only detected in an untreated sample of the control cell line HepG2 (see **Figure 40**).

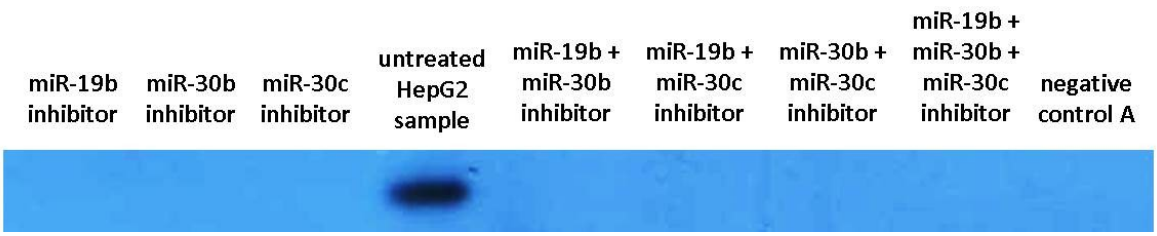

Figure 40: Western Blot analysis showing the effect of miR-inhibition (combination of inhibitors) on SOCS1 expression in CRL-5915. Inhibitors have been used with a final concentration of 100nM. An untreated HepG2 sample was used as control.

4. DISCUSSION

4.1 The role of BAP1 in malignant pleural mesothelioma

This study was published in *Pathology and Oncology Research*. [76]

Malignant pleural mesothelioma is an aggressive tumor that is resistant to current therapies [78] and due to its anatomical localization, it is a tumor in which early diagnosis is difficult and therefore MPM is often diagnosed in advanced stages when patients have a median survival of 6-12 months. But when patients are diagnosed at Stage IA, survival time of five or more years is not uncommon. [79, 80]There is an urgent need to know more about prognostic factors of outcome and driving forces, because of an increase of MPM worldwide.[81-84] In recent years, *BAP1* has been identified to be mutated in a wide variety of human tumors and it was stated that these germline mutations predispose to e.g. melanocytic tumors, meningioma, lung adenocarcinoma and malignant mesothelioma. [12, 85, 86] The existence of a *BAP1*-related cancer syndrome was reported, which is characterized by mesothelioma, uveal melanoma and possibly other cancer types. [86] Wiesner et al identified 19 *BAP1* germline mutation carriers in the three families they were investigating and they state that these mutation carriers are predisposed to the development of melanocytic skin lesions, uveal and cutaneous melanoma and mesothelioma with varying degrees of penetrance - only two patients with *BAP1* mutation were diagnosed with pleural mesothelioma. [87] It was reported that around 40% of MPM patients have a *BAP1* loss, a *BAP1* mutation or both and 32 different *BAP1* mutations have been identified so far. [88-90] Genomic alterations are seen frequently in MPM and *BAP1* gene inactivation occurs at very high frequency in patients with malignant epithelioid mesothelioma and this fact could also be useful for diagnosis. [90] It was also hypothesized that in patients who have a *BAP1* mutation and who have been exposed to asbestos, malignant mesothelioma predominates even though *BAP1* mutation alone may be sufficient to cause mesothelioma. [86]

While most of the published studies were dealing with the identification of specific mutations of the *BAP1* gene in MPM and other tumors and the consequences of mutant-BAP1 expression, the present study was focused on the impact of asbestos exposure on BAP1 expression and BAP1 as a possible prognostic factor of outcome. Most of the MPM cases used for the present study were not positively stained by the anti-BAP1 antibody

meaning that these cases most likely have a *BAP1* mutation. If this is equivalent to real *BAP1* mutations or caused by epigenetic downregulation of BAP1 still needs to be clarified in a subsequent study.

Asbestos exposure has no statistically significant effect on BAP1 expression in the 52 samples investigated. This indicates that asbestos exposure is not responsible for *BAP1* mutations or BAP1 downregulation in MPM. These results concur with previously published data where no correlation between *BAP1* mutation and asbestos exposure was detected. [88]

Several groups described the role of BAP1 in cell cycle progression and its function as a tumor suppressor. [13, 15, 91-93] Growth suppression *in vitro* and *in vivo* was achieved when cells - normally expressing mutant BAP1 – were re-expressing wild-type BAP1. [13, 15] Therefore it was expected that the expression of non-mutated BAP1 correlates with an increased overall survival and that mutations of this tumor suppressor gene lead to an earlier death. Surprisingly high BAP1 expression detected by immunohistochemistry correlates with shorter overall survival. That means that non-mutated*BAP1* resulting in BAP1 protein synthesis causes earlier death and therefore might cooperate with proteins causing progression and dismal outcome. In another study it was shown that there is no significant correlation between *BAP1* mutation and variables such as sex, histologic subtype and overall survival but a significant correlation of *BAP1* mutation and age was found – a mean age of 66.7 years in mutant *BAP1* compared to 58.6 years in wild-type *BAP1*. [88] These results are not confirmed by the present study since a statistically significant correlation between BAP1 expression and overall survival was detected and patients with wild-type BAP1 expression die earlier than those with no BAP1 expression, which indicates possible mutations in the *BAP1* gene.

BAP1 mutations were found in familial cases of MPM with no history of asbestos exposure. All of them were long-term survivors and showed negative immunohistochemical staining for BAP1. [86, 87] This goes along with the results obtained in the present study: improved survival in BAP1 negative MPM.

Only a few mutations common in malignant mesothelioma have been identified so far. Two frequent genetic alterations have been described: the most common are homozygous 9p21 deletions centered on *CDKN2A* found in up to 72% of tumors and 80% of MPM cell lines. [94] This deletion is predominantly found in short-term survivors and not in long-term survivors. [95]*NF2* loss through monosomy 22 or 22q deletions was described as another common event. [96] While several studies show that *BAP1* mutations frequently

occur and even predispose to malignant mesothelioma [79, 86, 88-90], one group described that there are no significant associations between *CDKN2A* loss and loss or mutation of *BAP1* or *NF2* which indicates that these three genetic events happen independently. [88]
To understand the cellular roles of BAP1, several groups have examined the proteins bound by BAP1 and possibly deubiquitinated by BAP1. Proteins identified include HCF1, ASXL1, ASXL2, FOXK1, FOXK2, ANKRD17, HAT1, UBE2O and AOF1. [97-99] BAP1 nuclear deubiquitinase seems to be involved in maintaining an appropriate level of regulatory ubiquitination of target histones, the HCF1 transcriptional co-factor and maybe other transcriptional proteins. [88, 92, 93] It has been reported that BAP1 binds to and deubiquitinates HCF1 in several cell lines and even in MPM cell lines [88, 97, 98] and that common BAP1 inactivation causes transcriptional deregulation in the pathogenesis of this highly lethal cancer. [88] Previous studies have shown that BAP1-HCF1 interaction may be important for HCF1-mediated growth effects.In doing so, HCF1 acts through modulation of transcription at E2F-responsive promoters. [80]Another research group looked specifically at the downstream targets of E2F – like Cyclin A2, E2F1, p107 and CDC25C – after BAP1 knockdown in MPM cell lines and they found that all the effectors were downregulated. These results go along with the possibility that BAP1 loss leads to post-translational inactivation of HCF1 and therefore downregulation of downstream E2F-responsive genes which are important for cell cycle progression. [88]

4.2 STAT signaling in malignant pleural mesothelioma

Parts of this study have already been published in *Virchows Archiv*.[33]

In previous investigations STAT1 was found to be upregulated [26] and turned out to function like an oncogene in MPM.[25] Therefore STAT1 function, the expression of the physiological inhibitor SOCS1 as well as the influence of IFN-γ on the STAT signaling pathway in MPM cell lines and human tissue samples was evaluated. Protein expression levels were evaluated by Western Blot and immunohistochemistry.
STAT1 was highly expressed in all six MPM cell lines and all tissue samples and it was impossible to increase STAT1 expression in MPM cell lines by IFN-γ treatment. The expression of pSTAT1-Y701 was already detected 15 minutes after IFN-γ treatment in MPM cell lines andprolonged treatment did not increase the expression any further. Phosphorylated STAT1-S727 was neither detected in untreated nor in IFN-γ treated

samples. Since pSTAT1-S727 was detected by immunohistochemistry, although at a very low level, it can be assumed that Western Blot analysis is not sensitive enough to detect these phosphorylated proteins within the total protein lysate of20µg. Phosphorylation is the prerequisite for STAT1 dimer formation, entry into the nucleus and DNA binding and gene activation.[100-102] However, it is not entirely clear, if both phosphorylation steps are necessary for dimer formation and DNA binding. Binding of STAT1 dimers to DNA induces transcription of several downstream targets such as SOCS1/3, the caspases Ice, Cpp32, and Ich-1, survivin and VEGF.[103, 104]

Survivin, a member of the family of inhibitor of apoptosis proteins, is known as a key regulator of mitosis and programmed cell death.[105] The overexpression of survivin is associated with resistance to chemotherapy or radiation therapy and is linked to poor prognosis.[106] Zimmermann et al. detected that IFN-γ induced STAT1 phosphorylation and they even examined the role of the IFN-γ signaling pathway on survivin expression in tumor specific T cells. They found that IFN-γ activated STAT1 binds to the survivin promoter site and activates survivin expression.[107] Since phosphorylation of STAT1 is even induced by IFN-γ in MPM cells, it is very likely that STAT1 functions as an oncogene through the STAT1/survivin pathway. A high survivin expression was even detected by IHC staining in the 52 MPM tissue samples used for the present study.This would nicely explain the quick development of resistance of MPM to chemotherapy. It seems that STAT1 does not induce proliferation but instead activates the expression of antiapoptotic proteins.

The impact of STAT1 expression on apoptosis – and cell cycle related genes was investigated. STAT1-mRNA was successfully knocked-down by using STAT1 siRNA in all three mesothelioma cell lines used for these experiments. The effect of STAT1 knock-down on the other components of the STAT signaling pathway differed between the cell lines: while CRL-5915 seems to compensate STAT1 knock-down by an upregulation of STAT5a, MSTO-211H and Hmeso show slightly upregulated expression levels of STAT3. SOCS1/2/3-mRNA as well as PIAS3 are upreglated in CRL-5915 while these mRNAs are only slightly upregulated or even downregulated in the other two cell lines. Most of the apoptosis- and cell cycle related genes were differentially expressed in MPM cell lines and only three genes (*F2R*, *IL10RA* and *CDKN1A*) were found to be either up- or downregulated in all cell lines. F2R and IL10RA belong to a group of receptors that bind and activate JAK proteins. [108, 109]CDKN1A, also known as p21, is a regulator of cell

cycle progression at the G1 phase, plays a regulatory role in S phase DNA replication and DNA damage repair and may be contributing in the execution of apoptosis. [110] Originally considered as a negative regulator of cell cycle and a tumor suppressor, it is now known that its function depends on its intracellular localization: when p21 is in the nucleus, it is a negative cell cycle regulator and tumor suppressor, whereas it acts like an oncogene by regulating migration, apoptosis and proliferation when localized in the cytoplasm. [111]*p21* was the first gene that was identified to be induced by p53[112] and it was shown that overexpression of p21 leads to growth arrest and that the increased expression is sufficient for the negative regulation of gene expression by p53 in H1299 (human non-small cell lung carcinoma cell line) cells. [113, 114]

STAT1 knock-down seems to have an effect on cell cycle progression and apoptosis by the upregulation of CDKN1A in mesothelioma cell lines used in the present study. However, no cell growth inhibition was detected microscopically after STAT1 knock-down. This indicates that STAT1 knock-down and the resulting upregulation of one gene are not enough to have an effect on proliferation and apoptosis in MPM cell lines. Anyway these results should be verified using other techniques to clarify if STAT1 has potential as a therapeutic target, which is of course only the case if proliferation and apoptosis are affected.

STAT3 was found to be lower expressed than STAT1 in all six MPM cell line and it was not possible to increase STAT3 expression by IFN-γ treatment. Phosphorylated STAT3-Y705 was not detected by Western Blot in MPM cell lines, but in a control cell lysate. This goes along with previous studies where phosphorylation of STAT3 was detected after Interleukin-6 treatment in different cell types. [115-118] In addition, an immunohistochemical staining with the anti-pSTAT3-Y705 antibody on tumor tissue samples was performed and a weak-positive but specific signal in a few cases was detected. These results indicate that only a very small amount of the downregulated STAT3 is phosphorylated on tyrosine 705 in MPM. STAT3 is known to have an oncogenic function and that it is constitutively activated in many human cancer cells.[119] It is involved in survivin upregulation and STAT3 activation can therefore inhibit apoptosis. The inhibition of STAT3 has been shown to result in downregulation of survivin expression.[105, 120] STAT3 is downregulated in MPM and only a very small part is activated by phosphorylation. These data indicate that STAT3 has no oncogenic function in MPM and that survivin expression is most probably not controlled by STAT3. Furthermore it was reported that STAT3 can be activated weakly by IFN-γ and that this

activation is much stronger in STAT1-null mouse embryo fibroblasts.[121] As STAT1 is upregulated in MPM, this could be an explanation for the missing activation of STAT3 by IFN-γ. Since the antiapoptotic function of STAT3 is probably taken over by STAT1, there might be no need for STAT3 activation.

STAT1 activity can be modulated through well characterized mechanisms including dephosphorylation, nuclear export and SOCS feedback inhibition. Additionally several negative regulators like PIAS, Nmi or SLIM are known. [122]PIAS1 binds to activated STAT1 dimers and PIAS3 specifically interacts with phosphorylated STAT3. Both can degrade pSTAT1/3 dimers by activating phosphatases within the nucleus, which in turn then dephosphorylate STAT dimers and furthermore facilitate SUMOylation for subsequent STAT1 degradation.[123, 124]PIAS1 is higher expressed than PIAS3 and both can degrade pSTAT1/3 dimers. But - given the high levels of STAT1 – might not inhibit their function. PIAS1 is a type 3 SUMOylase, butis not solely dedicated to STAT1 regulation [124, 125]and therefore their physiological function differs from that of SOCS proteins, which are induced in a classical negative feedback-loop, which is missing in MPM.

The negative regulator SOCS1 is normally translated and upregulated by STAT1, competes with STAT1 for the JAK1/2 binding site and thus abrogates the phosphorylation of STAT1 by JAK1/2.[121] In all MPM cases and cell lines SOCS1 protein was undetectable, which means that this negative feedback loop does not function, and STAT1 activation is not terminated by SOCS1.[126, 127]Constitutively STAT1 expression seems to provide MPM cells a selective growth and survival advantage. If this is only caused by missing SOCS1 expression or if other negative regulators play a role as well needs to be clarified by additional experiments.

STAT1 overexpression has been described to confer tumors resistance against radiation and cisplatin treatment.[128] Therefore better understanding of the mechanism underlying STAT1 activation and regulation could lead to successful strategies for targeting the STAT signaling pathway in MPM, probably by stimulating the negative feedback loop with analogues. It was reported previously that SOCS1 gene delivery cooperated with cisplatin plus pemetrexed to inhibit cell proliferation, invasiveness and induction of apoptosis in MPM cells. The authors hypothesize that SOCS1 gene delivery has a potent antitumor effect against MPM and that SOCS1 – in combination with cisplatin and pemetrexed – has potential for clinical use. [129] However, the effect of SOCS1 overexpression on STAT1/STAT3 expressionwas not investigated.

The expression pattern of STAT1, STAT3, SOCS1 and even SOCS3 on mRNA level differs from that on protein level: STAT1 and STAT3 were found to be downregulated compared to the housekeeping gene GAPDH in mesothelioma cell lines. It was possible to detect SOCS1 and SOCS3 mRNA – both were downregulated as well. The feasibility to detect SOCS mRNA but no SOCS protein in mesothelioma cell lines indicates that the translation process is inhibited or affected. And this is where miRNAs may come into play: they degrade mRNA or they prevent mRNA from being translated. Because of this fact and the promising results obtained in previous studies, where miRNA-30d-3p was identified as a possible regulator of pSTAT1-Y701 and maybe even STAT1 expression [26], the next step was to investigate the possible impact of miRNAs on the STAT signaling pathway in detail.

4.3 MicroRNAs in malignant pleural mesothelioma

The aggressiveness of malignant pleural mesothelioma is associated with genome and gene expression abnormalities, its diagnosis can be challenging and the knowledge about prognostic factors of outcome is poor. Therefore the identification of novel tumor markers may contribute to earlier detection, diagnosis and treatment of MPM. MiRNAs are often deregulated and function as oncogenes or tumor suppressors, they have potential as diagnostic markers and miRNA inhibitors can be used in disease treatment. This is why several research groups focused on the miRNA expression in MPM. [47, 58]

Specific miRNAs for each histopathological subtype have been identified as well as differentially expressed miRNAs in smokers compared to non-smokers. Guled et al. even reported that the miRNAs they identified, target genes most frequently affected in MPM like *CDKN2A*, *NF2*, *JUN*, *HGF* or *PDGFA*. [130]

MiR-126 was found to be downregulated in malignant tissue compared to normal pleura in different types of samples including serum, fresh tissue and FFPE samples. [68, 131, 132] One target of miR-126 is VEGF which can be found in high amounts in serum of MPM patients. Soluble mesothelin-related peptide (SMRP) is a specific marker for malignant mesothelioma. In subjects that had a high risk of developing MPM, a correlation between high levels of miR-126 and SMRP was found. These findings suggest that the association between miR-126 and SMRP could be used as a marker to detect MPM early. [68] High levels of VEGF were even found in human lung cancer cells, in which miR-126 was downregulated as well. [131] The downregulation of miR-126 in MPM was not confirmed

by the present study. By performing the miRNA profiling with 52 FFPE tumor tissue samples (epithelioid subtype), miR-126 was found to be highly upregulated.

MiRNAs belonging to the Oncomir-1 cluster (see Introduction) were found to be upregulated in MPM cells. MiRNAs, known to be downregulated in several tumors (miR-21, miR-29a, miR-30b and miR-106a), were even found to be deregulated. [133] These results go along with the findings of the present study: all mentioned miRNAs were upregulated.

Busacca et al. reported that miR-222 and miR-221 were downregulated in MPM cell lines. [134] Since these miRNAs are known to be negative regulators of the cyclin dependent kinase inhibitor (*CDKI*) p27 and the *PTEN* suppressor gene and are usually associated with poor prognosis, the downregulation of these miRNAs was somehow surprising. [135] In contrast to these results, miR-222 was found to be upregulated in MPM tumor tissue samples and MPM cell lines in the present study.

Subtype-related miRNAs were even correlated with better outcome: downregualtion of miR-30c was associated with better survival in MPM patients with sarcomatoid subtype, while this had no effect on epithelioid and biphasic subtypes. [134] In the present study, upregulation of miR-30c was detected in mesothelioma cell lines and epithelioid tumor tissue samples.

As mentioned previously, recurrent anomalies have been identified in MPM like the deletion of the 9p21.3 chromosome. It was shown that homozygous deletion of the miR-31 gene – which resides in the same area – and therefore a decreased expression, was associated with worse prognosis and short time to tumor recurrence. If miR-31 was re-expressed again, several important factors implicated in DNA replication and cell cycle progression were inhibited. These data indicate that miR-31 acts as tumor suppressor and has a high potential as therapeutic target. [67, 136]

That forcing the expression of specific miRNAs identifies potential targets for anti-cancer therapy, was shown by several studies. It was found that miR-1 was downregulated in MPM tissue compared to unaffected mesothelium. Overexpression of this miRNA induced inhibition of proliferation and apoptosis by increasing the expression of p16, p21, p53 and BAX while decreasing the expression of the antiapoptotic genes Survivin and BCL-2. [137] MiR-15 and miR-16 were found to be donwregulated in MPM tumor specimens and MPM cell lines. Forced expression of miR-15 and miR-16 resulted in growth inhibition in MPM cell lines but not in the normal mesothelial cell line Met5A. Re-expression of miR-16 even sensitized MPM cells to pemetrexed and gemcitabine. [138] In

contrast to that, miR-16 was found to be highly upregulated (compared to the endogenous control RNU44) in MPM tumor tissue samples in the present study. This difference may be caused by different histological subtype, patients' treatment or control groups.

Additionally it was reported that chemotherapeutic agents have an influence on miRNA expression: the agent Onconase – a single peptide chain that induces intracellular RNA degradation – induced an increase in miR-17* expression, while miR-30c was significantly downregulated in all cell lines as well as *NF-KB* and its downstream targets resulting in apoptosis and a less aggressive behavior. [139]

All these results demonstrate the advantages of miRNAs. Therefore the present study focused on the investigation of a totally deregulated signaling pathway and the possible impact of miRNAs. Three miRNAs (miR-17, miR-106a and miR-21) – targeting STAT3 – were found to be upregulated. However, none of these miRNAshas a statistically significant impact on STAT3 expression in malignant pleural mesothelioma. Since miR-21 is extremely upregulated and associated with a wide variety of human tumors, it is very likely that this miRNA plays an important role in MPM as well, even though STAT3 is not affected. This needs further investigations and correlations with other regulatory proteins involved in MPM proliferation and survival.

Four upregulated miRNAs (miR-19b, -30b, -30c and -222) have been identified, which are predicted to target SOCS1 and SOCS3. It was not possible to detect SOCS1/3 protein expression, but SOCS1/3-mRNA was detected in all cell lines even though the expression was downregulated in relation to the housekeeping gene GAPDH. These results suggest that the translation process might be inhibited or affected by miRNAs. Therefore high miRNA expression could definitely be the reason for downregulation or the missing expression of proteins. What has to be pointed out is that the same expression patterns have been detected for the control cell line HepG2: SOCS1/3-mRNA was downregulated whereas miR-19b, -30b, -30c and -222 were downregulated. Since SOCS1 protein is expressed in HepG2 cells, the identified miRNAs do not have an influence on SOCS expression in this cell line. However, as reported previously, results differ due to different subtypes or sample source of the same tumor [140] and it is not surprising that results vary between different types of tumors. Therefore it is possible that the identified miRNAs do not regulate the STAT signaling pathway in HepG2 cells but have a regulatory effect in MPM cell lines. Unfortunately it was not possible to affect STAT3 or SOCS1 expression in MPM cell lines by inhibiting miRNA expression.

Transfection efficiency has been tested by qPCR, which is definitely not the Gold standard. If transfection is inefficient, it is often because knockdown oligonucleotides are retained on the outside of the cell membrane or are sequestered in internal vesicles, physically separated from their miRNA targets in the cytoplasm. But during cell lysis these oligonucleotides are released and will interact with miRNAs in the lysate. Real-time PCR can therefore not distinguish between biologically relevant complexes that formed in the cytoplasm of transfected cells and complexes that formed following cell lysis. What was shown with this experiment was that all inhibitors were specifically working in general. However, the inhibitors (LNA^{TM} oligonucleotides) used in the present study, are single-stranded molecules and have therefore a lower molecular weight than the siRNAs used to knock-down STAT1 expression. Since these transfections were successfully performed, without problems using the same reagents, the transfections with miRNA inhibitors should have been successful as well.

MiRNA expression patterns have been evaluated between MPM FFPE samples and non-neoplastic pleura specimens, between cell lines and tumor tissues or between MPM subtypes and different expression patterns for a few miRNAs have been detected between tumor tissues and MPM cell lines. [65, 135, 141] Results are not the same due to different subtypes, sample sources, control groups, normalization techniques and qPCR and microarray analyses. This explains, why different research groups report different miRNA expression patterns, even though they are all investigating the same tumor. Due to the fact that data from cell lines do not always correlate in a biologically relevant manner with data from human tumors, it is not feasible to really compare *in vitro* and *in vivo* results. [140]

5. OVERALL CONCLUSIONS

The present study provides new evidence that STAT signaling is totally deregulated in MPM: STAT1 is upregulated, whereas STAT3 is downregulated. The physiologic regulation of STAT1 via SOCS1 is completely lost in MPM and it does not seem that the miRNAs identified by now, are the (only) reason for the missing expression of SOCS1 and SOCS3.Since it was shown that SOCS1 has a potent antitumor effect against MPM the reasons for the missing expression should be found.

Most likely STAT1 and phosphorylated STAT1 play a criticalrole in the pathogenesis of MPM by acting like an oncogene through activation of antiapoptotic molecules. MPM cell lines compensate STAT1 knock-down either by increasing the expression of STAT5a or STAT3, two genes which are generally considered to be oncogenes. The expression of CDKN1A/p21 was increased in all mesothelioma cell lines. The overexpression of p21 was shown to be sufficient for the negative regulation of gene expression by p53 in a human non-small cell lung carcinoma cell line. Unfortunately, no cell growth inhibition was detected microscopically after STAT1 knock-down in the mesothelioma cell lines investigated. This indicates that STAT1 knock-down and the resulting upregulation of one gene are not enough to have an effect on proliferation and apoptosis in MPM cell lines.

Therefore, further investigation need to be performed to identify additional apoptosis- and cell cycle related genes that are affected by STAT1 knock-down to clarify, if STAT1 has potential as therapeutic target in malignant pleural mesothelioma.

6. REFERENCES

1. Attanoos, R.L. and A.R. Gibbs, Pathology of malignant mesothelioma.*Histopathology*, 1997. **30**(5): p. 403-18.
2. Thompson, J.K., C.M. Westbom, and A. Shukla, Malignant mesothelioma: development to therapy.*J Cell Biochem*, 2014. **115**(1): p. 1-7.
3. Henderson, D.W., G. Reid, S.C. Kao, et al., Challenges and controversies in the diagnosis of malignant mesothelioma: Part 2. Malignant mesothelioma subtypes, pleural synovial sarcoma, molecular and prognostic aspects of mesothelioma, BAP1, aquaporin-1 and microRNA.*J Clin Pathol*, 2013. **66**(10): p. 854-61.
4. Ismail-Khan, R., L.A. Robinson, C.C. Williams, Jr., et al., Malignant pleural mesothelioma: a comprehensive review.*Cancer Control*, 2006. **13**(4): p. 255-63.
5. Carbone, M. and H. Yang, Molecular pathways: targeting mechanisms of asbestos and erionite carcinogenesis in mesothelioma.*Clin Cancer Res*, 2012. **18**(3): p. 598-604.
6. Zucali, P.A. and G. Giaccone, Biology and management of malignant pleural mesothelioma.*Eur J Cancer*, 2006. **42**(16): p. 2706-14.
7. Wagner, J.C., C.A. Sleggs, and P. Marchand, Diffuse pleural mesothelioma and asbestos exposure in the North Western Cape Province.*Br J Ind Med*, 1960. **17**: p. 260-71.
8. Ilgren, E.B. and K. Browne, Asbestos-related mesothelioma: evidence for a threshold in animals and humans.*Regul Toxicol Pharmacol*, 1991. **13**(2): p. 116-32.
9. World Health Organization - History of Fighting Against the Toxic Substance, Asbestos.*2012 November 26*, 2012: p. available from: http://www.asbestos.com/asbestos/who.php.
10. Carbone, M., S. Emri, A.U. Dogan, et al., A mesothelioma epidemic in Cappadocia: scientific developments and unexpected social outcomes.*Nat Rev Cancer*, 2007. **7**(2): p. 147-54.
11. Lopez-Rios, F., P.B. Illei, V. Rusch, and M. Ladanyi, Evidence against a role for SV40 infection in human mesotheliomas and high risk of false-positive PCR results owing to presence of SV40 sequences in common laboratory plasmids.*Lancet*, 2004. **364**(9440): p. 1157-66.
12. Wiesner, T., A.C. Obenauf, R. Murali, et al., Germline mutations in BAP1 predispose to melanocytic tumors.*Nat Genet*, 2011. **43**(10): p. 1018-21.

13. Jensen, D.E., M. Proctor, S.T. Marquis, et al., BAP1: a novel ubiquitin hydrolase which binds to the BRCA1 RING finger and enhances BRCA1-mediated cell growth suppression.*Oncogene*, 1998. **16**(9): p. 1097-112.
14. Jensen, D.E. and F.J. Rauscher, 3rd, BAP1, a candidate tumor suppressor protein that interacts with BRCA1.*Ann N Y Acad Sci*, 1999. **886**: p. 191-4.
15. Ventii, K.H., N.S. Devi, K.L. Friedrich, et al., BRCA1-associated protein-1 is a tumor suppressor that requires deubiquitinating activity and nuclear localization.*Cancer Res*, 2008. **68**(17): p. 6953-62.
16. Harbour, J.W., M.D. Onken, E.D. Roberson, et al., Frequent mutation of BAP1 in metastasizing uveal melanomas.*Science*, 2010. **330**(6009): p. 1410-3.
17. Shukla, A., M. Gulumian, T.K. Hei, et al., Multiple roles of oxidants in the pathogenesis of asbestos-induced diseases.*Free Radic Biol Med*, 2003. **34**(9): p. 1117-29.
18. Nowak, A.K., R.A. Lake, H.L. Kindler, and B.W. Robinson, New approaches for mesothelioma: biologics, vaccines, gene therapy, and other novel agents.*Semin Oncol*, 2002. **29**(1): p. 82-96.
19. Boutin, C., E. Nussbaum, I. Monnet, et al., Intrapleural treatment with recombinant gamma-interferon in early stage malignant pleural mesothelioma.*Cancer*, 1994. **74**(9): p. 2460-7.
20. Hand, A., K. Pelin, K. Mattson, and K. Linnainmaa, Interferon (IFN)-alpha and IFN-gamma in combination with methotrexate: in vitro sensitivity studies in four human mesothelioma cell lines.*Anticancer Drugs*, 1995. **6**(1): p. 77-82.
21. Hand, A.M., K. Husgafvel-Pursiainen, K. Pelin, et al., Interferon-alpha and -gamma in combination with chemotherapeutic drugs: in vitro sensitivity studies in four human mesothelioma cell lines.*Anticancer Drugs*, 1992. **3**(6): p. 687-94.
22. Hand, A.M., K. Husgafvel-Pursiainen, L. Tammilehto, et al., Malignant mesothelioma: the antiproliferative effect of cytokine combinations on three human mesothelioma cell lines.*Cancer Lett*, 1991. **58**(3): p. 205-10.
23. Phan-Bich, L., A. Buard, J.F. Petit, et al., Differential responsiveness of human and rat mesothelioma cell lines to recombinant interferon-gamma.*Am J Respir Cell Mol Biol*, 1997. **16**(2): p. 178-86.
24. Buard, A., C. Vivo, I. Monnet, et al., Human malignant mesothelioma cell growth: activation of janus kinase 2 and signal transducer and activator of transcription 1alpha for inhibition by interferon-gamma.*Cancer Res*, 1998. **58**(4): p. 840-7.

25. Kothmaier, H., F. Quehenberger, I. Halbwedl, et al., EGFR and PDGFR differentially promote growth in malignant epithelioid mesothelioma of short and long term survivors.*Thorax*, 2008. **63**(4): p. 345-51.
26. Arzt, L., H. Kothmaier, F. Quehenberger, et al., STAT signalling in malignant mesothelioma: Is there a regulatory effect of microRNAs? *Magazine of European Medical Oncology*, 2011. **4**(1): p. 38-42.
27. Rawlings, J.S., K.M. Rosler, and D.A. Harrison, The JAK/STAT signaling pathway.*J Cell Sci*, 2004. **117**(Pt 8): p. 1281-3.
28. Calo, V., M. Migliavacca, V. Bazan, et al., STAT proteins: from normal control of cellular events to tumorigenesis.*J Cell Physiol*, 2003. **197**(2): p. 157-68.
29. Espert, L., I. Dusanter-Fourt, and M.K. Chelbi-Alix, [Negative regulation of the JAK/STAT: pathway implication in tumorigenesis].*Bull Cancer*, 2005. **92**(10): p. 845-57.
30. Kile, B.T., B.A. Schulman, W.S. Alexander, et al., The SOCS box: a tale of destruction and degradation.*Trends Biochem Sci*, 2002. **27**(5): p. 235-41.
31. Starr, R. and D.J. Hilton, SOCS: suppressors of cytokine signalling.*Int J Biochem Cell Biol*, 1998. **30**(10): p. 1081-5.
32. Wormald, S. and D.J. Hilton, Inhibitors of cytokine signal transduction.*J Biol Chem*, 2004. **279**(2): p. 821-4.
33. Arzt, L., H. Kothmaier, I. Halbwedl, et al., Signal transducer and activator of transcription 1 (STAT1) acts like an oncogene in malignant pleural mesothelioma.*Virchows Arch*, 2014. **465**(1): p. 79-88.
34. Greenhalgh, C.J., D. Metcalf, A.L. Thaus, et al., Biological evidence that SOCS-2 can act either as an enhancer or suppressor of growth hormone signaling.*J Biol Chem*, 2002. **277**(43): p. 40181-4.
35. Schmitz, J., M. Weissenbach, S. Haan, et al., SOCS3 exerts its inhibitory function on interleukin-6 signal transduction through the SHP2 recruitment site of gp130.*J Biol Chem*, 2000. **275**(17): p. 12848-56.
36. Yoshimura, A., T. Ohkubo, T. Kiguchi, et al., A novel cytokine-inducible gene CIS encodes an SH2-containing protein that binds to tyrosine-phosphorylated interleukin 3 and erythropoietin receptors.*EMBO J*, 1995. **14**(12): p. 2816-26.
37. Kamizono, S., T. Hanada, H. Yasukawa, et al., The SOCS box of SOCS-1 accelerates ubiquitin-dependent proteolysis of TEL-JAK2.*J Biol Chem*, 2001. **276**(16): p. 12530-8.

38. Fire, A., S. Xu, M.K. Montgomery, et al., Potent and specific genetic interference by double-stranded RNA in Caenorhabditis elegans.*Nature*, 1998. **391**(6669): p. 806-11.
39. Montgomery, M.K., S. Xu, and A. Fire, RNA as a target of double-stranded RNA-mediated genetic interference in Caenorhabditis elegans.*Proc Natl Acad Sci U S A*, 1998. **95**(26): p. 15502-7.
40. Stark, G.R., I.M. Kerr, B.R. Williams, et al., How cells respond to interferons.*Annu Rev Biochem*, 1998. **67**: p. 227-64.
41. Elbashir, S.M., W. Lendeckel, and T. Tuschl, RNA interference is mediated by 21- and 22-nucleotide RNAs.*Genes Dev*, 2001. **15**(2): p. 188-200.
42. Elbashir, S.M., J. Harborth, W. Lendeckel, et al., Duplexes of 21-nucleotide RNAs mediate RNA interference in cultured mammalian cells.*Nature*, 2001. **411**(6836): p. 494-8.
43. Hammond, S.M., E. Bernstein, D. Beach, and G.J. Hannon, An RNA-directed nuclease mediates post-transcriptional gene silencing in Drosophila cells.*Nature*, 2000. **404**(6775): p. 293-6.
44. Martinez, J., A. Patkaniowska, H. Urlaub, et al., Single-stranded antisense siRNAs guide target RNA cleavage in RNAi.*Cell*, 2002. **110**(5): p. 563-74.
45. NCBI, RNA Interference.*http://www.ncbi.nlm.nih.gov/projects/genome/probe/doc/TechRnai.shtml*.
46. Dorsett, Y. and T. Tuschl, siRNAs: applications in functional genomics and potential as therapeutics.*Nat Rev Drug Discov*, 2004. **3**(4): p. 318-29.
47. Meola, N., V.A. Gennarino, and S. Banfi, microRNAs and genetic diseases.*Pathogenetics*, 2009. **2**(1): p. 7.
48. Gregory, R.I., K.P. Yan, G. Amuthan, et al., The Microprocessor complex mediates the genesis of microRNAs.*Nature*, 2004. **432**(7014): p. 235-40.
49. Shenouda, S.K. and S.K. Alahari, MicroRNA function in cancer: oncogene or a tumor suppressor? *Cancer Metastasis Rev*, 2009. **28**(3-4): p. 369-78.
50. Cai, X., C.H. Hagedorn, and B.R. Cullen, Human microRNAs are processed from capped, polyadenylated transcripts that can also function as mRNAs.*RNA*, 2004. **10**(12): p. 1957-66.
51. Carthew, R.W., Gene regulation by microRNAs.*Curr Opin Genet Dev*, 2006. **16**(2): p. 203-8.

52. Denli, A.M., B.B. Tops, R.H. Plasterk, et al., Processing of primary microRNAs by the Microprocessor complex.*Nature*, 2004. **432**(7014): p. 231-5.
53. Han, J., Y. Lee, K.H. Yeom, et al., The Drosha-DGCR8 complex in primary microRNA processing.*Genes Dev*, 2004. **18**(24): p. 3016-27.
54. Lee, Y., C. Ahn, J. Han, et al., The nuclear RNase III Drosha initiates microRNA processing.*Nature*, 2003. **425**(6956): p. 415-9.
55. Bohnsack, M.T., K. Czaplinski, and D. Gorlich, Exportin 5 is a RanGTP-dependent dsRNA-binding protein that mediates nuclear export of pre-miRNAs.*RNA*, 2004. **10**(2): p. 185-91.
56. Gregory, R.I., T.P. Chendrimada, N. Cooch, and R. Shiekhattar, Human RISC couples microRNA biogenesis and posttranscriptional gene silencing.*Cell*, 2005. **123**(4): p. 631-40.
57. Lim, L.P., N.C. Lau, P. Garrett-Engele, et al., Microarray analysis shows that some microRNAs downregulate large numbers of target mRNAs.*Nature*, 2005. **433**(7027): p. 769-73.
58. Zhang, B., X. Pan, G.P. Cobb, and T.A. Anderson, microRNAs as oncogenes and tumor suppressors.*Dev Biol*, 2007. **302**(1): p. 1-12.
59. Hayashita, Y., H. Osada, Y. Tatematsu, et al., A polycistronic microRNA cluster, miR-17-92, is overexpressed in human lung cancers and enhances cell proliferation.*Cancer Res*, 2005. **65**(21): p. 9628-32.
60. Hammond, S.M., RNAi, microRNAs, and human disease.*Cancer Chemother Pharmacol*, 2006. **58 Suppl 1**: p. s63-8.
61. Johnson, C.D., A. Esquela-Kerscher, G. Stefani, et al., The let-7 microRNA represses cell proliferation pathways in human cells.*Cancer Res*, 2007. **67**(16): p. 7713-22.
62. Johnson, S.M., H. Grosshans, J. Shingara, et al., RAS is regulated by the let-7 microRNA family.*Cell*, 2005. **120**(5): p. 635-47.
63. Takamizawa, J., H. Konishi, K. Yanagisawa, et al., Reduced expression of the let-7 microRNAs in human lung cancers in association with shortened postoperative survival.*Cancer Res*, 2004. **64**(11): p. 3753-6.
64. Benjamin, H., D. Lebanony, S. Rosenwald, et al., A diagnostic assay based on microRNA expression accurately identifies malignant pleural mesothelioma.*J Mol Diagn*, 2010. **12**(6): p. 771-9.

65. Gee, G.V., D.C. Koestler, B.C. Christensen, et al., Downregulated MicroRNAs in the differential diagnosis of malignant pleural mesothelioma.*Int J Cancer*, 2010.**127**(12): p. 2859-69.
66. Pass, H.I., C. Goparaju, S. Ivanov, et al., hsa-miR-29c* is linked to the prognosis of malignant pleural mesothelioma.*Cancer Res*, 2010. **70**(5): p. 1916-24.
67. Ivanov, S.V., C.M. Goparaju, P. Lopez, et al., Pro-tumorigenic effects of miR-31 loss in mesothelioma.*J Biol Chem*, 2010. **285**(30): p. 22809-17.
68. Santarelli, L., E. Strafella, S. Staffolani, et al., Association of MiR-126 with soluble mesothelin-related peptides, a marker for malignant mesothelioma.*PLoS One*, 2011. **6**(4): p. e18232.
69. Kirschner, M.B., Y.Y. Cheng, B. Badrian, et al., Increased circulating miR-625-3p: a potential biomarker for patients with malignant pleural mesothelioma.*J Thorac Oncol*, 2012. **7**(7): p. 1184-91.
70. Janssen, H.L., H.W. Reesink, E.J. Lawitz, et al., Treatment of HCV infection by targeting microRNA.*N Engl J Med*, 2013. **368**(18): p. 1685-94.
71. Clinicaltrials.gov, A Multicenter Phase I Study of MRX34.*http://clinicaltrials.gov/show/NCT01829971*, 2013.
72. Exiqon, LNA technology *http://www.exiqon.com/lna-technology*, 2013.
73. Arzt, L., H. Kothmaier, F. Quehenberger, et al., Evaluation of formalin-free tissue fixation for RNA and microRNA studies.*Exp Mol Pathol*, 2011. **91**(2): p. 490-495.
74. Reale, F.R., T.W. Griffin, J.M. Compton, et al., Characterization of a human malignant mesothelioma cell line (H-MESO-1): a biphasic solid and ascitic tumor model.*Cancer Res*, 1987. **47**(12): p. 3199-205.
75. Shukla, A., J.M. Hillegass, M.B. MacPherson, et al., Blocking of ERK1 and ERK2 sensitizes human mesothelioma cells to doxorubicin.*Mol Cancer*, 2010. **9**: p. 314.
76. Arzt, L., F. Quehenberger, I. Halbwedl, et al., BAP1 protein is a progression factor in malignant pleural mesothelioma.*Pathol Oncol Res*, 2014. **20**(1): p. 145-51.
77. Pichiorri, F., S.S. Suh, M. Ladetto, et al., MicroRNAs regulate critical genes associated with multiple myeloma pathogenesis.*Proc Natl Acad Sci U S A*, 2008. **105**(35): p. 12885-90.
78. Flores, R.M., H.I. Pass, V.E. Seshan, et al., Extrapleural pneumonectomy versus pleurectomy/decortication in the surgical management of malignant pleural mesothelioma: results in 663 patients.*J Thorac Cardiovasc Surg*, 2008. **135**(3): p. 620-6, 626 e1-3.

79. Carbone, M., L. Korb Ferris, F. Baumann, et al., BAP1 cancer syndrome: malignant mesothelioma, uveal and cutaneous melanoma, and MBAITs.*J Transl Med*, 2012. **10**(1): p. 179.
80. Flores, R.M., Surgical options in malignant pleural mesothelioma: extrapleural pneumonectomy or pleurectomy/decortication.*Semin Thorac Cardiovasc Surg*, 2009. **21**(2): p. 149-53.
81. Belli, C., D. Fennell, M. Giovannini, et al., Malignant pleural mesothelioma: current treatments and emerging drugs.*Expert Opin Emerg Drugs*, 2009. **14**(3): p. 423-37.
82. Neragi-Miandoab, S., Multimodality approach in management of malignant pleural mesothelioma.*Eur J Cardiothorac Surg*, 2006. **29**(1): p. 14-9.
83. Paleari, L., N. Rotolo, A. Imperatori, et al., Osteopontin is not a specific marker in malignant pleural mesothelioma.*Int J Biol Markers*, 2009. **24**(2): p. 112-7.
84. Treasure, T. and A. Sedrakyan, Pleural mesothelioma: little evidence, still time to do trials.*Lancet*, 2004. **364**(9440): p. 1183-5.
85. Abdel-Rahman, M.H., R. Pilarski, C.M. Cebulla, et al., Germline BAP1 mutation predisposes to uveal melanoma, lung adenocarcinoma, meningioma, and other cancers.*J Med Genet*, 2011. **48**(12): p. 856-9.
86. Testa, J.R., M. Cheung, J. Pei, et al., Germline BAP1 mutations predispose to malignant mesothelioma.*Nat Genet*, 2011. **43**(10): p. 1022-5.
87. Wiesner, T., I. Fried, P. Ulz, et al., Toward an Improved Definition of the Tumor Spectrum Associated With BAP1 Germline Mutations.*J Clin Oncol*, 2012.**30**(32): p. e337-40.
88. Bott, M., M. Brevet, B.S. Taylor, et al., The nuclear deubiquitinase BAP1 is commonly inactivated by somatic mutations and 3p21.1 losses in malignant pleural mesothelioma.*Nat Genet*, 2011. **43**(7): p. 668-72.
89. Ladanyi, M., M.G. Zauderer, L.M. Krug, et al., New Strategies in Pleural Mesothelioma: BAP1 and NF2 as novel targets for therapeutic development and risk assessment.*Clin Cancer Res*, 2012.**18**(17): p. 4485-90
90. Yoshikawa, Y., A. Sato, T. Tsujimura, et al., Frequent inactivation of the BAP1 gene in epithelioid-type malignant mesothelioma.*Cancer Sci*, 2012. **103**(5): p. 868-74.
91. Kittler, R., L. Pelletier, A.K. Heninger, et al., Genome-scale RNAi profiling of cell division in human tissue culture cells.*Nat Cell Biol*, 2007. **9**(12): p. 1401-12.

92. Mallery, D.L., C.J. Vandenberg, and K. Hiom, Activation of the E3 ligase function of the BRCA1/BARD1 complex by polyubiquitin chains.*EMBO J*, 2002. **21**(24): p. 6755-62.
93. Schlabach, M.R., J. Luo, N.L. Solimini, et al., Cancer proliferation gene discovery through functional genomics.*Science*, 2008. **319**(5863): p. 620-4.
94. Illei, P.B., V.W. Rusch, M.F. Zakowski, and M. Ladanyi, Homozygous deletion of CDKN2A and codeletion of the methylthioadenosine phosphorylase gene in the majority of pleural mesotheliomas.*Clin Cancer Res*, 2003. **9**(6): p. 2108-13.
95. Dacic, S., H. Kothmaier, S. Land, et al., Prognostic significance of p16/cdkn2a loss in pleural malignant mesotheliomas.*Virchows Arch*, 2008. **453**(6): p. 627-35.
96. Thurneysen, C., I. Opitz, S. Kurtz, et al., Functional inactivation of NF2/merlin in human mesothelioma.*Lung Cancer*, 2009. **64**(2): p. 140-7.
97. Machida, Y.J., Y. Machida, A.A. Vashisht, et al., The deubiquitinating enzyme BAP1 regulates cell growth via interaction with HCF-1.*J Biol Chem*, 2009. **284**(49): p. 34179-88.
98. Misaghi, S., S. Ottosen, A. Izrael-Tomasevic, et al., Association of C-terminal ubiquitin hydrolase BRCA1-associated protein 1 with cell cycle regulator host cell factor 1.*Mol Cell Biol*, 2009. **29**(8): p. 2181-92.
99. Sowa, M.E., E.J. Bennett, S.P. Gygi, and J.W. Harper, Defining the human deubiquitinating enzyme interaction landscape.*Cell*, 2009. **138**(2): p. 389-403.
100. Ma, J. and X. Cao, Regulation of Stat3 nuclear import by importin alpha5 and importin alpha7 via two different functional sequence elements.*Cell Signal*, 2006. **18**(8): p. 1117-26.
101. Wenta, N., H. Strauss, S. Meyer, and U. Vinkemeier, Tyrosine phosphorylation regulates the partitioning of STAT1 between different dimer conformations.*Proc Natl Acad Sci U S A*, 2008. **105**(27): p. 9238-43.
102. McBride, K.M., G. Banninger, C. McDonald, and N.C. Reich, Regulated nuclear import of the STAT1 transcription factor by direct binding of importin-alpha.*Embo J*, 2002. **21**(7): p. 1754-63.
103. Kumar, A., M. Commane, T.W. Flickinger, et al., Defective TNF-alpha-induced apoptosis in STAT1-null cells due to low constitutive levels of caspases.*Science*, 1997. **278**(5343): p. 1630-2.
104. Klampfer, L., The role of signal transducers and activators of transcription in colon cancer.*Front Biosci*, 2008. **13**: p. 2888-99.

105. Mita, A.C., M.M. Mita, S.T. Nawrocki, and F.J. Giles, Survivin: key regulator of mitosis and apoptosis and novel target for cancer therapeutics.*Clin Cancer Res*, 2008. **14**(16): p. 5000-5.
106. Kanwar, R.K., C.H. Cheung, J.Y. Chang, and J.R. Kanwar, Recent advances in anti-survivin treatments for cancer.*Curr Med Chem*, 2010. **17**(15): p. 1509-15.
107. Zimmerman, M., D. Yang, X. Hu, et al., IFN-gamma upregulates survivin and Ifi202 expression to induce survival and proliferation of tumor-specific T cells.*PLoS One*, 2010. **5**(11): p. e14076.
108. NCBI, F2R coagulation factor II (thrombin) receptor *http://www.ncbi.nlm.nih.gov/gene/2149*.
109. NCBI, IL10RA interleukin 10 receptor, alpha *http://www.ncbi.nlm.nih.gov/gene/3587*.
110. NCBI, CDKN1A cyclin-dependent kinase inhibitor 1A (p21, Cip1).*http://www.ncbi.nlm.nih.gov/gene/1026*.
111. Romanov, V.S., V.A. Pospelov, and T.V. Pospelova, Cyclin-dependent kinase inhibitor p21(Waf1): contemporary view on its role in senescence and oncogenesis.*Biochemistry (Mosc)*, 2012. **77**(6): p. 575-84.
112. el-Deiry, W.S., T. Tokino, V.E. Velculescu, et al., WAF1, a potential mediator of p53 tumor suppression.*Cell*, 1993. **75**(4): p. 817-25.
113. Lohr, K., C. Moritz, A. Contente, and M. Dobbelstein, p21/CDKN1A mediates negative regulation of transcription by p53.*J Biol Chem*, 2003. **278**(35): p. 32507-16.
114. Wang, Y., G. Blandino, and D. Givol, Induced p21waf expression in H1299 cell line promotes cell senescence and protects against cytotoxic effect of radiation and doxorubicin.*Oncogene*, 1999. **18**(16): p. 2643-9.
115. Berishaj, M., S.P. Gao, S. Ahmed, et al., Stat3 is tyrosine-phosphorylated through the interleukin-6/glycoprotein 130/Janus kinase pathway in breast cancer.*Breast Cancer Res*, 2007. **9**(3): p. R32.
116. Braun, D.A., M. Fribourg, and S.C. Sealfon, Cytokine response is determined by duration of receptor and signal transducers and activators of transcription 3 (STAT3) activation.*J Biol Chem*, 2013. **288**(5): p. 2986-93.
117. Russell, M.A., A.C. Cooper, S. Dhayal, and N.G. Morgan, Differential effects of interleukin-13 and interleukin-6 on Jak/STAT signaling and cell viability in pancreatic beta-cells.*Islets*, 2013. **5**(2): p. 95-105.

118. Yang, X., L. Liang, X.F. Zhang, et al., MicroRNA-26a suppresses tumor growth and metastasis of human hepatocellular carcinoma by targeting IL-6-Stat3 pathway.*Hepatology*, 2014.**59**(5): p. 1874-85

119. Bromberg, J., Stat proteins and oncogenesis.*J Clin Invest*, 2002. **109**(9): p. 1139-42.

120. Aoki, Y., G.M. Feldman, and G. Tosato, Inhibition of STAT3 signaling induces apoptosis and decreases survivin expression in primary effusion lymphoma.*Blood*, 2003. **101**(4): p. 1535-42.

121. Qing, Y. and G.R. Stark, Alternative activation of STAT1 and STAT3 in response to interferon-gamma.*J Biol Chem*, 2004. **279**(40): p. 41679-85.

122. Schindler, C., D.E. Levy, and T. Decker, JAK-STAT signaling: from interferons to cytokines.*J Biol Chem*, 2007. **282**(28): p. 20059-63.

123. Liao, J., Y. Fu, and K. Shuai, Distinct roles of the NH2- and COOH-terminal domains of the protein inhibitor of activated signal transducer and activator of transcription (STAT) 1 (PIAS1) in cytokine-induced PIAS1-Stat1 interaction.*Proc Natl Acad Sci U S A*, 2000. **97**(10): p. 5267-72.

124. Ungureanu, D., S. Vanhatupa, N. Kotaja, et al., PIAS proteins promote SUMO-1 conjugation to STAT1.*Blood*, 2003. **102**(9): p. 3311-3.

125. Lee, J.H., S.M. Park, O.S. Kim, et al., Differential SUMOylation of LXRalpha and LXRbeta mediates transrepression of STAT1 inflammatory signaling in IFN-gamma-stimulated brain astrocytes.*Mol Cell*, 2009. **35**(6): p. 806-17.

126. Madonna, S., C. Scarponi, O. De Pita, and C. Albanesi, Suppressor of cytokine signaling 1 inhibits IFN-gamma inflammatory signaling in human keratinocytes by sustaining ERK1/2 activation.*Faseb J*, 2008. **22**(9): p. 3287-97.

127. Lesinski, G.B., J.M. Zimmerer, M. Kreiner, et al., Modulation of SOCS protein expression influences the interferon responsiveness of human melanoma cells.*BMC Cancer*, 2010. **10**: p. 142.

128. Klampfer, L., Signal transducers and activators of transcription (STATs): Novel targets of chemopreventive and chemotherapeutic drugs.*Curr Cancer Drug Targets*, 2006. **6**(2): p. 107-21.

129. Iwahori, K., S. Serada, M. Fujimoto, et al., SOCS-1 gene delivery cooperates with cisplatin plus pemetrexed to exhibit preclinical antitumor activity against malignant pleural mesothelioma.*Int J Cancer*, 2013. **132**(2): p. 459-71.

130. Guled, M., L. Lahti, P.M. Lindholm, et al., CDKN2A, NF2, and JUN are dysregulated among other genes by miRNAs in malignant mesothelioma -A miRNA microarray analysis.*Genes Chromosomes Cancer*, 2009. **48**(7): p. 615-23.
131. Liu, B., X.C. Peng, X.L. Zheng, et al., MiR-126 restoration down-regulate VEGF and inhibit the growth of lung cancer cell lines in vitro and in vivo.*Lung Cancer*, 2009. **66**(2): p. 169-75.
132. Tomasetti, M., S. Staffolani, L. Nocchi, et al., Clinical significance of circulating miR-126 quantification in malignant mesothelioma patients.*Clin Biochem*, 2012. **45**(7-8): p. 575-81.
133. Volinia, S., G.A. Calin, C.G. Liu, et al., A microRNA expression signature of human solid tumors defines cancer gene targets.*Proc Natl Acad Sci U S A*, 2006. **103**(7): p. 2257-61.
134. Busacca, S., S. Germano, L. De Cecco, et al., MicroRNA signature of malignant mesothelioma with potential diagnostic and prognostic implications.*Am J Respir Cell Mol Biol*, 2010. **42**(3): p. 312-9.
135. Andersen, M., M. Grauslund, M. Muhammad-Ali, et al., Are differentially expressed microRNAs useful in the diagnostics of malignant pleural mesothelioma? *APMIS*, 2012. **120**(9): p. 767-9.
136. Ivanov, S.V., J. Miller, R. Lucito, et al., Genomic events associated with progression of pleural malignant mesothelioma.*Int J Cancer*, 2009. **124**(3): p. 589-99.
137. Xu, Y., M. Zheng, R.E. Merritt, et al., miR-1 induces growth arrest and apoptosis in malignant mesothelioma.*Chest*, 2013. **144**(5): p. 1632-43.
138. Reid, G., M.E. Pel, M.B. Kirschner, et al., Restoring expression of miR-16: a novel approach to therapy for malignant pleural mesothelioma.*Ann Oncol*, 2013. **24**(12): p. 3128-35.
139. Goparaju, C.M., J.D. Blasberg, S. Volinia, et al., Onconase mediated NFKbeta downregulation in malignant pleural mesothelioma.*Oncogene*, 2011. **30**(24): p. 2767-77.
140. Truini, A., S. Coco, A. Alama, et al., Role of microRNAs in malignant mesothelioma.*Cell Mol Life Sci*, 2014.**71**(15): p. 2865-78.
141. Balatti, V., S. Maniero, M. Ferracin, et al., MicroRNAs dysregulation in human malignant pleural mesothelioma.*J Thorac Oncol*, 2011. **6**(5): p. 844-51.

7. APPENDIX

The following publications resulted from this dissertation:

Arzt, L; Kothmaier, H; Halbwedl, I; Quehenberger, F; Popper, HH;
Signal transducer and activator of transcription 1 (STAT1) acts like an oncogene in malignant pleural mesothelioma.
Virchows Archiv 2014; **465**(1): 79-88. Doi: 10.1007/s00428-014-1584-8

Arzt, L; Quehenberger, F; Halbwedl, I; Mairinger, T; Popper, HH;
BAP1 Protein is a Progression Factor in Malignant Pleural Mesothelioma.
Pathol Oncol Res. 2014; **20**(1):145-151. Doi: 10.1007/s12253-013-9677-2